NOTTINGHAM TRENT UNIVERSITY

Innovative co-simulation tool for assessment and optimisation of energy consumption in deep retrofitted buildings

Giorgio Cucca

A thesis submitted in partial fulfilment of the requirements of Nottingham Trent University for the degree of Doctor of Philosophy in Civil Engineering

July 2021

Dedication

Needless to say, my first thought is for you, it's been 24 years now, I miss you, but I also know that you are walking next to me on this journey called life. **Vittoria** and **Fabio**, I cannot put into words the love and gratitude I feel for you, all of this is for you, the best mother, and the best brother/father I could ever have.

Acknowledgments

I want to express all my gratitude to my supervisors Prof. Anton Ianakiev and Dr. Marisela Mendoza. The constant support, guidance and all the invaluable advice Dr. Ianakiev provided me during this journey have been vital and helped my growth not only as researcher but as person too. Special thanks also go to Ahmad, the best colleague one can hope for.

And thanks obviously to my friends, first and foremost Nicola, the second brother life gave me, and thanks also to Andrea, Agnese, all the guys from the "Taverna", and all the Bernardini.

Abstract

The building sector has a strong impact in terms of energy consumption and greenhouse gasses emissions, for this reason the scientific community is dedicating an increasing attention to this sector. In this context, the REMOURBAN H2020 project has carried out a pilot deep refurbishing work on a small cluster of 10 homes. The interventions included the implementation of passive energy saving measures to the buildings envelope and the replacement of the old heating system, based on individual gas boilers, with an all new hybrid energy-supply system capable of satisfy both the space heating and the domestic hot water demand. This retrofitting scheme aims to achieve near-zero-energy homes level of performance at reasonable cost by offsetting part of the energy demand renewable energy produced in loco. The new layout is designed as a local low temperature district heating system and includes ground source heat pumps, photovoltaic panels, electric, and thermal energy storage devices. The management of the complex hybrid system requires a suitable control strategy to optimise the energy consumption and consequently running cost. With this purpose a co-simulation tool has been developed, coupling a model of the energy system built using Dymola/Modelica and the EnergyPlus model of the buildings. A subsequent expansion of the case study to a total of 27 dwellings highlighted the modularity of the co-simulation tool, as well as its ease of scalability. The co-simulation tool allows a precise assessment of the building energy performance before and after the refurbishment. It has also been used to develop different control strategies aiming to reduce the energy consumption from the grid, maximize the self-consumption of photovoltaic energy and ultimately move away from fossil fuel to sustainable energy resources.

Table of Contents

List of figures

List of tables

Chapter 1: Introduction

According to the Intergovernmental Panel on Climate Change (IPCC), human activities have been the dominant cause of the observed warming since the beginning of the industrial era. The human induced global warming has already reached 1°C (likely between 0.8°C and 1.2°C) compared to the pre-industrial levels, the increasing rate seems to be comprised between 0.1 and 0.3°C per decade (Allen *et al.*, 2018) . If no action is taken to stop the climate change, then this increase is likely to reach a value of 2°C with severe consequences on the environment and therefore on public health and economy. In Europe weather related disaster could affect up to two-thirds of the population, 16% of the Mediterranean climate zone may become arid and the annual damage due to river floods could rise from the current €5 billion per year up to €112 billion per year. (European Commission, 2018b). A summary of the climate change impact on Europe is reported in Figure 1.1

Arctic region
Temperature rise much larger than global average
Decrease in Arctic sea ice coverage
Decrease in Greenland ice sheet
Decrease in permafrost areas
Increasing risk of biodiversity loss
Some new opportunities for the exploitation of natural resources and for sea transportation
Risks to the livelihoods of indigenous peoples

Atlantic region
Increase in heavy precipitation events
Increase in river flow
Increasing risk of river and coastal flooding
Increasing damage risk from winter storms
Decrease in energy demand for heating
Increase in multiple climatic hazards

Mountain regions
Temperature rise larger than European average
Decrease in glacier extent and volume
Upward shift of plant and animal species
High risk of species extinctions
Increasing risk of forest pests
Increasing risk from rock falls and landslides
Changes in hydropower potential
Decrease in ski tourism

Coastal zones and regional seas
Sea level rise
Increase in sea surface temperatures
Increase in ocean acidity
Northward migration of marine species
Risks and some opportunities for fisheries
Changes in phytoplankton communities
Increasing number of marine dead zones
Increasing risk of water-borne diseases

Boreal region
Increase in heavy precipitation events
Decrease in snow, lake and river ice cover
Increase in precipitation and river flows
Increasing potential for forest growth and increasing risk of forest pests
Increasing damage risk from winter storms
Increase in crop yields
Decrease in energy demand for heating
Increase in hydropower potential
Increase in summer tourism

Continental region
Increase in heat extremes
Decrease in summer precipitation
Increasing risk of river floods
Increasing risk of forest fires
Decrease in economic value of forests
Increase in energy demand for cooling

Mediterranean region
Large increase in heat extremes
Decrease in precipitation and river flow
Increasing risk of droughts
Increasing risk of biodiversity loss
Increasing risk of forest fires
Increased competition between different water users
Increasing water demand for agriculture
Decrease in crop yields
Increasing risks for livestock production
Increase in mortality from heat waves
Expansion of habitats for southern disease vectors
Decreasing potential for energy production
Increase in energy demand for cooling
Decrease in summer tourism and potential increase in other seasons
Increase in multiple climatic hazards
Most economic sectors negatively affected
High vulnerability to spillover effects of climate change from outside Europe

Figure 1.1 Impact of the climate change on Europe (European Commission, 2018b)

The European Union is on the frontline addressing the root causes of the climate change, the 2030 climate and energy framework includes EU-wide targets and policy objectives for the period from 2021 to 2030.

Key targets for 2030:

- At least 40% cuts in greenhouse gas emissions (from 1990 levels)
- At least 32% share for renewable energy
- At least 32.5% improvement in energy efficiency. ("2030 Climate & Energy Framework,")

Furthermore on November 28th 2018 the European Commission presented a long term strategic vision for a competitive carbon neutral economy by 2050 (European Commission, 2018a)

The United Kingdom is tackling and responding to climate change through the Climate Change Act 2008, which initially stated that "*It is the duty of the Secretary of State to ensure that the net UK carbon account for the year 2050 is at least 80% lower than the 1990 baseline*" (Parliament of the United Kingdom, 2008). However, The Committee on Climate Change (CCC) recommended in his report "Net Zero the UK's contribution to stopping global warming" to set a new emission target for the UK with a net zero greenhouse gases (GHGs) emission by 2050. In the light of this the Climate Change Act has been amended in 2019, setting the new target to a 100% reduction (HM Government, 2019). The CCC has classified the options for emission reduction in three categories:

- Core options: are those low-cost low-regret options that make sense under most strategies to meet the 80% 2050 target. For most the Government has already made commitments or begun to develop policies (although in many cases these need to be strengthened).
- Further Ambition: options are more challenging and/or more expensive than the Core options but are all likely to be needed to meet the net-zero target (which represents the current goal).
- Speculative options: currently have very low levels of technology readiness, very high costs, or significant barriers to public acceptability. It is very unlikely they would all become available. Some of these options would be required to reach net-zero GHGs emission domestically.

Options for all of these three categories are indicated for different sectors, such as, power production, buildings, industry, transport and others. (Committee on Climate Change, 2019a, 2019b)

The building sector in particular has a substantial impact on energy consumption, it accounts for about the 40% of the energy demand in the European Union (Sajn, 2016) and 32% in the world (Mauro *et al.*, 2015). In the UK, direct greenhouse gas emissions from buildings were 85 $MtCO_2$ in 2017, 17% of the total; taking into account also indirect emissions the value rises to 26% of the total[1] as shown in Figure 1.2 (Committee on Climate Change, 2019a).
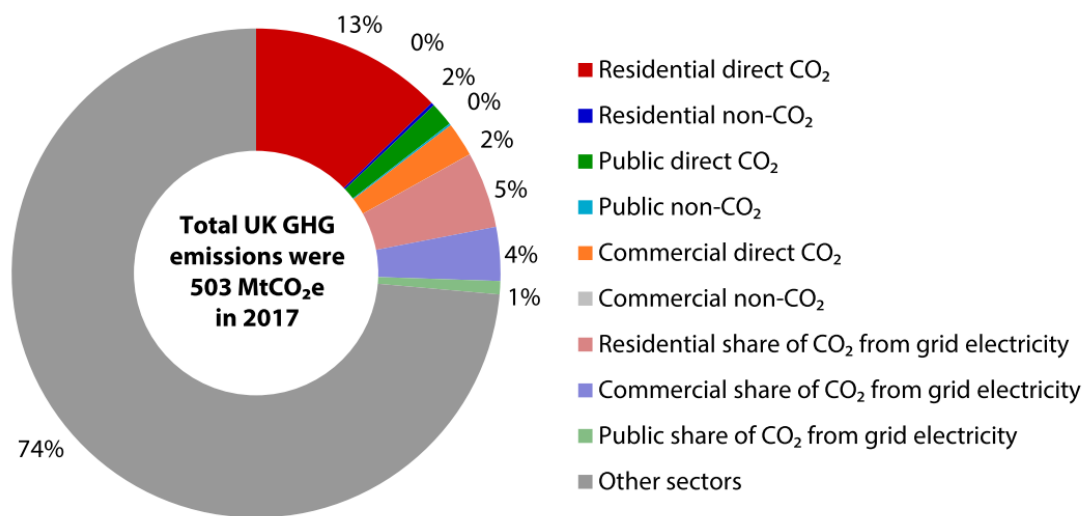
Figure 1.2 Building sector emissions by source (Committee on Climate Change, 2019a)

These numbers are significant and they explain why the reduction of the energy demand is becoming more and more important (Neroutsou, 2016). The CCC itself underlines how having low-carbon heating systems by 2050 was already a desirable goal for the initial 80% reduction target, but becomes necessary when the target is a carbon neutral 2050 (Committee on Climate Change, 2019b). Research has shown that the replacement rate of existing buildings with new buildings is quite low, about 1-3% per annum (Ma et al., 2012), and therefore the 80% of the actual building stock is expected to be still occupied in 2050 (Thorpe, 2010). At European level about two thirds of the buildings were built

---

[1] Direct emissions are from sources that are owned or controlled by the reporting entity. Indirect emissions are a consequence of the activities of the reporting entity but occur at sources owned or controlled by another. Indirect emissions are currently most commonly associated with electricity use. (Committee on Climate Change, 2019a)

when energy efficiency requirements were very poor or not present at all, almost 50% of the boilers for instance were installed before 1992 and they run with an efficiency equal to 0.6 or less (Ascione, Bianco, De Masi, et al>, 2017). In this scenario, refurbishing existing buildings is a necessary path for the reduction of GHGs (Ascione, Bianco, De Stasio, et al., 2017), the European Commission itself states that given the replacement rate an higher renovation rate is needed (European Commission, 2018b).

In terms of refurbishment the main interventions indicated by the CCC in both the "Core Options" and "Further ambitions" are:

- Efficiency improvement (in terms of reduced energy demand)
- Low-carbon heating systems (i.e., heat pumps, biomethane and networked low-carbon heat)

In the Core scenario the total abatement in terms of GHGs is of 66 $MtCO_2e$ with residual emissions of up to 20 $MtCO_2e$.

The efficiency improvement will provide a 21% reduction in homes energy demand thanks to improvements in the building's envelope; in terms of low-carbon heat both low carbon-heat networks and heat pumps are considered.

In the Further Ambitions scenario on the other hand the total abatement is estimated in 83 $MtCO_2e$. The result is achieved thanks to a better fabric energy efficiency capable of deliver a 25% emission reduction; and more advanced technologies, like hydrogen utilization and a wider utilization of heat pumps. One of the alternative options in the Further Ambition scenario is the full electrification of the heating compartment with no utilization of hydrogen (Committee on Climate Change, 2019a).

1.1. Rationale

The need for a strong reduction in GHGs emission has brought a lot of attention on buildings energy efficiency. Both the single countries and political and economic unions like the European Union have set specific regulation and targets in order to achieve significant emissions reduction (European Commission, 2018c, 2018d; HM Government, 2019). As stated in the previous section specific interventions on the existing building stock and the heating systems are necessary to achieve these targets, but it is very important to underline that efficient device need to be well controlled and assembled in order to reach high efficiency performances (Peeters *et al.*, 2008). This means that a refurbishment intervention must not just rely on good design practices, but also that there

is a need for the optimization of the systems. This study will focus on a complex hybrid energy system installed within the renovation work of a 10 homes district in Nottingham (expanded to 27 homes during the PhD), concentrating on the impact of the retrofitting and the consequences of the control strategies on the overall performances of the refurbishment.

Nowadays very powerful building performance simulation (BPS) tools are available. Software like EnergyPlus (U.S. Department of Energy's (DOE) Building Technologies Office (BTO), n.d.), IDA ICE (EQUA Simulation AB) or TRNSYS (University of Wisconsin System) perform very well in terms of evaluation of annual building energy performance (Nouidui and Wetter, 2014), and allow a detailed analysis of the building behaviour and complex phenomena like thermal zones coupling and solar radiation effects (Ascione, Bianco, *et al.*, 2016). These software on the other hand fall short when it comes to have a proper representation of the control system (Nouidui and Wetter, 2014; 'EnergyPlus Essentials', 2021). BPS tools can also be used to improve the energy performances of the building using a "parametric simulation method" approach; according to this method, the input of each variable is varied, within a proper range, in order to see the effects on some objective functions while keeping constant other variables (Nguyen, Reiter and Rigo, 2014; Ascione *et al.*, 2015). This method has limitations because computationally expensive and also because these tools present a limit in terms of complexity of the analysed system. Different software like Modelica-Dymola (Dassault Systèmes) are capable of providing a better control on the management of the energy systems facilitating the optimisation process. Coupling building energy modelling tools with their vast libraries, their user-friendly interface, and their capability of importing complex geometries from CAD files, with a platform like Dymola, provides an opportunity to develop and optimise control strategies for the energy systems, overcoming de facto the limitations of BPS tools.

In this work DesignBuilder (DesignBuilder Software Ltd) has been selected as interface for the utilization of EnergyPlus, this because is currently the most comprehensive and user-friendly interface (Yu *et al*, 2015). This software has been coupled with Dymola creating a powerful co-simulation tool capable of optimising and assessing the performance of the whole system (buildings plus new energy systems) created by the deep refurbishment intervention.

1.2. Research aim and objectives

The aim of this research is to optimise the management of complex domestic, multi-element, energy generation and storage systems, through both active strategies to manage electrical and thermal energy and passive strategies to optimise the building fabric.

The research has the following objectives:

- Build a model to investigate the existing building structures and plants using building performance simulation tools like DesignBuilder and IDA ICE, and other modelling software like Dymola/Modelica
- Compare and validate the results of simulated model with monitored data from the case study.
- Investigate the performances of the whole energy system (photovoltaic system, ground source heat pumps, thermal and electric storage) in the case study.
- Develop and optimize new operation management procedures in order to find the most efficient way to run the system and meanwhile guarantee the maximum energy saving for that specific configuration.

1.3. The REMOURBAN project

As stated in this section retrofitting the existing buildings stock is crucial to achieve the future targets in terms of GHGs emissions. In this context, the City of Nottingham participated in the REMOURBAN H2020 project, which aims at the development and validation in three lighthouse cities (Valladolid-Spain, Nottingham-UK and Tepebasi/Eskisehir-Turkey) of a sustainable urban regeneration model that leverages the convergence area of the energy, mobility and ICT sectors. The REMOURBAN project provided the case study for this research, a total of 27 homes (initially 10), divided between two blocks of terraced houses and two blocks of bungalows, were subject to a deep refurbishment intervention. The retrofitting included both active and passive measures to improve the energy performance and the living standards of the dwellings. For this research an extensive and detailed simulation work has been carried out on the case study to assess the effect of the refurbishment and develop appropriate control strategies for the new energy system.

There is a great number of standards regarding low energy buildings, but most of these are related to new buildings. When it comes to the retrofitting of existing buildings the number of applicable standards reduces drastically. Among the applicable standards, the

majority deals only with certain retrofitting aspects. EnerPHit standard adapts the respective requirements and parameters for the retrofit of existing building to a near Passivhaus standard. The EnerPHit standard is strongly efficient and allows the building to reach consistent energy performance, but on the other hand, it is very expensive and not always affordable from an economical point of view (Neroutsou, 2016). The total cost of the technical intervention in those cases could be close to the value of the entire houses and therefore not economically sustainable. This project instead, research the development of a near zero energy building, called 2050 Homes, where the energy consumption is partially offset by local microgeneration of renewable energy. The details of the entire standard are tailored to each market and differ on details. While EnerPHit concept focuses in reducing the energy demand to a very low point, the design of 2050 Homes using new technologies such as prefabricated facades, insulated rooftops with solar panels, and smart heating looks for a balanced combination between passive and active measures (Energiesprong Foundation). The requirements of the 2050 Homes do not specify how the reduction in energy demand is achieved, and they are not linked to a system of deep retrofitting, as long as the energy consumption from external energy sources can be reduced to the required minimum. Therefore, the design is very flexible, being the energy saving target focussed on achieving near zero energy. This demonstration of 2050 Homes intent to show how we can rethink the way we procure and the business models around deep retrofitting to make it viable. Rather than being prescriptive, in this development we are procuring an output performance specification, with a performance guarantee.

Chapter 2: Literature review

2.1. Introduction

The reduction of greenhouse gas emission is arising as a crucial challenge for all the countries around the world. The building sector, considering its impact on the carbon emissions, plays a central role in this effort. Reducing the environmental impact of the building sector requires passive and active measures. Passive actions include improvements to the building envelope, while active measures include upgrades to heating, ventilation air conditioning (HVAC) systems, lighting etc (Sadineni, Madala and Boehm, 2011). Understanding how the performance of the building fabric are defined and how active measures effect the overall energy demand of dwellings is a key factor to achieve the targets set by the Climate Change Act and European Union. This chapter aims to provide an overview of these topics and a summary of the latest development in the computer aided building energy analysis, which nowadays is an essential tool to define the energy performance of a building.

2.2. Building envelope

The building envelope is defined by Sadineni, Madala and Boehm, (2011) as "*what separates the indoor and outdoor environments of the building*". According to the Approved Document L2B (HM Government, 2010 L2B) it includes walls, floor, windows, roof windows and roof-lights.

An energy efficient building envelope is necessary to have an energy efficient building, the following paragraphs will list the different parameters which characterise the building envelope defining its efficiency.

Pacheco, Ordóñez and Martínez (2012), divided the parameters that define the building energy requirements in two main categories as reported in Table 2.1.

Table 2.1 Parameters defining building energy demand

Physical–environmental parameters	Design parameters
Daily outside temperature (°C)	Shape factor
Solar radiation (W/m2)	Orientation
Wind direction and speed (m/s)	Transparency ratio
	Thermal–physical properties of building materials
	Distance between buildings

Physical–environmental parameters will not be analysed in this work which is focused on existing buildings. For the same reason shape factor, orientation and transparency ration will be only introduced considering that they do not change in case of refurbishment. In Attention will focus, in a dedicated paragraph, on the thermal-physical properties of the building materials, which define the thermal behaviour of the envelope.

2.2.1. Shape factor

The shape factor (or shape coefficient) is defined as the ratio between the building's thermal envelope area and its internal volume. This factor measures the compactness of the building (Danielski, Fröling and Joelsson, 2012).

$$SF = \sum \frac{S_i}{V} \left(\frac{m^2}{m^3} \right)$$
Eq. 2-1

As expressed in Eq. 2-1, where $\sum S_i$ represents the external surface and V the internal volume, the shape factor quantifies the building area exposed to the external conditions (Granadeiro *et al.*, 2013). This means that for a specific volume a lower shape factor indicates a smaller area exposed, so, in principle, a reduced energy demand due to the diminished heat exchange with the environment.

2.2.2. Orientation

Building orientation as one of the greatest impacts on the energy demand of the buildings, and combined with a proper shape factor can reduce the energy demand by 36% (Abanda and Byers, 2016). A proper orientation can maximise solar gains, with important benefits both in terms of heating energy demand but also in terms of lighting energy consumption (Wong and Fan, 2013).

2.2.3. Transparency ratio

The transparency ratio, also called window to wall ratio (WWR) (Çağlar, Gedik and Gökdemir, 2020) or glazing ratio represents the ratio between the glazing area and the gross (i.e., not glazed walls shall be included in the value) external wall area. The optimum value for the WWR changes according to the orientation of the wall. In the UK climate the best values for the WWR are 25% for a South facing façade, 20% for facades oriented toward East or West and in case of North facing wall the glazed surfaces should be kept at minimum (LETI, 2020).

2.3. Thermal-physical properties of the building materials

The thermal-physical properties of the building materials define the behaviour of the building envelope in terms of heat transmission, hence its performance. This paragraph will provide an insight of the most important ones, summarising the parameters that are generally used to define the performance of a construction, is not intended however as a handbook of such a vast topic, and only the topics needed for a better understanding of this research work will be treated. Before that also an overview of the heat transmission mechanism will be provided.

2.3.1. Heat transmission

Heat is the energy that is transferred between the system and the environment because of a temperature difference between them (Halliday, Resnick and Walker, 2014). Heat naturally flows from the system at higher temperature to the system at lower temperature with the total energy remaining constant. Heat transfer is divided into three main mechanisms:

- Conduction
- Convection
- Radiation

In the building envelope heat is transferred by elements like walls, roofs, floors and windows through the aforementioned mechanisms, a review of these processes follows.

2.3.1.1. Conduction

Conduction is defined by McMullan (2017) as "*the transfer of heat energy through a material without the molecules of the material changing their basic positions*". Conductive heat transfer is, according to (Asadi *et al.*, 2018), a combination of energy transport by free electrons and molecular vibration.

The Fourier's Law quantifies the amount of heat flowing, per unit area, through a surface as expressed by Eq. 2-2.

$$q = -\lambda \nabla T = -\lambda \left(i \frac{\partial T}{\partial x} + j \frac{\partial T}{\partial y} + k \frac{\partial T}{\partial z} \right) \qquad \text{Eq. 2-2}$$

In case of unidirectional flow, the equation is simplified to:

$$q = -\lambda \frac{\partial T}{\partial x} \qquad \text{Eq. 2-3}$$

Considering a specific area, A, it's possible to express the heat flow rate as in Eq. 2-4.

$$Q = Aq = -A\lambda \frac{\partial T}{\partial x} \qquad \text{Eq. 2-4}$$

Where:

- Q = heat flow (W)
- A = area (m²)
- q = heat flux (W/m²)
- λ = thermal conductivity (W/mK)
- $\frac{\partial T}{\partial x}$ = temperature gradient.

Thermal conductivity is a parameter which defines the rate at which heat flows across a material under specific conditions, specifically it is the heat flow (in Watt) through a thickness of 1 m of material with a ΔT equal to 1 K and a surface equal to 1 m². Conductivity is a parameter which differ in different materials, materials with high λ are generally refer to as conductor materials (e.g., metals), whereas materials with a low to moderate λ are known as insulators. The reciprocal of conductivity is known as resistivity and measured in m·K/W

2.3.1.2. Convection

Convection is defined as the heat transfer between a surface and a fluid flowing on it (Kothandaraman, 2012). Convection is usually the prevalent form of heat transfer in liquid and gases whereas it does not occur in solids. The heat transfer due to convection can be defined using the Newton's law for cooling:

$$Q = hA(T_s - T_\infty)$$ Eq. 2-5

Where:

- Q = heat flow (W)
- h = convection coefficient (W/m²K)
- A = area (m²)
- T_s = surface temperature
- T_∞ = fluid temperature at distance from the surface

The value of the convection coefficient (or convective heat transfer coefficient) is affected by several factors: fluid properties like density, viscosity, and specific heat; fluid velocity and geometry of the surface. Considering that these properties change with temperature and location the convection coefficient will vary from point to point.

Convection can be classified as natural convection or forced convection. In the first case the fluid movement is induced by the expansion of the heated fluid which correspond to a reduction in density, due to the different in density the colder fluid displaces the warmer one causing it to rise. In turn the colder fluid it is heated, and the process repeated creating the so called "convection current". In the forced convection on the other hand, the fluid is moved by external means like pumps or fans (McMullan, 2017).

2.3.1.3. Radiation

Thermal exchange through radiative transfer occurs between surfaces in visual contact regardless the presence of a medium between them. The heat transfer rate between the surfaces follows Eq. 2-6:

$$Q = A\sigma\varepsilon(T_1^4 - T_2^4)$$
<div align="right">Eq. 2-6</div>

Where:

- Q = heat flow (W)
- A = area (m²)
- σ = Stefan-Boltzmann Constant ($5.6703 \cdot 10^{-8}$ (W/m^{2}K^4))
- ε = emissivity
- T_1 and T_2 = surfaces temperature (in Kelvin)

Thermal radiation it is emitted by matter irrespectively to temperature and is part of the electromagnetic spectrum (Kothandaraman, 2012).

2.3.2. Thermal transmittance (U-value) and thermal resistance (R-value)

According to Green, Hope and Yates (2015) the two primary mechanism through which buildings lose heat are:

- Heat conduction through the building envelop.
- Convective losses due to ventilation.

In order to quantify the heat transferred through a particular section of a building (e.g., a wall) two parameters are used, the thermal transmittance (U-value) and the thermal resistance (R-value). The U-values (or overall heat transfer coefficient) indicates the rate of heat flow through a surface with area 1 m² and with 1 K of ΔT between the two sided of the surface. On the other hand, thermal resistance (used to calculate the U-value) is defined as the opposition to the heat flow offered by a particular component (McMullan, 2017).

The R-value is calculated as:

$$R = \frac{s}{\lambda}$$
<div align="right">Eq. 2-7</div>

Where:

- R = thermal resistance (m²·K/W)
- s = thickness of the material (m)
- λ = thermal conductivity (W/mK)

Eq. 2-7 clearly shows how the R-value is function of the thermal conductivity of the material and depends also on the thickness of the analysed component.

As mentioned, R is used to calculate the transmittance, specifically the latter can be defined as the reciprocal of the sum of the resistance of all the n layers composing a specific component and the internal and external surface resistance. Eq. 2-8 shows the generic equation used to define the U-value[2]:

$$U = \cfrac{1}{R_{in} + \cfrac{s_1}{\lambda_1} + \cfrac{s_2}{\lambda_2} + \cdots \cfrac{s_n}{\lambda_n} + R_{ex}}$$
Eq. 2-8

Where:

- U = thermal transmittance (W/m²K)
- s = thickness of the material of each of the n layers (m)
- λ = thermal conductivity of the material of each of the n layers (W/mK)
- R_{in} = internal surface resistance (m²·K/W)
- R_{ex} = external surface resistance (m²·K/W)

The surface resistance R_s (R_{in} and R_{ex} in the equation) is defined as

$$R_s = \cfrac{1}{h_c + h_r}$$
Eq. 2-9

Where:

- R_s = surface resistance (m²·K/W)
- h_c = convection coefficient (W/m²K)
- h_r = radiation coefficient (W/m²K)

The coefficients h_c and h_r depend on different parameters, like direction of the heat flow, surface properties (like emissivity), temperature and climatic effects. Both are different for the internal and external surface, respectively.

---

[2] Thermal resistance of the different layer expressed as R = s/λ

2.4. Ventilation

As stated in 2.3.2 ventilation is one of the two main processes through which a building loses heat. The CIBSE Guide B2: Ventilation and ductwork (CIBSE, 2015), defines ventilation as "*the process by which fresh air is provided to occupants and concentrations of potentially harmful pollutants are diluted and removed from a space*", underlining as it can account for 50% or more of the heating/cooling losses. Similar values are provide by Dodoo, Gustavsson and Sathre (2011) which estimate the impact on energy demand in a range between 30 and 60%. In case of heating, ventilation (and infiltrations, which are undesired air leakages) increase the heat demand due to the rise of the "ventilation heat loss" i.e., the heat that must be supplied to warm up the external air at the same temperature of the internal one (Green, Hope and Yates, 2015). It is evident, in the light of the values provided, that ventilation and airtightness play a crucial role in the energy efficiency of a building.

CIBSE (2015) identifies three main methods to provide ventilation:

- Natural ventilation
- Mechanical ventilation
- Hybrid or mixed-mode ventilation.

Natural ventilation, as suggested by the name is due to natural phenomena being driven by forces like wind and buoyancy. The wind-driven ventilation is caused by the wind pressure on the building, and therefore it is influenced by the terrain surrounding the structure, its shape, and the direction and speed of the wind within respect to the building. On the other hand, slack or buoyancy-driven ventilation is caused by the pressure difference between inside and outside of the building due to the temperature difference. Buoyancy-driven ventilation can often achieve the same magnitude of the natural one, having, consequently, a significant effect on the total ventilation.

Mechanical ventilation relies on fans to provide ventilation and it is therefore independent from natural forces. Main functions of mechanical ventilation systems are :

- Providing fresh air ventilation.
- Assist the natural cooling of a building when the outside temperature is lower than the internal.
- Distribution of the air from eventual HVAC systems.

Compared to natural ventilation mechanical ventilation gives the opportunity, using adequate systems, of recovering part of the heat from the exhaust air using it to pre-heat the incoming air, in this case the system is define as Mechanical Ventilation with Heat Recovery (MHVR), a schematic representation is shown in Figure 2.1.
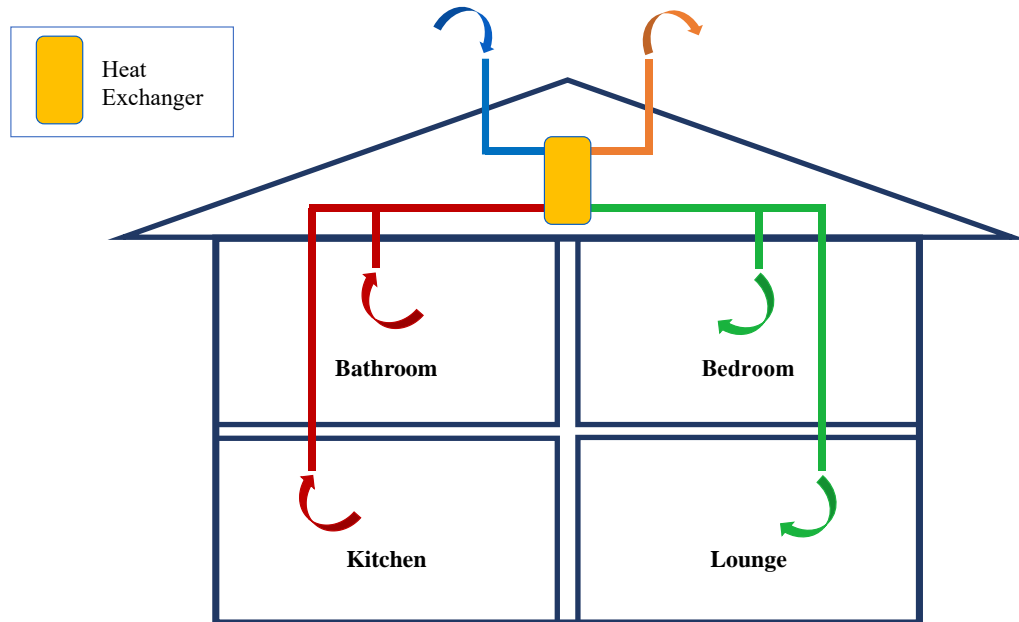
Figure 2.1 MVHR schematic representation

2.5. Energy efficiency measures

As stated in section 2.1 the improvement of the energy performance of a building can be achieved through passive or active measures (or, obviously, a combination of the two). In the following paragraphs an overview of these two types of energy efficiency practices will be provided.

2.5.1. Passive measures

Passive measures aim to reduce the energy demand of the building by reducing the energy losses through the building envelop (including the ones due to ventilation), but also with the increase of natural heating (or cooling), and natural lighting (Amirifard, Sharif and Nasiri, 2019). Among all the passive measures the improvement of the thermal insulation has been identified as the most efficient and impacting one (Dylewski and Adamczyk, 2011) (Al-Homoud, 2005).
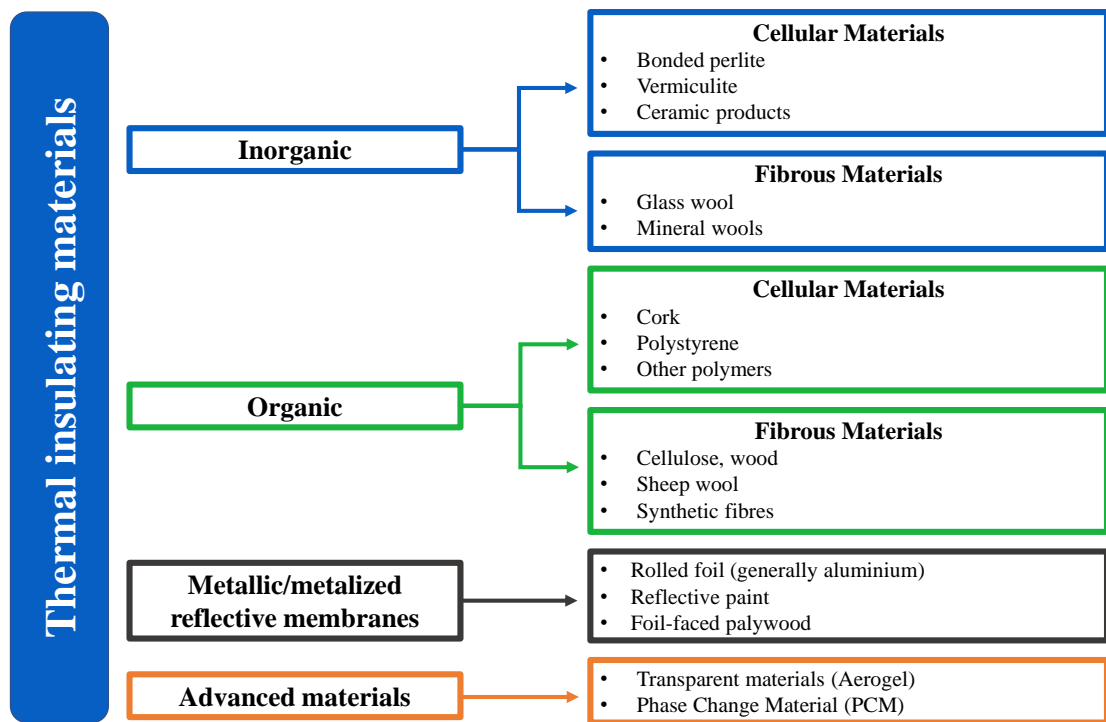
Figure 2.2 Insulating materials classification

A vast number of insulating material, capable of providing great improvement in terms of U-value (i.e., reduce the thermal loss through the envelope), are nowadays available on the market, (Sadineni, Madala and Boehm, 2011) provided a classification of them visible in Figure 2.2. However, adding (or increasing) insulation to the building envelope has to be done in an accurate way. The performance of the building envelope will not be influenced only by the thickness of the thermal insulation, but also by where and how the insulation has been applied. Insulation should be used to reduce thermal bridges (zones in which the thermal resistance is lower than the surrounding areas (Branco, Tadeu and Simoes, 2004)) which, as underlined by Galadanci *et al.* (2020), can increase the heat loss by up to 9%. The position of the thermal insulation is crucial also under the point of view of the thermal mass. The later can be defined as the capacity of a structure to accumulate and store heat energy (Amirifard, Sharif and Nasiri, 2019). Installing the insulation on the external surface of the building envelope in fact, allows to use all the wall thickness to store heat. This means that (in case of heating) the heat energy requires more time to diffuse from the inside to the outside of the building, consequently the internal temperature will be more stable with beneficial effects on comfort and energy efficiency.

In section 2.4 the considerable impact of ventilation on the building energy efficiency has been highlighted. Undesired ventilation (infiltrations) should be kept at minimum, using

airtightness retrofitting measures which can significantly reduce the energy loss being, furthermore very cost effective (Roberts, 2008).

It is important to consider that opaque surfaces are not the only components of the building envelope, also windows, roof windows, and roof-lights are part of it, and they play an important role in its efficiency accounting for 30 to 50% of the heat losses in the winter (Gustavsen *et al.*, 2011). Also for these elements the U-value is an important parameters when it comes to define their energy efficiency. Considering that in each fenestration glazing cover most of the surface its U-value is going to have a considerable impact on the U-value of the entire structure. Technology in the glazing field has seen a tremendous progress in recent years and a considerable number of technical solutions are available, multilayer (double or triple) glazing, vacuum glazing, low emissivity coatings, glazing cavity filled with gasses like Argon and Xenon are only some of the available solutions. All of them aim to reduce the heat loss and keep the heat into the building. Speaking of glazing however there are other factors that must be considered. Fenestrations are in fact vital in terms of natural light supply and solar gains. Modern windows are capable of reflecting portions of the solar radiation (generally in the infrared and ultraviolet spectrum) allowing at the same time the visible fraction to pass through. These properties are crucial when it comes to avoid overheating, together with proper shading structures (Amirifard, Sharif and Nasiri, 2019). It is important to underline that specific coating allow windows to keep inside the infrared emission coming from the internal building environment reducing the heat demand.

Many other passive measures exist, solution like green roofs, ventilated roofs, Trombe walls, walls with PCM incorporated, and so on, but the analysis of all these technical solution falls outside the field of this research work, the paragraph however provided an overview of the topic useful to understand the work done on the case study.

2.5.2. Active measures

Active energy efficient measures aim to reduce the building energy consumption with interventions which include the upgrade of the building service system and energy saving control strategies (Chen *et al.*, 2020). Other measures which aim to offset (completely or partially) the energy consumption of the building with renewable energies are classified as active measures too (Serrano-Jiménez *et al.*, 2019). In terms of building systems one of the most common interventions is the upgrade of the lighting system. Older systems such as the incandescent light bulb have been banned or are being phased out in many

countries including the European Union and the USA (Howarth and Rosenow, 2014). Nowadays the compact fluorescent lamps are diffused worldwide and represent the most common solution, representing a massive step forward compared to the old bulbs. Light-emitting diodes (LED) however are capable of even better performance, Chen *et al.* (2020) highlight how a LED lamps combined with dimming technology can provide a 40% reduction in lighting energy consumption.

The number of possible interventions on the heating system is vast and a detailed analysis of each possible intervention is not within the aims of this work, this paragraph will only focus on the main ones and with the assumption that the baseline system (the one that will generally be replaced) is a gas boiler, which is, in fact, the most diffused solution in the England, covering about the 92% of the central heating systems (MHGLC, 2018). Gas boilers efficiency improved dramatically during the years, and condensing boilers account for 66% of the total, compared to 2% in 2001.
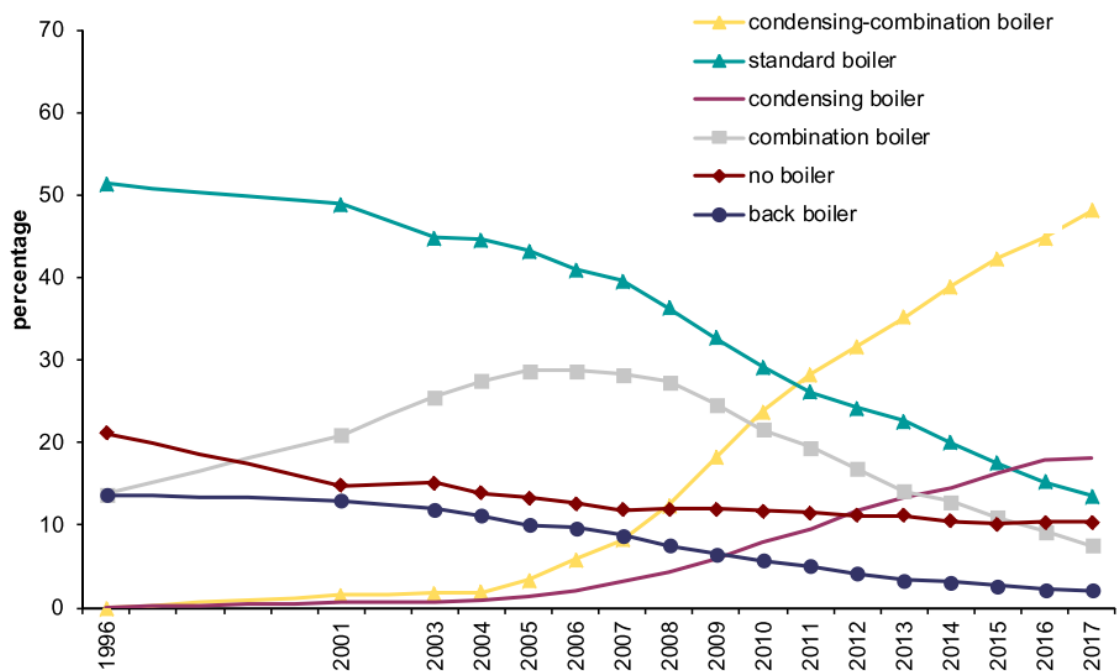
Figure 2.3 Boiler typologies in England (MHGLC, 2018)

Gas boiler even taking into account the improvements in efficiency (which in latest models easily ranges above 90%) still rely on the combustion of a fossil fuel, this puts them in an "uncomfortable" position considering the push towards the electrification of heating systems (Committee on Climate Change, 2019a), furthermore, as previously stated most of them in Europe run with an efficiency equal to 60% or less (Ascione, Bianco, De Masi, et al, 2017). Gas boiler can be replaced by several systems, like district

heating (often fed with waste heat), cogenerations systems, biomass boilers, etc...nevertheless this paragraph, considering the case study of the PhD, will focus on full electric heating systems and renewable energy sources. Not considering the highly inefficient electric room heaters and electric storage heaters (MHGLC, 2018) heat pumps (HPs) are the systems of choice for the electrification of the heating system.

Heat pumps can be defined as a form of heat engine which transfer heat energy from a source at low temperature to a source at higher temperature using mechanical work (Rees, 2016), Figure 2.4 shows a schematic view of a heat pump.
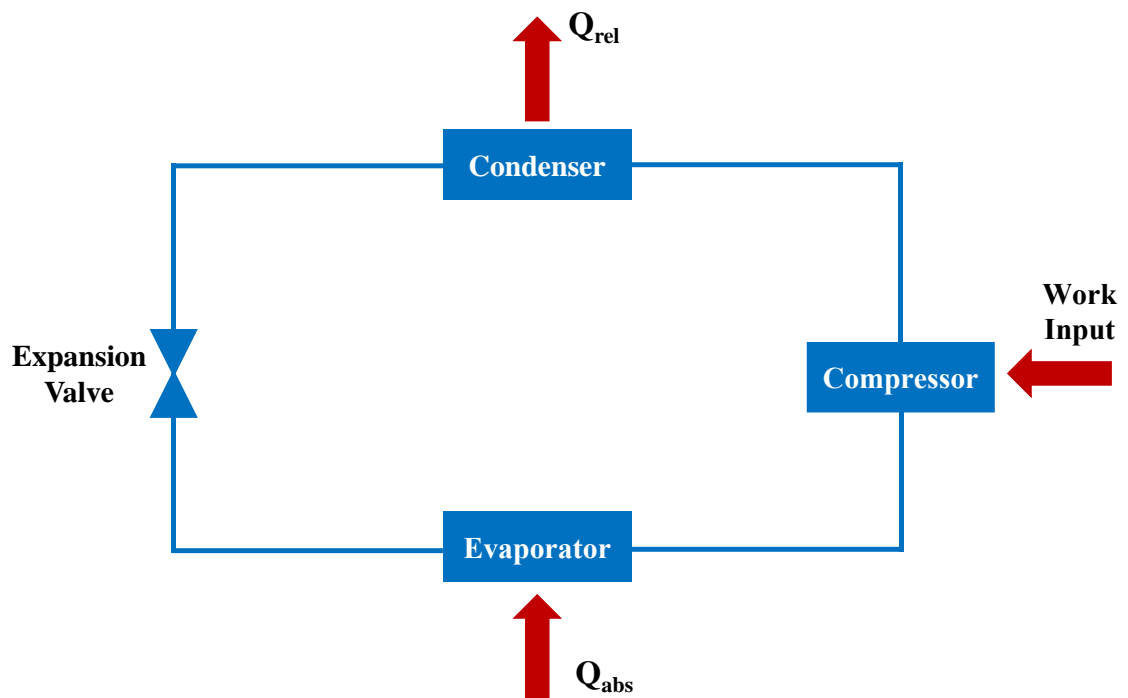
Figure 2.4 Heat pump generic layout

The refrigerant in the circuit is compressed using external supplied energy, the fluid is then sent to the condenser where it releases heat during the condensation phase, the fluid leaving the condenser reaches the expansion valve where its pressure is reduced before it enters the evaporator where it will change phase again absorbing heat. Through this cycle HPs are capable to subtract heat from the external environment at low temperature and "pump" it in the internal environment at higher temperature. They can operate in the other direction too, removing heat from the building and discharging it in the external environment, this happens when HPs are used for cooling rather than heating. An important parameter which defines the performance of a heat pump is the so-called Coefficient Of Performance (COP), defined by (CIBSE, 2016) as the ratio between the heat output at the condenser and the power input absorbed by the compressor. COP value

is function of the working temperature of condenser and evaporator; therefore, it is subject to considerable variations according to these two temperatures. Modern HPs show COP values in nominal conditions which are often above 3 or 4, it is imperative to underline that this does not mean that HPs can "produce" more heat than the energy they absorb, what they do is moving (or pumping) heat from one heat source to another.

Heat pumps can be categorised in different ways, for example according to the heat source, in this case the three principal categories are:

- Air source heat pumps (ASHP).
- Ground source heat pumps (GSHP).
- Water source heat pumps (WSHP).

Air source heat pumps use the external air as heat source extracting energy from it to heat the building interiors. This kind of heat pumps are subject to large falls in terms of COP value when the air temperature drops. Ice can build up on the external evaporator if the temperature is low, and in this case the HP will require defrosting cycles to operate, this has detrimental effects on the performance of the HP. It is common in some cases (e.g., swimming pools) to use as heat source exhaust air coming from ventilation systems increasing the COP and, at the same time, recovering heat that would otherwise go wasted.

Ground source heat pumps utilise the ground as heat source rather than air, this is due to the fact that the soil temperature is usually above the air temperature and, unlike air, the ground temperature below 2m from the surface remains reasonably stable throughout the year (CIBSE, 2016). A higher and more constant temperature translates in higher average COP for the HP which leads to considerable savings in terms of energy. GSHPs can exchange heat with the ground through two kinds of heat exchanger, the horizontal one in which a coil is buried at a depth of roughly 1.5 m, and vertical one, in this case the pipework is installed into boreholes with variable depth. The fluid

Water source heat pumps make use of water as heat source, either water aquifer or surface water like rivers or lakes. The target just like for GSHP is to exchange heat with a medium at higher and more constant temperature than the air. In case of water source HPs, the Environmental Agency imposes strict rules to the amount of heat that can be extracted, and temperature difference between the flow and the return.

As said another way to categorise HPs is according to the heating source and the heat distribution medium Table 2.2.

Table 2.2 Heat pump typologies

Type of HP	Heat source	Heat distribution medium
Air-to-air	Air (outdoor or ventilation exhaust)	Air
Air-to-water	Air (outdoor or ventilation exhaust)	Water
Water-to-air	Ground/Water	Air
Water-to-water	Ground/Water	Water

The different kinds of heat source have already been described, concerning the heat distribution medium it can be air or water. Air-to-air and water-to-air systems use air as medium for heating the internal space, most diffused example being the ducted ventilation air supply. Air-to-water and water-to-water on the other hand use water as heat vector, generally is water at low temperature (compared to the usual working temperature of boiler and radiators systems) used in floor heating systems, water radiators (with proper sizing), and domestic hot water (DHW) production.

Thanks to the high COP heat pumps can deliver considerable savings in terms of energy used for space heating or DHW production. It must be noted however, that electricity (which is the main energy vector used to run the HPs) is more expansive than gas, hence an accurate design is required to avoid low COP values which could erode the energy savings.

Another typology of retrofitting which falls under the category of active measure is the installation of local renewable energy production systems, generally PV systems (for electricity production) and thermal solar systems (used for the production of hot water).

"*Photovoltaics is the direct conversion of light into electricity at the atomic level. Some materials exhibit a property known as the photoelectric effect that causes them to absorb photons of light and release electrons. When these free electrons are captured, an electric current results that can be used as electricity*." (Knier, 2008)

The production of electricity in loco is often used in combination with both passive and active measures, frequently in combination with electric energy storage (EES) systems.

The combination of HPs, PV, EES lead to systems significantly more complicated than a simple gas boiler, de facto such plants are not only heating system, but rather hybrid energy systems where different energy sources and vectors are combined to cover not only the building heating demand (which however remains their first duty) but also offset the other energy needs of the building. Hybrid energy systems are complex equipment which require a precise design and an efficient control strategy, this is where energy modelling and simulation becomes essential.

2.6. Building energy modelling

2.6.1. SAP

Building energy performance are assessed in the UK using the Standard Assessment Procedure (SAP) (BRE, 2014). SAP is not a modelling tool but rather "*the methodology used by the Government to assess and compare the energy and environmental performance of dwellings*" (*Standard Assessment Procedure - GOV.UK*, 2013). The procedure works on the bases of a standardised assumptions which allows a comparison between different dwellings in terms of: energy use per normalised floor area, CO_2 emissions and a fuel-cost-based energy efficiency rating.

SAP provide a framework to assess the energy demand in dwellings and is used for compliance testing, it is not in other words a precise and reliable tool when it comes to define the energy performance of a buildings which diverge form the standard assumptions within it (Palmer and Passivhaus Trust, 2020). This limitation is clearly highlighted by a study on 410 homes showed in Figure 2.5.
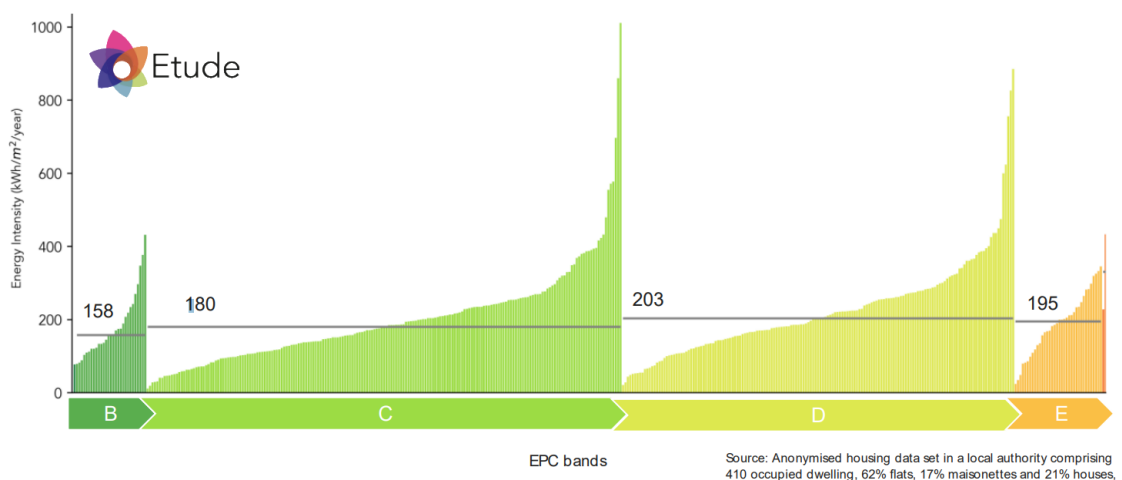
Figure 2.5 Disconnection between EPC band and metered energy consumption (The future of SAP calculations - Etude, n.d.)

When more precise results are required, especially for complex and not-standard scenarios more sophisticated instruments are needed to assess the performance of buildings and their systems.

2.6.2. Definition of building energy modelling and evolution in time.

According to the BEM Library (*Introduction: EnergyPlus Essentials — EnergyPlus 9.6*, n.d.):

"*Building Energy Modelling (BEM)*[3] *is the practice of using computer-based simulation software to perform a detailed analysis of a building's energy use and energy-using systems. The simulation software works by enacting a mathematical model that provides an approximate representation of the building. BEM includes whole-building simulation as well as detailed component analysis utilizing specialized software tools that address specific concerns, such as moisture transfer through building materials, daylighting, indoor air quality, natural ventilation, and occupant comfort. BEM offers an alternative approach that encourages customized, integrated design solutions, which offer deeper savings. Using BEM to compare energy-efficiency options directs design decisions prior to construction. It also guides existing building projects to optimize operation or explore retrofit opportunities.*"

Building simulation finds its roots in the 1960s having a consistent expansion in the 1970s, during these years research was mostly focused on theories and algorithms of load and energy estimation. The oil crisis emphasized building simulation as an instrument to transform energy-intensive buildings in more efficient environments (Hong, Chou and Bong, 2000). The work of those years put the bases for the development of a vast number of simulation packages (Augenbroe, 2002). Thanks to substantial investments in R&D by the US Department of Energy (also in terms of sponsorships) and the diffusion of desktop computers, software like TRNSYS, DOE-2 (Hirsch, n.d.), and ESP (University of Strathclyde, 2019) were developed. Nevertheless, building energy modelling remained mostly confined to the research world due to cost and complexity (Hong, Chou and Bong, 2000). It is in the 1990s, in a period of increased awareness of the buildings' environmental impact, that personal computer and graphical user interface became

---

[3] The same topic can be addressed with other names, such as Building Simulation, Building Performance Simulation, Building Energy Simulation and Building Performance Modelling

accessible to a broader public, making building energy simulation (BES) available not only for the researchers but also for the professional community (Wang and Zhai, 2016).

The need for improving building energy performance inevitably leads to the utilization of building performance simulation tool, as stated by Hong, Chou and Bong (2000) in fact "*Only computer-aided simulation holds the key to improving building energy efficiency*". This efficiency depends not only on the performance of the building envelope or the HVAC system as independent components, but a holistic analysis is also necessary to understand the effect that individual modification will have on the building as a whole. Building modelling allows the user to answer question that might arise in a decision-making context, predicting the effects of retrofitting interventions for example (De Wit, 2004).

2.6.3. Modelling approach

In scientific modelling it is possible to divide models in two categories (Andrea *et al.*, 2008): *Diagnostic* i.e. models that can be used to better understand the laws behind a given system under analysis, and *Prognostic* i.e. models used to predict the behaviour of a system starting from a well-defined set of governing laws. Coakley, Raftery and Keane (2014) define the building energy simulation models as prognostic law- driven simulation tools, under the consideration that they are used to forecast the performance of a complex system given a well-defined set of laws and inputs.

Harish and Kumar (2016) identified three main approaches in building energy modelling: the *law-driven* approach (or *forward*), the *data-driven* approach (or *inverse*) and the *grey-box* approach.

The *law-driven* approach (in Figure 2.6 the step by step procedure for this kind of approach) relies on a given set of laws governing a specific system to assess and foresee its behaviour under pre-defined conditions (Coakley, Raftery and Keane, 2014). These models show a high accuracy thanks also to the advanced computing techniques.

Step 1: Acquire climate data as per location of the building under study

Step 2: Acquire building design data

Step 3: Heat plant characteristics

Step 4: Building operating schedules

Step 5: Simulate the model as per the desired simulation periods

Step 6: Predict the net energy (peak or average values) consumption patterns

Step 2.1: Acquire building geographical characteristics: location, orientation, etc…

Step 3.1: Type of HVAC system

Step 2.2: Acquire building construction data: building material properties etc…

Step 3.2: Type and characteristics of the HVAC subsystems: AHU, Coil units, etc.

Figure 2.6 Steps for forward approach as for (Harish and Kumar, 2016)

The building energy simulation models developed with the *data-driven* approach (also called black-box models), do not require a knowledge of the intrinsic nature of the modelled phenomenon, they make use of statistical or mathematical models which relate a set of influential input parameters to measured outputs. The *grey-box* approach uses a mix of both law-driven and data-driven, relying on a physical mode of the building system and hen with statistical analyses identifies important factors representative of certain key and aggregated physical parameters. The latter approach very useful in some fields (like the faulty detection analysis) find limited application in the building sector.

Some authors (Coakley, Raftery and Keane, 2014) identify also another approach as sub-category of the law-driven one. The *detailed model calibration*, this approach is based on a detailed forward model of the building system in which some parameters and inputs are tuned in order to march measured data from the building. This procedure delivers the most precise prediction of the building behaviour and being intrinsically linked to the real building also provides a very reliable platform on which is possible testing the impact of specific parameter changes (e.g., retrofitting intervention analysis).

To simulate building energy performance three main thermal building models are currently used, zonal, multizonal and Computational Fluid Dynamics (CFD) methods. Each of these methods has its peculiarities, and the selection of the physical method depends mostly on the problem that has to be solved (Foucquier *et al.*, 2013). On the other hand, all the most widespread software used in building energy modelling, namely TRNSYS, EnergyPlus, IDA-ICE, and ESP-r, (Foucquier *et al.*, 2013; Mazzeo *et al.*, 2020) use the multizonal method, also called nodal method. In this approach every building zone

is seen as a homogeneous volume characterised by uniform state variables and approximated to a node described by a unique pressure, temperature, concentration, etc…The thermal transfer equation is solved for each node in the system that could represent a wall, a room or the exterior of the building but also more specific loads like internal gains (from occupancy or equipment) or the heating system (Foucquier *et al.*, 2013).

As aforementioned TRNSYS, EnergyPlus, IDA-ICE, and ESP-r represent the most diffused building performance simulation tools, in the following paragraphs some of them will be presented.

2.6.4. ESP-r

ESP-r (Environmental Systems Performance – Research) is an integrated modelling tool which allows the simulation of visual, acoustic, and thermal performance of buildings. Similarly to other software (e.g. EnergyPlus or DOE-2) requires the user to input data regarding geometry, HVAC system, components and schedules (Coakley, Raftery and Keane, 2014).

The first prototype of ESP-r was developed by Joe Clarke as part of his PhD research. In the following years, the software has been refined thanks also to Dr Don McLean and funding's that, through the years, have been provided by UK Science and Engineering Research Council. In late 1980s the Energy Simulation Research Unit (ESRU) was formed, and ESP-r development continued as part of ESRU research portfolio. Software improvement carried on for decades thanks especially to researchers from the University of Strathclyde but also from other institutions like the Lawrence Berkeley Laboratory or the Eindhoven University of Technology (University of Strathclyde, 2002).

Tavares *et al.* (2016) carried out a study on the control of electrochromic glasses in buildings refurbishment. The research work carried out with ESP-r compared the heating and cooling loads resulting from the utilization of different types of glazing. The study shows how the retrofitting with electrochromic could potentially lead to an increased heating demand but also to a reduction in cooling needs (the simulation represent a Mediterranean climate) which makes the total energy demand drop. Different control strategies have been developed showing that a differentiation in the control logic between the heating and cooling season. The software highlights also the importance of bespoke solutions for the different facades (i.e., different orientation).

Asaee, Ugursal and Beausoleil-Morrison (2016) used ESP-r as simulation engine in their research work. Aim of the study is the assessment of the impact (in terms of energy consumption and GHGs emission) of air to water heat pump and PV retrofit on the Canadian house stock. The system tested is hybrid and also includes an auxiliary oil or natural gas boiler, which however is rarely needed according to the simulations. Results show that roughly 20% of the Canadian building stock is suitable for the installation of such a system, highlighting that the HP+PV heating in those homes would reduce the energy consumption of the entire Canadian house stock by 16% and the CO2 emissions by 12% with a fossil fuel consumption in the retrofitted homes close to zero.

2.6.5. TRNSYS

TRNSYS has been developed in the 1970s by University of Wisconsin and University of Colorado, since then it has been constant updated and improved (Mcdowell *et al.*, 2017) by an international collaboration of Thermal Energy System Specialists, the University of Wisconsin-Solar Energy Laboratory (USA), Centre Scientifique et Technique du Bâtiment (France) and TRANSSOLAR Energietechnik (Germany). The software is extremely flexible and has been used through the decades to simulate building, application of solar energy but even biological process (Duffy *et al.*, 2009). Based on FORTRAN code TRNSYS is used to simulate transient systems with two parts, the kernel, and the library. The first processes input files, solves the system, and determines convergence, the second includes a number of user modifiable models.

Valdiserri *et al.* (2015) used TRNSYS to evaluate the effects of refurbishment interventions on a tertiary building supposed to be located in two cities at different latitude (i.e., climatic zones) in Italy. Two scenarios have been simulated, one with retrofitting focused only on the opaque structures (walls, roof and floors), and one with improved highly efficient glazing. Results showed consistent energy savings but also the impact of the climatic zone on the economic feasibility of the intervention.

Another study about energy assessment of envelope retrofitting was carried out by Terés-Zubiaga *et al.* (2015) using TRNSYS. A total of 64 possible combinations of different energy saving measures have been simulated. The model was validated through comparison against data monitored in the real building in north Spain. The simulation work highlighted the positive effects of the different intervention capable to reach not only the standards required for refurbished buildings but also for new ones. Results from TRNSYS were also used to carry out an economic analysis of the different combinations

proving that most of them where beneficial from both the point of view of energy and economic.

The flexibility of TRNSYS makes possible its utilisation in several co-simulation, Kübler and Norrefeldt (2014) for example coupled TRNSYS and Dymola to improve the simulation of the airflow/air temperature in atria. The coupling showed however instabilities and had to be improved with new scripts before finally achieving good correlation between co-simulated and measured data.

Nageler *et al.* (2019) used TRNSYS in a co-simulation framework with IDA ICE and Dymola to analyse a large-scale district heating network. In this framework IDA ICE is used to simulate the different buildings, Dymola the district heating network while TRNSYS is used to model the hybrid energy supply unit. The latter is represented by the waste heat of a dairy and a gas auxiliary heater. The framework allows to model the interactions between building, network, and heat supply, including the investigation of seasonal heat storage (using a pit). Results shows a reduction in carbon emissions and the possibility of using the framework to avoid the oversizing of the plant (considering climate change scenarios)

2.6.6. EnergyPlus

"*EnergyPlus is a whole building energy simulation program that engineers, architects, and researchers use to model both energy consumption—for heating, cooling, ventilation, lighting and plug and process loads—and water use in buildings*." (U.S. Department of Energy's (DOE) Building Technologies Office (BTO), n.d.). First released in 2001 its development started in 1997 ('EnergyPlus Essentials', 2021) to address the shortcoming of two other software in which it has its roots, BLAST and DOE-2 (Crawley *et al.*, 2001). EnergyPlus is, according to Ferrara, Monetti and Fabrizio (2018), the most diffused tool for energy performance calculation.
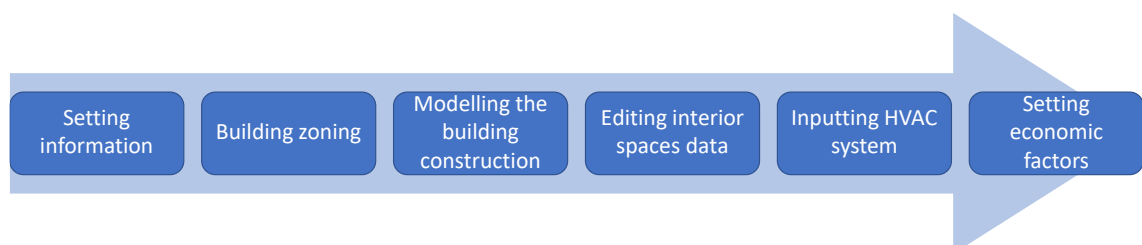
Figure 2.7 Modelling process in EnergyPlus

Yu *et al.* (2015) divided the modelling process in EnergyPlus into six phases (Figure 2.7):

Setting information – In this process the user has to provide building location and weather information, an overall representation of the building has to be described too. This includes, among others, building dimensions, internal and external walls, windows, doors, ceilings, roofs, and floors. Furthermore lighting equipment, occupancy, working schedule as well as HVAC system operating parameters are set.

Building zoning – The zone partition is not a geometric concept but rather a thermodynamic one, the surface building elements which constitute the overall architectural model are in fact divide in heat transfer surfaces and thermal storage surfaces. This implies that two close zones with the same air-conditioning set can be zoned in different space because of different orientation, on the other hand, two zones located in different areas in space can be designed as hot zone due to the same temperature setpoint.

Modelling the building construction – In this process, once completed the zoning of the construction, the user classifies the building surfaces according to the temperature setpoint. In order to reduce the complexity and number of the surfaces is possible to define all the same constructed surfaces as an equivalent surface in a hot zone. This principle applies to windows and shadings too. Further simplification can arrive from stitching complex surfaces into basic geometry.

Editing interior spaces data – Internal loads can be affected by occupancy, ventilation, infiltration, lighting, and equipment. Design load, peak load and corresponding timetables can be used in EnergyPlus to describe the indoor load.

Inputting HVAC system – Inputting the HVAC system could be difficult, and the user is required to have a good knowledge of the modelled system. Third party interface software like DesignBuilder provide a much user friendly and easier interface to operate

Setting economic factors – With the proper set of inputs EnergyPlus is capable of not only performing a building energy evaluation but, after the inputting of the energy rates, a cost analysis too.

The underlying calculation method for building thermal zones in EnergyPlus is a heat balance model based, among others, on the following assumptions about the room air temperature and surfaces (i.e., windows, walls, ceilings, and floors):

- Uniform air temperature throughout;

- Uniform surface temperatures;

- Uniform long and short-wave irradiation;

- Diffuse radiating surfaces;

- One dimensional heat conduction.
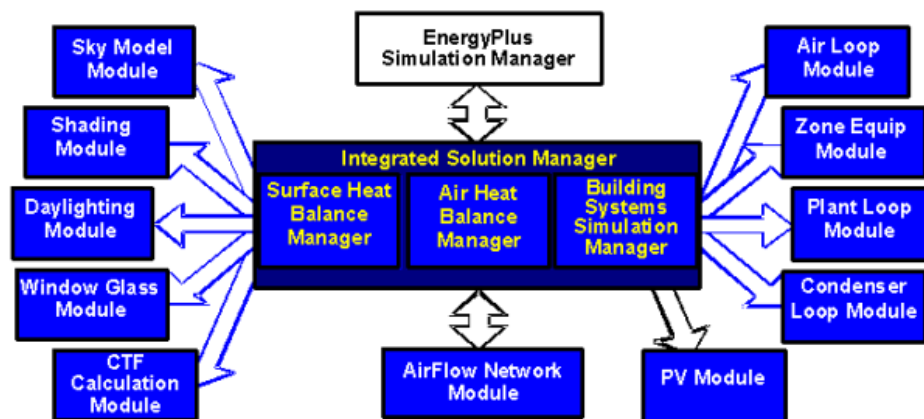
Figure 2.8 EnergyPlus integrated simulation manager

Figure 2.8 shows the integrated simulation manager in EnergyPlus, which works as an interface between the modules that manage the heat balance (of surfaces and air) in the different zones, and the building system simulation modules. The surface heat balance module defines a number of parameters including conduction, convection, radiation and mass transfer effects, furthermore inside and outside heat balance are simulated. On the other hand, the air in the zone is "managed" by the air mass balance module, which works with several mass streams like infiltrations, ventilation and exhaust air. It also accounts the thermal mass of the air in the zone and assesses convective heat gains. Other modules are present (and thanks to the modularity of the code could be added). The list includes for example the Daylighting module which calculates interior illuminance due to daylight, glare from windows, electric lighting control and much more including complex fenestration systems (light shelfs, blinds etc…). It is also present the AirFlow Network Module which improves the calculation of multi-zone airflow.

The integration between all the different modules is with no doubts one of the strong points of EnergyPlus, zone conditions are directly connected and interact with the Building Systems Simulation providing a better overall understanding of the simulated system (Crawley *et al.*, 2001).

EnergyPlus has been used by Murano *et al.* (2017) to analyze the potential imbalance in refurbished buildings in different climate zones in Italy. Three building archetypes were studied, a single-family home, a block of flats and an office building. These building were simulated in two cities with consistent differences (due to latitude and proximity to the sea) in terms of climate. Results show that the reduction of the U-value could lead to imbalance of opposite energy demand from the building (heating and cooling). The reduction in heating demand is in fact coupled to an increase of the cooling demand in all the analysed cases.

Becchio *et al.* (2015) carrier out an assessment research work with EnergyPlus. The authors compared a consistent number of energy efficiency measures for a high-performance dwelling. Analyzed measures included both passive and active interventions. The study showed that near zero energy levels were achievable with conventional solutions (like high efficiency boilers), a good level of insulation and a large number of PV panels, same performance have been reached with more advanced heating systems (air-to-air heat pumps), a high level of insulation and again a large PV plant. To achieve net zero energy levels on the other hand, more sophisticated technical systems were required (HPs, mechanical ventilation, and heat recovery) together with high levels of insulation and a substantial number of PV panels.

Arabzadeh Saheli, Lari and Kasaeian Ziarati (2019) used EnergyPlus in a research work about hybrid energy systems, in this case a combination of wind and PV generators coupled with batteries and gas generators. EnergyPlus has been used to evaluate the energy demand from the case study while the optimisation process was carried out using another software (*HOMER - Hybrid Renewable and Distributed Generation System Design Software*, n.d.). The research identified the three most suitable combinations of the energy systems listed above, with the combination wind-gas generator being the most economical and the solution with PV, wind turbines, gas generators, and batteries the most efficient in terms of GHGs emissions.

2.6.7. DesignBuilder

The first version of DesignBuilder was released in 2005 as the first Graphical User Interface (GUI) for EnergyPlus. According to DesignBuilder Software Ltd (*DesignBuilder Software Ltd - About Us*, 2019) *"DesignBuilder's advanced building performance simulation tools minimise modelling time and maximise productivity as a result of considerable investment in user interface technology and an uncompromising*

approach to software design. Models either imported from BIM or built quickly within DesignBuilder provide fully-integrated performance analysis including: energy and comfort, HVAC, daylighting, cost, design optimisation, CFD, BREEAM/LEED credits, and reports complying with several national building regulations and certification standards"

Andarini (2014) described DesignBuilder as a powerful tool for modelling 3D building geometries and assessing the energy performance combining rapid building modelling with state of the art dynamic simulation. It also have an extensive templates library for a large number of different buildings providing simulation inputs for occupancy schedule, envelop construction, or lighting systems (Wasilowski and Reinhart, 2009).

DesignBuilder uses the easy to operate OpenGL solid modeler, the user can also import CAD files to construct the 3D building and use weather files in .epw format. Time intervals of the running period can be divided from annual/monthly down to daily, hourly, or sub-hourly. The results output shows the building energy performance in terms of both fuel and electricity consumption, it is also possible to define the heating and cooling as well as the CO_2 output (Yu *et al.*, 2015).

DesignBuilder has been used by Ascione, De Masi, *et al.* (2016) in an optimisation study focused on the performance of residential buildings in Mediterranean climate. Different glazing types and sizes, walls constructions, and roof constructions have been evaluated to define the optimal solution in terms of minimization of heating and cooling loads. The case study (a small dwelling) was simulated in four different cities, Madrid (Spain), Nice (France), Naples (Italy), and Athens (Greece). The research indicates the best solutions for the reduction of the heating load as well as the cooling one. When it comes to the best "all conditions" solutions, factors like thermal mass, WWR, solar absorbance and emissivity of the roof show to be very important as well as U-value and selective glazing.

Liang *et al.* (2017) carried out a study analyzing and optimizing the impact of passive retrofitting measures on a rural dwelling in China. The model built in DesignBuilder has been validated with the actual energy consumption of the house. Results show that after the refurbishment the building energy consumption drop by 23% with also a consistent improvement in terms of comfort with the average internal temperature moving from 10.5°C to roughly 15°C.

Rahman, Rasul and Khan (2010) used DesignBuilder to analyse a number of energy saving measures applied to a large institutional building in Rockhampton (Australia). The model built in DesignBuilder has been calibrated and validated against data measured on site. At this point the potential of each energy conservation measure has been evaluated, showing the effectiveness of both zero investment measures (e.g., changing temperature setpoints), passive and active measures, which combined could provide a reduction in energy demand close to 42%.

2.6.8. IDA ICE

The first version of IDA ICE was released in 1998, the software is defined by the developers (EQUA Simulation AB, 2016a) as: *"a dynamic multi-zone simulation application for accurate study of indoor climate of individual zones as well as the energy consumption of an entire building."*

IDA ICE is widely used to simulate the internal climate of buildings regarding comfort indices, operative temperature, humidity, energy utilisation and CO_2 production (Soleimani-Mohseni, Nair and Hasselrot, 2016).

Niemelä, Kosonen and Jokisalo (2017) carried out with IDA ICE an analysis in terms of energy performance and environmental impact of cost-effective retrofitting solutions for a large building in Finland. IDA-ICE has been used dynamic building simulation engine in combination with an optimisation tool developed by the Aalto University. The study investigated over 220 million possible combinations and the results show the effectiveness of heat pump systems in reducing the CO_2 emissions in large multi-families blocks.

A research work was conducted by Liu *et al.* (2014) to investigate the effects of refurbishment interventions on 11 buildings located in a cold region of Sweden (Gävleborg region). Using IDA ICE, the authors studied the impact of three different retrofitting packages (which all include both passive and active energy saving measures) on the performance of the buildings. All the packages presented savings in terms of primary energy consumption and CO_2, the study demonstrate that a 50% CO_2 reduction is feasible in the Gävleborg region especially combining solar or PV panels with new heating systems.

Soleimani-Mohseni, Nair and Hasselrot (2016) investigated the performance of a high rise-high energy efficiency building in countries with very diverse climate, specifically

Sweden, Slovenia (where the original building is located), Croatia and United Arab Emirates. The results from IDA ICE have been evaluated considering the requirements for passive buildings. Simulation outcomes showed that the building has an excess in heating demand when simulated in Sweden whereas the cooling load is too high in the other location. A number of interventions on the building envelope have been evaluated to bring the building toward the passive house standard, the requirements however were only met in the Slovenian climate, different and bespoken intervention need to be investigated for more extreme climates.

Wang, Ploskić and Holmberg (2015) studied the performance of low temperature heating (LTH) in residential buildings in Sweden. The authors analysed the impact of LTH combined with five different retrofitting interventions (improved air tightness, heat recovery in the existent ventilation system, improved fenestration, improved roof insulation, improved wall insulation). IDA ICE highlights that all the five proposed interventions are capable of reducing the primary energy demand by more than 20% while delivering optimal comfort. Furthermore, the combination of all the five interventions, together with the LTH reduce the primary energy demand by 52.8%.

2.6.9. Dymola

The first ideas behind Dymola were developed by Dr Hilding Elmqvist as part of his PhD, in 1996 Dynasim (a company founded by Elmqvist) started the development of a new modelling language (Modelica) which was released in 1999 with Dymola being the first commercial tool to support the new language. In 2006 has been acquired by Dassault Systèmes.

Dymola can be defined as: *"an integrated environment for developing models in the Modelica language and a simulation environment for performing experiments"* (Bruck *et al.*, 2002)

Dymola supports hierarchical object-oriented modelling allowing the description in increasing detail of systems, sub-systems, and components of a model. Numerous libraries of reusable components and composite acausal connectors are available for Dymola covering many engineering fields (Dassault Systèmes AB, 2017).

The software is extremely versatile and nowadays it is used in field like aerospace, industrial equipment, automotive and motorsport, as well as building and energy systems.

As said Dymola is based on the Modelica language, the latter is an equation-based, acausal, object-oriented modelling language designed for component oriented multi-domain modelling of dynamic systems. Modelica thanks to its object-oriented model construction gives the opportunity to expert in different disciplines (e.g., HVAC and controls engineers) to simultaneously develop their respective process interfacing them latter (Wetter and Haugstetter, 2006). All this translate in a reduced development time of the model.

He, Xiong and Shi (2017) developed a model of the renewable energy system of a real world net-zero-energy community located in the USA (Florida). Using Dymola they took advantage of the model reuse to reduce the development time (while also been facilitated in the debugging). The results show a very good matching between the PV power output provided from the simulation and the real output measured in the community. The authors highlight also how the general physical interface in Modelica will allow them to effortlessly connect the developed system to other energy system models.

He *et al.* (2014) carried out a study to evaluate Dymola as a tool for building energy and control system simulation. The authors used components available in the Modelica Standard Library (Modelica Association, 2013) and in the Building library (Wetter, Zuo and Nouidui, 2011). A single zone HVAC system has been built with related control system; the authors showed how Dymola has a problem analysis capacity which goes beyond the possibilities of traditional BEP tool.

Wetter and Haugstetter (2006) have compared Dymola (Modelica) with TRNSYS in building energy modelling. The work focused particularly on the model development time which often dominates the total time spent for the conduction of numerical experiments. The authors achieved a considerable reduction in model development time, with Dymola being 5 to 10 times quicker. The construction of large models is facilitated by the hierarchical architecture which allows the user to reuse sub-models and facilitates debugging. Authors also stated that Dymola is capable of control analysis that are not possible in TRNSYS and even if the HVAC library is larger in TRNSYS the time required for the development is significantly higher than in Modelica.

2.6.10. Software comparison

A number of different building energy modelling software have been reviewed in this chapter, Table 2.3 provides a summary of strengths and weaknesses of each tool. This analysis guided the decision on which tool to use in this research work, the reasons behind the decision are explained in higher detail in paragraph 3.2.

Table 2.3 BEM software comparison

BEM tool	Advantages	Disadvantages
ESP-r	Powerful tool, excellent to simulate new technologies, open source. Extensively validated.	Long learning process, requires a user with high expertise and know-how. Lack of documentation and relatively low diffusion (compared to the other software).
TRNSYS	Very diffused, large library available, already tested in co-simulation works.	Longer model development time compared to other software (up to ten times). Instability problems in some co-simulation works. Better software available for control system development (e.g., Dymola).
EnergyPlus	It is the most diffused tool for energy performance calculation, showed high compatibility with a number of other software, regular updates are released. Already tested in co-simulation.	Not user friendly interface, requires coding skills.
DesignBuilder	GUI for EnergyPlus, vast library available, user friendly interface and compatible with CAD files. Optimisation tool available.	Falls short in terms of building energy systems controls, simulation time might become a problem according to the desired outputs and time steps
IDA ICE	Powerful tool, very detailed building systems simulation, possibility to modify the code behind the different components	Lack of capacity to simulate photovoltaic plants with required accuracy or EES, unfriendly graphic interface, computational time consistently higher than DesignBuilder/EnergyPlus
Dymola	Supports hierarchical object-oriented modelling, large library with reusable components available. Extremely versatile. Already tested in co-simulation. Excellent for control development	Used alone, for the simulation of complicated buildings, could lead to overcomplicated models.

Chapter 3: Methodology

In this thesis the modelling of energy performance of individual residential properties, part of a multi- property case study, will be done using the *Calibrated Simulation approach* (Fumo, 2014). The choice of this approach was based on the lack of real monitored data antecedent the retrofitting (this approach is often used for new building construction).

Models using DesignBuilder and IDA ICE software have been implemented to simulate the case study in pre-refurbishment conditions in order to obtain a baseline in terms of heating demand. The models have been then modified including the retrofitting measures (both active and passive) simulating the post-refurbishment conditions. A first comparison between these models provides the simulated energy savings.

After the interventions were physically installed, the monitored heat consumption from the case study has been compared to the simulated post intervention energy consumption.

Using the monitored data, it has been possible to calibrate the post-retrofitting model, matching the real energy demand. To define the baseline the interventions have been removed from the model, and running it with the physical properties and heating system of the not refurbished case study, has been possible to extract the results in terms of pre-intervention heat demand

The simulation calibration process has been important for the validation of the simulations and the baseline consumption and, furthermore, to understand if differences between the monitored results and the simulated post-retrofit results were acceptable.

3.1. Approach

The simulation process in the case study using the *Calibrated Simulation approach* was as follows:

- Energy simulation of the residential properties was performed using DesignBuilder and IDA ICE software platforms. This procedure aimed to provide an element of verification of the simulation results by comparing data obtained through two different simulation platforms.
- The preliminary simulation showed very close results between the two building energy simulation platforms. The research however has been continued only with DesignBuilder/EnergyPlus for three main reasons:

- - Ease of integration with Dymola to carry out the co-simulation process.
  - Lack of capacity of IDA ICE to simulate photovoltaic plants with required accuracy or EES[4].
  - Consistent difference in terms of simulation time.
- Monitoring data about the heat consumption was collected on site. The monitoring phase is crucial as it provides the values necessary for the calibration and validation process. In this work the thermal energy demand (for both space heating and domestic hot water production) from the different homes has been collected.
- The monitored and simulated data were compared, and the model refined until desired degree of fidelity was achieved. This specific step is the calibration and validation phase and will be discussed in greater detail in Chapter 7:
- After achieving simulation compliance, the retrofitting measures have been removed from the model resulting in reliable simulated baseline consumption. This is another phase of the *Calibrated Simulation approach.* Once the model is calibrated and validated in "refurbished conditions" it is assumed that removing all the modifications (to the building envelope) implemented during the retrofitting work, the model (which still carries the modification applied to temperature set points and heating hours) will provide simulation results representative of the pre-refurbishment condition.
- Co-simulation models have been developed combining two different software platforms: DesignBuilder/EnergyPlus providing the building energy loads, and Dymola simulating the performance of the hybrid energy system. This software combination is meant to take advantage of the strong points of each software to provide a more powerful tool especially from the point of view of the building systems' control.
- The energy savings were defined by comparing the energy results before and after the retrofitting. In this phase the results from the calibrated model running in the co-simulation, and the baseline model (modified as explained above) are compared, assessing the benefits of the retrofitting.

---

[4] This is valid for the release available at the specific time in which the project was carried out, successive releases have not been investigated.

- The co-simulation has been used to develop and analyse different control strategies for the energy system, results have been assessed with different performance indexes.

3.2. Software used

Strengths and weaknesses of a number of BEM (or BPS) tools have been highlighted in Table 2.3, but only three have been used in this research work. They are, as mentioned before, DesignBuilder (a GUI for EnergyPlus), IDA ICE and Dymola. The author decided to not use ESP-r mostly because of the long learning curve, and because the software is not as diffused as other ones taken into account. TRNSYS has been considered, but the literature review showed Dymola to be faster in terms of model developing, and the reported instability in co-simulation works persuaded the author to focus on DesignBuilder, IDA ICE and Dymola The first two have been selected because of the user friendly interface, the large libraries they incorporate and the reliability due to their widespread utilisation. Considering the complexity of the energy system in the case study, and the aim of the research, a more detailed control for the energy system itself was required, the author decided to take advantage of the potentialities offered by the co-simulation technique. As underlined by Nicolai and Paepcke (2017) the utilisation of Dymola/Modelica alone could lead to overcomplicated models, especially when dealing with large buildings with many different zones, which can make the process error-prone. For this reason, is convenient take advantage of the strong points of the different software using a BPS tool like DesignBuilder/EnergyPlus to model and simulate the building while using Dymola/Modelica to simulate the energy system and the adequate control strategies.

Chapter 4: Co-Simulation

Co-simulation represent a technique that allows individual component models described by algebraic or discrete equations to be simulated by different simulation tools running simultaneously and exchanging data during runtime.

Co-simulation is relatively new modelling approach. Cabonare *et al.* (2019) used EnergyPlus and Dymola for a co-simulation tool intended for the optimization of comfort levels in a demand controlled ventilation scheme. Borkowski *et al.* (2016) carried an optimisation study about advanced control strategies for adaptive building skins working with EnergyPlus and Dymola, the object of the investigation was a single room at an office development. Favoino *et al.* (2016) developed a simulation framework to evaluate the control and performance of photovoltachromic switchable glazing using in this case EnergyPlus and MATLAB platforms. A more articulated work was carried out by Yang *et al.* (2018), EnergyPlus and Dymola were used as part of an integrated tool chain to study a new hotel building HAVC system, with lake-source HPs. Other works use different software like NANDRAD (Nicolai and Paepcke, 2017) in combination with Dymola or a Building Control Virtual Test Bed (BCVTB) as a link between Dymola and EnergyPlus (or other similar software) to analyse HVAC systems, especially in terms of effective control (Nouidui and Wetter, 2014). To the best of the authors' knowledge, however, in literature co-simulation models of hybrid energy systems, operating at small district level like the one developed in this research, are not present. By using the software EnergyPlusToFMU developed by Lawrence Berkeley National Laboratory (Lawrence Berkeley National Laboratory, n.d.) a Functional Mock-up Unit (FMU) was created to couple the two software platforms, EnergyPlus and Dymola. This link package is written in Python and allows users to export EnergyPlus as an FMU for co-simulation using the Functional Mock-up Interface. The FMU imported in a software like Dymola will work as a slave to the master software (Modelica/Dymola in this case) and can utilise the interface in a standardised way exchanging data as input and output signals.

Figure 4.1 shows an example where the heat flow defined in the master software is used in the FMU (i.e., in EnergyPlus) to calculate the temperature in a room.
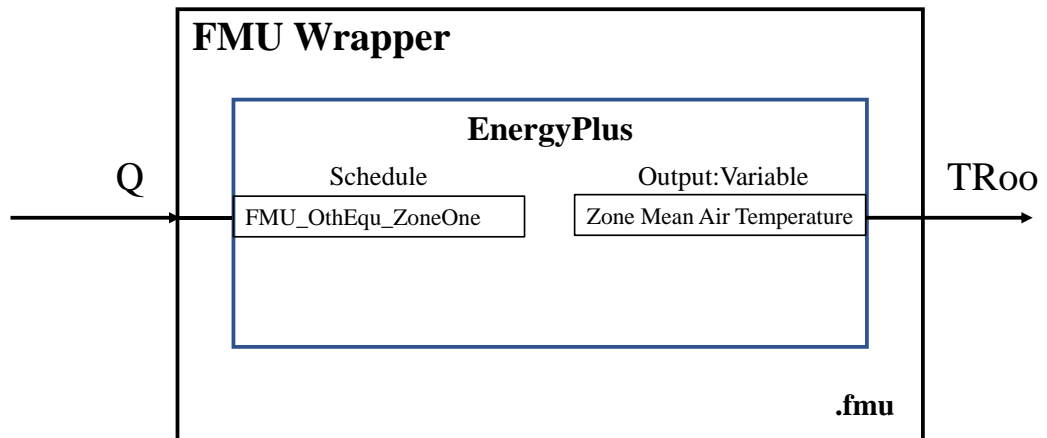
Figure 4.1. FMU example

In this work the co-simulation is used for coupling EnergyPlus and Dymola. The latter works as a master software with EnergyPlus used to simulate the building and its energy demand, and Dymola used to simulate the energy system with all its components.

4.1. FMU generation

Using the FMU block the model developed on EnergyPlus / DesignBuilder was imported in the Dymola environment, creating a co-simulation tool where the building performances in terms of energy demand and losses due to the envelope are simulated in EnergyPlus, whereas the entire energy system and relative control systems are implemented in Dymola (Figure 4.9).

The FMU provides to Dymola the values of:

- weather data,
- building heat demand (as mass flow and temperature required for SH and DHW),
- PV electric energy generation.

Dymola sends back to the FMU the temperature of the low and high heat storage, used to define respectively the temperature of the radiators and DHW supply. Dymola allows the maximum level of freedom in terms of control system and makes very easy to the user to carry on comparative evaluation changing different parameters.

4.1.1. FMU creation and mathematical description

Before analysing the computational steps in the model is worth to describe how the FMU has been created and what unique features were required for this specific study.

The FMU is generated from the EnergyPlus Input Data File (IDF) that EnergyPlus automatically creates after every simulation. The IDF file has been customised by the author to satisfy the specific requirements of this research work.

In the IDF a script representing two fictitious boilers was implemented: one boiler is dedicated to the SH (Figure 4.2) the second to the DHW (Figure 4.3). The idea behind this is to provide these two fictitious boilers with outlet temperature values calculated in Dymola for both the SH and DHW circuits. The mass flow in these two systems will be defined by EnergyPlus itself depending on the temperature value received from Dymola, this means that the heating system simulated in Dymola/Modelica will "de facto" provide the heat for the buildings simulated in EnergyPlus.

```
PlantComponent:TemperatureSource,
    Boiler,                                     !- Name of water component in below loop
    Boiler Water Inlet Node,                    !- Inlet Node
    Boiler Water Outlet Node,                   !- Outlet Node
    Autosize,                                   !- Design Volume Flow Rate
    Scheduled,                                  !- Temperature Specification Type
    10,                                         !- Source Temperature
    Boiler Schedule;                            !- Source Temperature Schedule Name

EXTERNALINTERFACE:FUNCTIONALMOCKUPUNITEXPORT:TO:SCHEDULE,
    Boiler Schedule,                            !- Match the Schedule Name above
    Any Number,
    <Fluid Temp Variable from GSHP>,            !- Variable from Dymola
    0;                                          !- Initial value

SetpointManager:Scheduled,
    HW Loop Setpoint Manager,                   !- Name of Setpoint Manager in the loop
    Temperature,
    Boiler Schedule,                            !- Same schedule as above.
    HW Loop Supply Side Outlet;                 !- Node name
```

Figure 4.2 Fictitious SH boiler loop script

```
PlantComponent:TemperatureSource,
    DHW Loop Water Heater,                      !- Name of water component in below loop
    DHW Loop Water Heater DHW Inlet Node,       !- Inlet Node
    DHW Loop Water Heater DHW Outlet Node,      !- Outlet Node
    Autosize,                                   !- Design Volume Flow Rate
    Scheduled,                                  !- Temperature Specification Type
    10,                                         !- Source Temperature
    DHW Loop Water Heater Schedule;             !- Source Temperature Schedule Name

EXTERNALINTERFACE:FUNCTIONALMOCKUPUNITEXPORT:TO:SCHEDULE,
    DHW Loop Water Heater Schedule,             !- Match the Schedule Name above
    Any Number,
    <Fluid Temp Variable for DHW>,              !- Variable from Dymola
    0;                                          !- Initial value

SetpointManager:Scheduled,
    DHW Loop Setpoint Manager,                  !- Name of Setpoint Manager in the loop
    Temperature,
    DHW Loop Water Heater Schedule,             !- Same schedule as above.
    DHW Loop Supply Side Outlet;                !- Node name
```

Figure 4.3 Fictitious DHW boiler loop script

The first part of the script (Plant Component Temperature Source) defines the pseudo-loop, specifically the mock source of fluid. A number of different parameters are specified

in this script. The first three lines define the heat source, "Boiler" and "DHW Loop Water Heater" for SH and DHW loop respectively, and the related inlet and outlet.

The following parameter is named "Design Volume Flow Rate", as displayed in both Figure 4.2 and Figure 4.3 this factor is set to *Autosize*. With this set up the mass flow in the SH loop and DHW loop is calculated by EnergyPlus itself accordingly to the heat requirement and the temperature of the flow. In section 6.5 will be explained how this value is exported and used in Dymola. The "Temperature Specification Type" identifies how the fluid temperature is defined, being set to *Scheduled* it will have the value specified by the "Name of Setpoint Manager in the loop" in the third part of the script in Figure 4.2 and Figure 4.3. In this same part of the script the name of the variable that carries the temperature value are indicated, and the node to which it applies, *HW Loop Supply Side Outlet* and *DHW Loop Supply Side Outlet* respectively. These nodes, as represented in DesignBuilder are highlighted in Figure 4.4 and Figure 4.5, the nodes are the points in the loop in which the temperature calculated in Dymola is applied to the EnergyPlus model. To do so an interface between the two software is required, this is defined in the second part of the script (EXTERNALINTERFACE: FUNCTIONALMOCKUPUNITEXPORT:TO:SCHEDULE). The port from which the temperature for the SH loop is imported is called *<Fluid Temp Variable from GSHP>*, whereas the one for the DHW is *<Fluid Temp Variable for DHW>*.The two ports are visible in Figure 4.8**.** When the co-simulation is running the temperature source (i.e., the *Boiler* and the *DHW Loop Water Heater*) will provide water at the specified temperature at these points.

HW Loop Supply Side Outlet
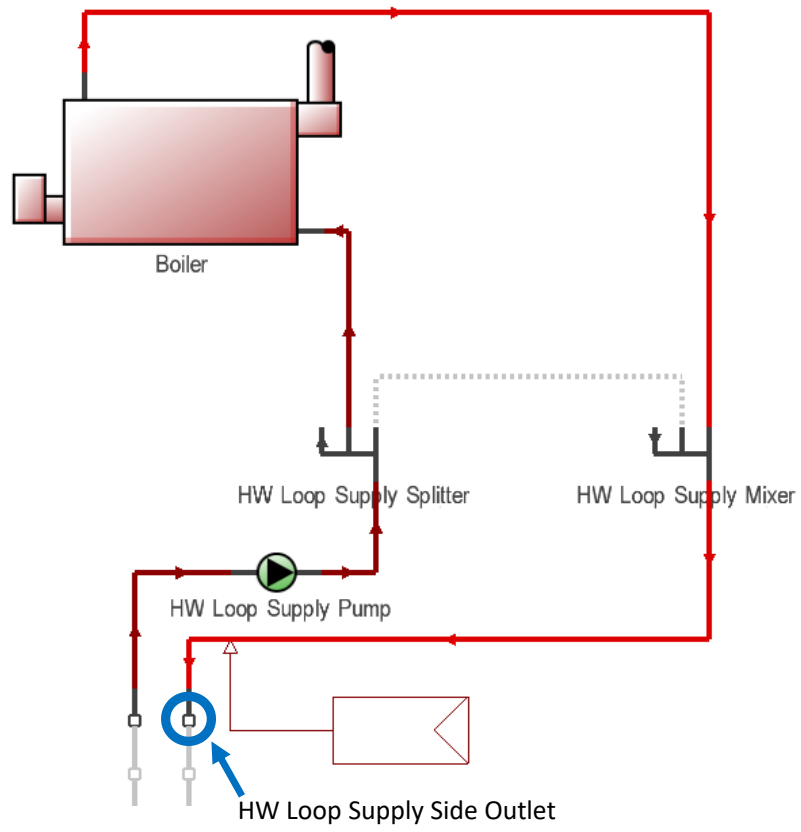
Figure 4.4 Space Heating loop

DHW Loop Supply Side Outlet
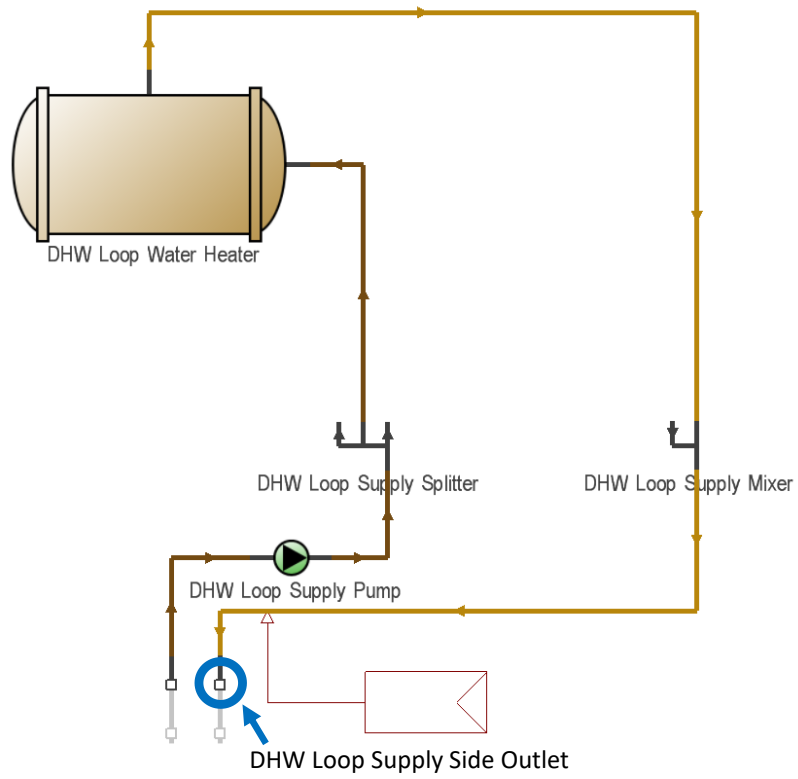
Figure 4.5 Domestic Hot Water supply loop

```
ExternalInterface:FunctionalMockupUnitExport:From:Variable,
    Boiler Water Outlet Node,                                    !- Output:Variable Index Key Name
    System node temperature,                                     !- Output:Variable Name
    Boiler_Water_Outlet_Temp;                                    !- FMU Variable Name

ExternalInterface:FunctionalMockupUnitExport:From:Variable,
    Boiler Water Inlet Node,                                     !- Output:Variable Index Key Name
    System node temperature,                                     !- Output:Variable Name
    Boiler_Water_IN_Temp;                                        !- FMU Variable Name

ExternalInterface:FunctionalMockupUnitExport:From:Variable,
    Boiler Water Outlet Node,                                    !- Output:Variable Index Key Name
    System Node Mass Flow Rate,                                  !- Output:Variable Name
    Boiler_Water_Outlet_Flow;                                    !- FMU Variable Name

ExternalInterface:FunctionalMockupUnitExport:From:Variable,
    DHW Loop Water Heater DHW Inlet Node,                        !- Output:Variable Index Key Name
    System node temperature,                                     !- Output:Variable Name
    DHW_Water_Inlet_Temp;                                        !- FMU Variable Name

ExternalInterface:FunctionalMockupUnitExport:From:Variable,
    DHW Loop Water Heater DHW Outlet Node,                       !- Output:Variable Index Key Name
    System node temperature,                                     !- Output:Variable Name
    DHW_Water_Outlet_Temp;                                       !- FMU Variable Name

ExternalInterface:FunctionalMockupUnitExport:From:Variable,
    DHW Loop Water Heater DHW Outlet Node,                       !- Output:Variable Index Key Name
    System Node Mass Flow Rate,                                  !- Output:Variable Name
    DHW_Water_Outlet_FlowRate;                                   !- FMU Variable Name

ExternalInterface:FunctionalMockupUnitExport:From:Variable,
Environment,                                                     !- Output:Variable Index Key Name
    Site Outdoor Air Drybulb Temperature, timestep;             !- Output:Variable Name
    T_out_drybulb_temp;                                          !- FMU Variable Name

ExternalInterface:FunctionalMockupUnitExport:From:Variable,
    Whole Building,                                              !- Output:Variable Index Key Name
    Facility Total Produced Electric Energy,                     !- Output:Variable Name
    PV_El;                                                       !- FMU Variable Name

ExternalInterface:FunctionalMockupUnitExport:From:Variable,
    Whole Building,                                              !- Output:Variable Index Key Name
    Facility Total Building Electric Demand Power,               !- Output:Variable Name
    El_power;                                                    !- FMU Variable Name
```

Figure 4.6 External interfaces as defined in the IDF file

To allow a two-way communication between the FMU and Dymola, setting up of a so called "External Interface" is required. Examples of external interfaces are the already discussed ports to import the temperature signal from Dymola to EnergyPlus. Other interfaces are required to export the required values from EnergyPlus to Dymola. Specific scripts have been created to export each variable (Figure 4.6) generating ports to export the following parameters:

- SH boiler outlet temperature (*Boiler_Water_Outlet_Temp*) expressed in °C

- SH boiler temperature (*Boiler_Water_IN_Temp*) expressed in °C

- SH boiler mass flow (*Boiler_Water_Outlet_Flow*) expressed in kg/s

- DHW boiler outlet temperature (*DHW_Water_Outlet_Temp*) expressed in °C

- DHW boiler temperature (*DHW_Water_Inlet_Temp*) expressed in °C

- DHW boiler mass flow (*DHW_Water_Outlet_FlowRate*) expressed in kg/s

- Outdoor air-dry bulb temperature (*T_out_drybulb_temp*) expressed in °C

- Facility electric power demand (El_power) expressed in Watt

- Electricity produced by the PV roof (*PV_El*) expressed in Joule

Other interfaces (providing the reading for parameters like temperature in different rooms) where implemented to provide a real time verification of the functioning of the systems. These external interfaces are not necessary for the model to operate but are an important aid for the user, an example is displayed in Figure 4.7.

```
ExternalInterface:FunctionalMockupUnitExport:From:Variable,
    N32FrontFirstFloor:Lounge,                          !- Output:Variable Index Key Name
    Zone Operative Temperature,                          !- Output:Variable Name
    Lounge32_OP_TEMP;                                    !- FMU Variable Name

ExternalInterface:FunctionalMockupUnitExport:From:Variable,
    N28FrontSecondFloor:Bedroom,                         !- Output:Variable Index Key Name
    Zone Operative Temperature,                          !- Output:Variable Name
    Bedroom28_OP_TEMP;                                   !- FMU Variable Name
```

Figure 4.7 External interfaces for room temperatures

Once finalised the IDF has been converted to FMU using both EnergyPlusToFMU package and Python interpreter. The FMU as visible in Dymola is showed in Figure 4.8.
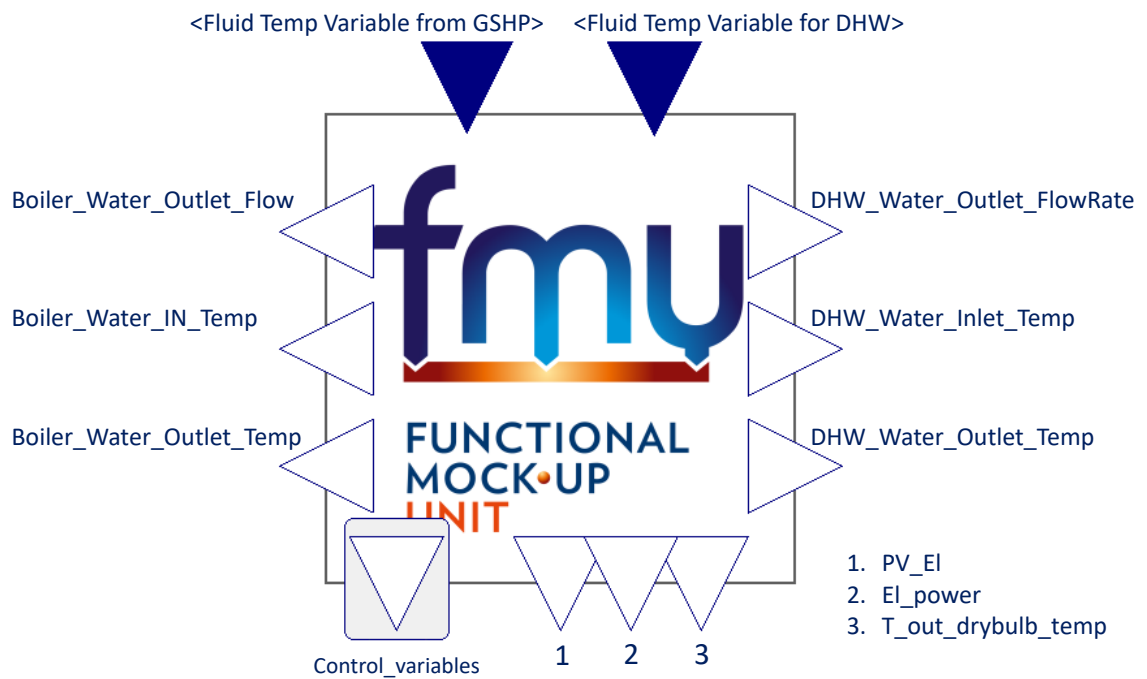
Figure 4.8 FMU block (variable names at the bottom have been replaced with numbers to help the reader)

At this point Energy Plus, as the slave programme {1}, is packaged in the FMU for co-simulation and Dymola as a master programme {2} supports the import of the FMU for co-simulation. Each programme solves initial value ordinary differential equations that are coupled through the FMU to the differential equations of the other programme. When for a general step (k) EnergyPlus computes the sequence:

$$(x\{1\}(k+1) = f\{1\}(x\{1\}(k), x\{2\}(k)) \qquad \text{Eq. 4-1}$$

Dymola similarly computes the sequence:

$$(x\{2\}(k+1) = f\{2\}(x\{2\}(k), x\{1\}(k)) \qquad \text{Eq. 4-2}$$

With initial conditions:

$$(x\{1\}(k=0) = x\{1,0\}) \qquad \text{Eq. 4-3}$$

and

$$(x\{2\}(k=0) = x\{2,0\}) \qquad \text{Eq. 4-4}$$

To advance from time step (k) to the next time step (k+1) each of the two programmes uses its own integration algorithm. At the end of the time step Energy plus {1} sends its new state x{1}(k+1) to Dymola {2} and receive from Dymola the state x{2}(k+1).

Dymola as the master of the two simulation programmes imports the FMU and manages the data exchange between the two programmes. As a procedure this co-simulation scheme is equal to an Explicit Euler integration scheme (Virgin, 2019).

4.1.2. Computational steps

In Figure 4.9 is possible to see a schematic representation of the co-simulation tool with the data flow between the different blocks. In the energy system block present six sub-systems are present. The subsystems represent (clockwise order) the control system, the heat pumps, the thermal energy storages, the boreholes and the battery block that is comprehensive of its own battery control system.
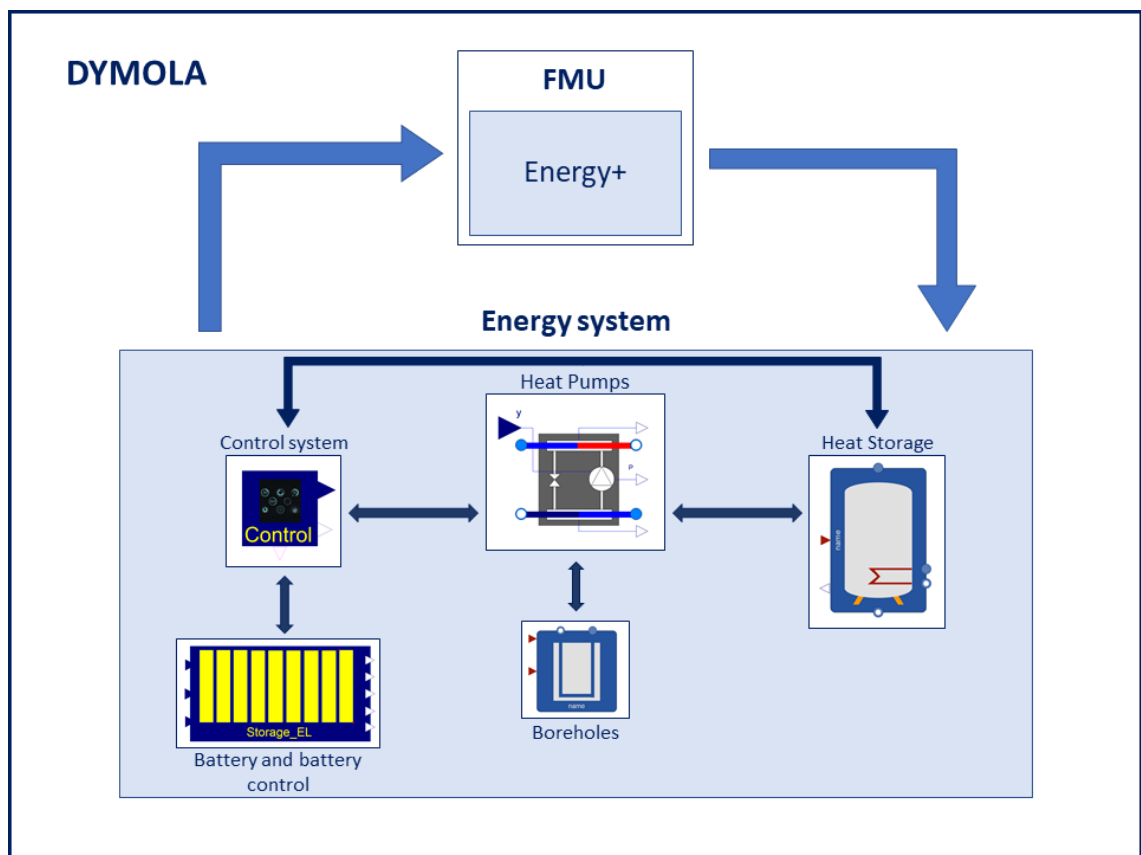
Figure 4.9. Co-simulation model scheme

As an explicit integration scheme sufficient number of steps needs to be used to maintain stability of the solution.

The simulation is dynamic, and the values are elaborated simultaneously with steps of 900 seconds (15 minutes). In each step all the following processes take place.

- The heat demand for SH and DHW (defined as the value of mass flow and return temperature of the water in the SH and DHW circuits) is sent by the FMU to the TESs (two TES are present, one for SH and one for DHW) defining the temperature and mass flow at the inlet of the heat exchanger at the top of the two TES.

- Temperature sensors are present at the outlet of the heat exchanger in each TES, the signals from these sensors are sent back to the FMU defining the temperature of the water that the two fictitious boilers send to SH and DHW circuits.

- HPs with their control system are also connected to the TESs. Depending on the temperature and the hour of the day the control system sends an on/off signal to the HPs keeping the TESs temperature within a range specified by the user. The same control system operates the pumps in the hydraulic systems between the boreholes and HPs and between HPs and TES.

- The FMU also provides the value of the PV energy production and the electricity consumption of the buildings. These two values, together with the electricity demand from the heat pumps are the input of the "battery and battery control" block. The control logic directly implemented into the battery control block manage the battery circuit and simulate different control strategies taking into account numerous constrains like the state of charge of the battery, the power required by the HP, the power supplied by the PV panels and the power demand of the buildings.

At this stage, in the control of the energy system, co-simulation shows all its usefulness, the number of parameters that is possible to control and the level of detail are one step ahead compared to a standard BPS tool, which on the other hand is still very useful when it comes to apply modification in terms of building envelope or occupant behaviour.

Chapter 5: Case Study: West Walk development

5.1. Location and climate

The case study is located in Nottingham (United Kingdom), the city has a warm and temperate climate with an average yearly rainfall of 648 mm. In the Koppen-Geiger climate classification Nottingham falls under the Cfb category (Temperate oceanic climate, Figure 5.1) with no dry season and warm summer. The driest month of the year is February with an average of 46 mm while August with 60 mm has the highest average rainfall. In terms of temperature July and January are respectively the warmer and colder months of the year with an average temperature of 17.2 °C in July and 2.9 °C in January, the average annual temperature stands at 9.8 °C.
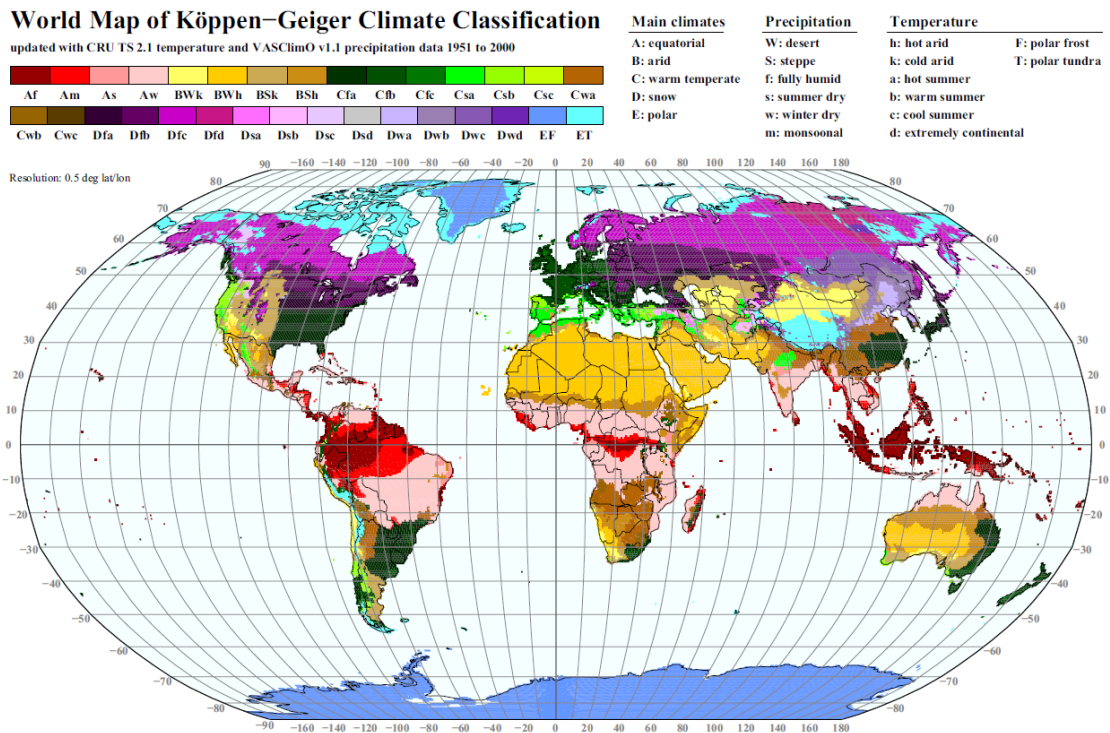
Figure 5.1 Köppen−Geiger Climate Classification (Kottek et al., 2006)

Due to the position (Latitude: 52°58'12"N and Longitude: 1°10'48"W) the Sun's location changes consistently during the year, the Sun is at its highest on June 21st (60.4°) and at its lowest on December 21st (13.5°), this factor has a consistent effect on the solar energy available in the different months of the year.

5.2. Pre-refurbishment conditions

The initial case study was a small cluster of thirteen houses in Sneinton, Nottingham, built in the 1960s, nine of them are terraced William Moss houses (Michelle, Ianakiev and García-fuentes, 2017) and four are bungalows (Figure 5.2 and Figure 5.3[5]).

Figure 5.2 Satellite view of the initial case study (Already subjected to refurbishment)

---

[5] Refurbishment work started before the beginning of the PhD therefore a full picture of the site before the retrofitting intervention is not available)

Figure 5.3 Case study during the refurbishment work

Every terraced home includes a kitchen, two bedrooms, a toilet, a bathroom and a lounge, all connected by a staircase (Figure 5.4). The bungalows on the other hand are divided in hall (circulation zone), kitchen, bathroom, bedroom, and lounge (Figure 5.8).

5.2.1. Main block building envelope
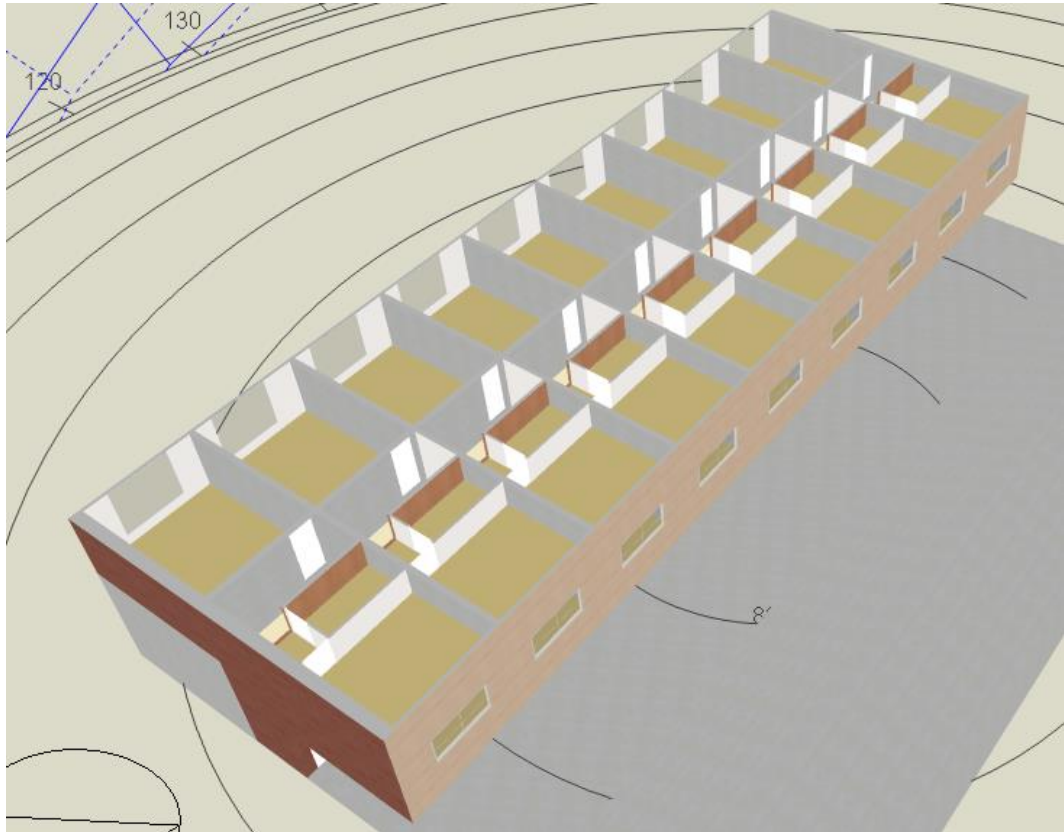
Figure 5.4. Section of the main block from DesignBuilder

The main building has raft foundation and load bearing precast concrete panels which work also as separation between the different terraced houses. Storey-height infill timber frame panels were fixed between the precast panels, and tiles hung on timber battens. The external walls were originally specified with glass fibre insulation within the timber panels, the insulation however is in very poor conditions slumped or affected by damp. The end walls are cladded with bricks, the roof is covered in bitumen tiles, with an asymmetrical section, a vertical element (facing west) cladded with cooper is present and visible in the top part of Figure 5.5 (Michelle, Ianakiev and García-fuentes, 2017).

Figure 5.5 End terrace wall pre-refurbishment

The two end terrace walls (Figure 5.5) have the stratigraphy listed in Table 5.1 (starting from the outside layer):

Table 5.1 End-terrace walls stratigraphy

Material	Thickness (mm)	Thermal Conductivity λ (W/mK)
Brick wall	120	0.72
Air gap	50	R=0.18 (m²K/W)
EPS	25	0.04
Pre-casted concrete	170	2.5

The resultant U value however is theoretical because of the poor conditions of the EPS layer; but for simulation purposes this theoretical U value will be used, putting the simulation in a conservative position. A pre-casted steel reinforced concrete wall (170 mm thick) which goes from the ground up to the roof separates the different homes. This wall has no insulation so there is a consistent heat flow between the different homes. The front and back facades are built with timber frames filled with a glass wool insulation as in Table 5.2:

Table 5.2 Facades stratigraphy

Material	Thickness (mm)	Thermal Conductivity λ (W/mK)
Weatherboard	10	0.14
Glass wool	90	0.04
Plasterboard	10	0.25

The U value of the façade wall is an approximation too, there are indeed several thermal bridges, because of the wooden frame and the concrete separation wall additionally, as mentioned, the build quality is low, the insulation does not cover all the space inside the timber frame, leaving several empty gaps which contribute to decrease the overall U value of the façade.

Figure 5.6. Back of the building before the refurbishment

It is important to underline that the entrances to the different homes are in a porch that runs under the first floor of the building. In this zone the floor of the first-floor rooms (i.e., the kitchens) directly faces the outside affecting the energy performances of the building. The floor of every kitchen indeed is poorly insulated, the space between the joists is filled with glass wool, but also in this case there are several gaps and spaces without insulation. For simulation purposes, the stratigraphy considered is the following:

Table 5.3 External floor

Material	Thickness (mm)	Thermal Conductivity λ (W/mK)
Chipboard	15	0.15
Wooden frame	150	R=0.3150 (m²K/W)
Glass wool	50	0.04
Chipboard	10	0.15

The ground floor in the storeroom (facing the ground) is assumed as concrete 100 mm thick. The store-rooms are on the backside of the building, they are basically open spaces, considering that they are closed just with wood boards installed by the tenants. This means that the floor of the room above them (the living room in every home) is facing temperatures almost equals to the external ones. This causes consistent heat losses because the floor of the living rooms is made by simple wooden joists without any insulation. The facade at the ground level under the porch is composed by a brick wall (120 mm thick) and a wooden frame covered with plasterboard, no insulation is present, its stratigraphy is showed in Table 5.4.

Table 5.4 Ground floor façade

Material	Thickness (mm)	Thermal Conductivity (W/mK)
Brick wall	120	0.72
Air gap	170	R=0.18 (m²K/W)
Plasterboard	10	0.25

All the internal walls are dry walls 70 mm thick, except for the wall between the stairs and the rooms facing the backyard which is a concrete wall 100 mm thick. The pitched

roof of the building is covered with bitumen tiles and has a very thin insulation (roughly 30 mm of glass wool).
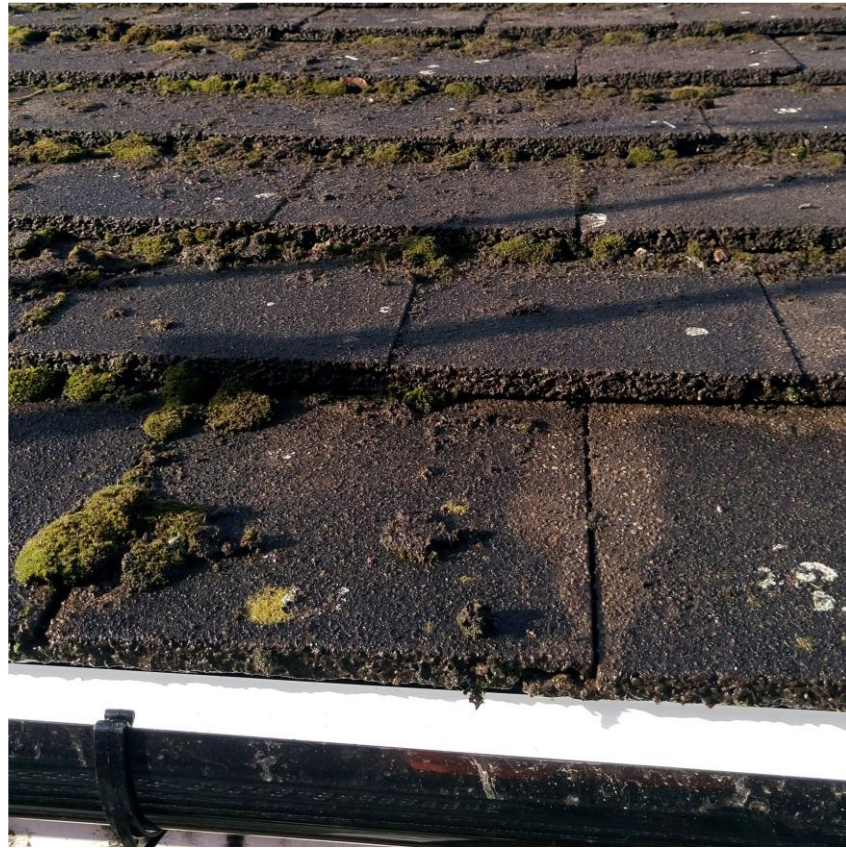
Figure 5.7 Bitumen tiles on the main building

The space under the roof is empty and non-heated. The floor of the under roof space is covered with a layer of glass wool with very variable thickness. The insulation is not only uneven, but massive gaps (in same cases more than 0.7 m) between the insulation and the external walls are present too, in one home the insulation is totally absent. Figure 5.10, which shows the insulation in the loft of one of the bungalows provides a better understanding of the general poor conditions of the buildings. To represent this complex situation in the model assumptions had to be made, therefore a 100 mm thick layer of mineral wool between the joists has been considered, with plasterboard on the bottom. This assumption puts the model in a conservative position.

5.2.2. Bungalows building envelope

As mentioned, the bungalows are divided into four rooms, kitchen, bathroom, bedroom, and lounge, plus a hall/circulation zone (Figure 5.8).
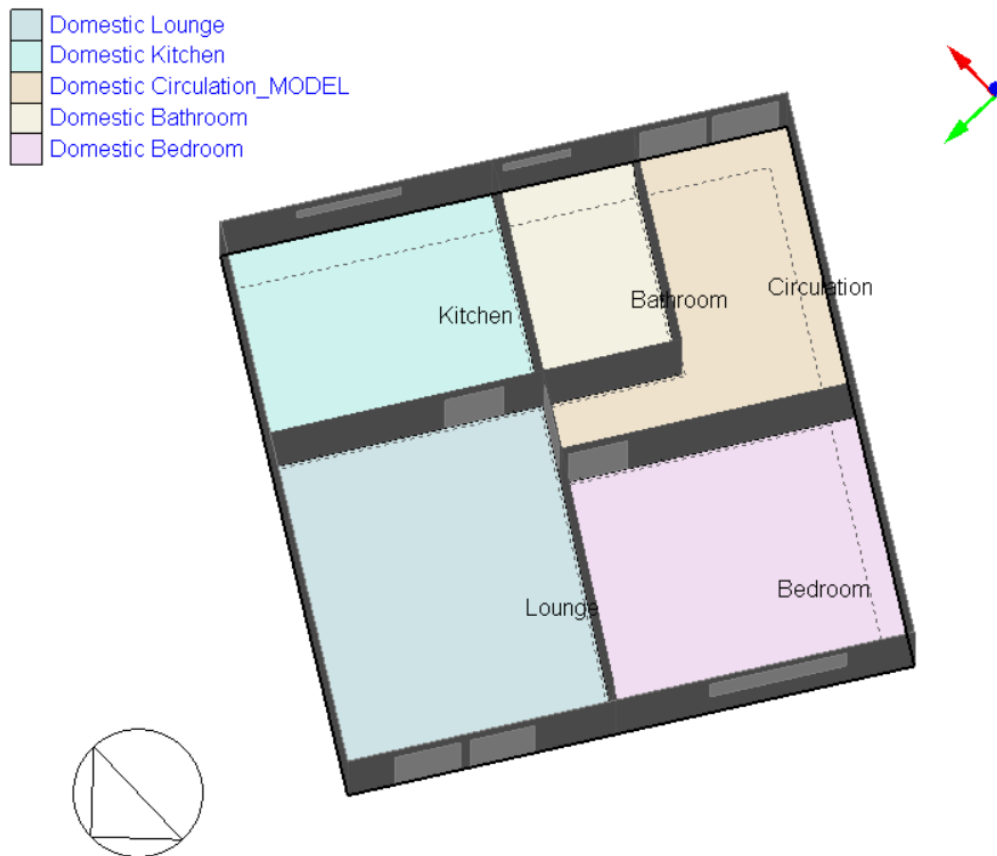
Figure 5.8 Bungalow floor plan from Design Builder

As the main building the bungalows too have raft foundations and load bearing precast concrete panels which work also as separation between the different apartments. On the other hand, the rear and front façade show a different construction compared to the main building. The bungalows facade facing the main building was built as a single concrete wall 170 mm thick (external wall of hall, kitchen and bathroom), whereas the facade facing the street (external walls of bedroom and lounge visible in Figure 5.9) had a wooden structure filled with 90 mm of glass wool (layers in Table 5.5)

Table 5.5 Bungalows' façade facing the main road

Material	Thickness (mm)	Thermal Conductivity λ (W/mK)
Weatherboard	10	0.14
Glass wool	90	0.04
Plasterboard	10	0.25
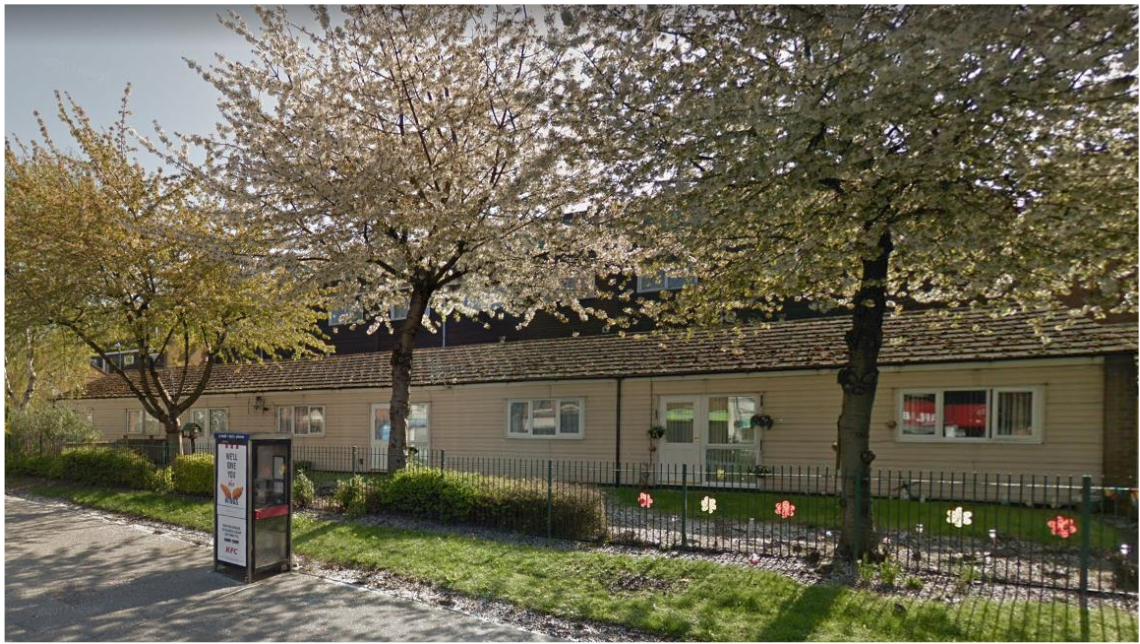
Figure 5.9 Bungalows pre-retrofitting

Figure 5.10 Loft insulation in one of the bungalows

5.2.3. Windows and ventilation

Essential part of the building envelope are the windows, the building comes with double glazed UPVC windows, the glazes are 3 mm thick whereas the air gap is 6 mm. The building envelope is leaky, the result of the blower door test is 8.74 m³/(m²hr)@50Pa, this value may seem good, but it is important to consider that two walls of each homes are made in solid concrete, so all the leaks are concentrated in the front and back façade. The ventilation values considered (Table 5.6) are the ones suggested by The Chartered Institution of Building Services Engineers (CIBSE) Guide A and by the Approved Document F: ventilation (2010 edition incorporating 2010 and 2013 amendments) (CIBSE, 2006)(HM Government, 2013).

Table 5.6 Ventilation values

Room	Supplied air rate (l/s)	Supplied air rate (ac/h)
Kitchen	13	
Toilet		>5 (5.1)
Bathroom	8	
Bedrooms		0.8
Living areas		0.8
Stairs		0.5

5.2.4. Pre-refurbishment heating system

Before refurbishment every house was provided with a 28 kW gas combi boiler (Baxi Duo-tec Combi 28 HE) responsible for the production of domestic hot water (DHW) and for space heating (SH) of the house itself. Radiators, fed with a double string system, are present in every room except the toilet, dimensions of the different radiators are specified in Table 5.7.

Table 5.7 Radiators dimensions

Room	Width (m)	Height (m)
Stairs	0.95	0.60
Kitchen	1.10	0.60
Bedroom1	1.10	0.60
Lounge	1.75	0.60
Garden room	1.20	0.60
Bathroom	0.65	0.60
Bedroom 2	1.10	0.60

5.3. Post-Refurbishment

5.3.1. Building envelope

The refurbishing of the building has been carried out following the "Energiesprong" (Energiesprong Foundation, n.d.) approach, only seven of the nine houses and three out of four bungalows, own by the local housing provider have been refurbished. The privately-owned middle terrace home, one of the end-terrace homes and one of the

bungalows, remain in the pre-refurbishment conditions due to the existing financial restrictions; this brings the total of the retrofitted homes to 10. The Energiesprong approach is based on the utilization of prefabricated components, so the building facades have been covered with an external wall, the end terrace walls have been refurbished and the building has now a new rooftop which incorporates a photovoltaic (PV) plant. The new façade wall, applied directly over the old one, helps to eradicate the thermal bridges and increase substantially the insulation level of the building. In Table 5.8 is reported the stratigraphy of the new external wall applied on the old one.

Table 5.8. External insulation added on the old facades

Material	Thickness (mm)	Thermal Conductivity λ (W/mK)
Weatherboard	10	0.14
Air gap	50	R=0.18 (m²K/W)
Chipboard	10	0.15
Glass wool	200	0.04
Vapour barrier	-	-
Air gap	40	R=0.18 (m²K/W)
Chipboard	10	0.15

The refurbishment of the end terrace wall consisted of polyurethane insufflation foam placed into the cavity between the external brick and the internal concrete load-bearing wall, replacing the air gap and the old EPS insulation. The roof renovations consist of a new glass wool insulation layer placed on top of the old one in this way covering also parts that were not insulated before. The total thickness of the glass wool insulation layers is now 270 mm.

Figure 5.11 Case study after the refurbishment intervention

A new room has been added to each home by converting the external store into a garden room/new living room (the new façade wall has been installed as a front wall). Another intervention on the building envelope has been the application of a 200 mm thick glass wool external insulation on the ground floor wall and a 150 mm one on the kitchen floor. The external wall/cladding is offset manufactured and installed in a single step operation (Figure 5.12).

The bungalows facades have been cladded with a new pre-fabricated module similar (but not identical) to the one used in the main building; the module consists of the layers in Table 5.9. Bungalow's roof, unlike the one in the main building was not retrofitted increasing the insulation layer on the loft. On the contrary a new pitched roof was installed, the new roof has a 250 mm mineral wool insulation and, on the side opposite the main building, PV panels incorporated in the structure (the side facing the main block is covered with tiles). The different layers are listed in Table 5.10.

Table 5.9 Bungalow added insulation

Material	Thickness (mm)	Thermal Conductivity λ (W/mK)
Weatherboard	10	0.14
Air gap	38	R=0.18 (m²K/W)
Chipboard	10	0.15
Mineral wool	190	0.035
Chipboard	10	0.15
Vapour barrier	-	-
Air gap (against old façade)	50	R=0.18 (m²K/W)

Figure 5.12. Installation of a prefabricated façade module

Table 5.10 Bungalow roof post-retrofitting

Table 5.10 Bungalow roof post-retrofitting

Material	Thickness (mm)	Thermal Conductivity λ (W/mK)
Tiles	6	0.85
Air layer (non-ventilated)	85	R=0.16 (m²K/W)
Mineral wool	250	0.035
Chipboard	10	0.15

The work on the building envelope has reduced the infiltration value to 6 m³/(m²hr)@50Pa. The value of air changes to living rooms and bedrooms is now 0.5 ac/h (so in the lower band of the values suggested by CIBSE), is possible to presume that the thermal bridges have been almost completely eradicated (this reduces the risk of mould). The radiators in the retrofitted houses have not been changed, it is assumed that by improving the building fabric after the refurbishment work, the energy consumption will be substantially reduced, and the old heating elements will be able to provide necessary heat. New double-glazed windows with 6-20-6 low emissivity glazing and Argon filling have been installed (Figure 5.13).

Figure 5.13. Back façade of the building after the retrofitting

5.3.2. Heating system

The heating system has been completely changed, the gas boilers have been removed and replaced by completely new, advanced, low temperature heating system. The system includes ground source heat pumps, thermal energy storage (TES), and electric energy

storage. The block now is configured as a micro low temperature district heating (LTDH) network.

The heat in the system is generated by two different GSHPs with a total thermal power of 32.4 kW. One of the GSHPs is used to heat the water up to 55°C the second can, if necessary, heat the water up to 65°C. The GSHPs are connected to 5 boreholes 130 m deep, and they have a COP of respectively 4.15 and 4.16 (B0/W35 ΔT 5 K EN 14511) (British Standards Institution, 2018). The thermal storage is composed by two hot water tanks with a total capacity of 4 m³ (Figure 5.15), the EES on the other hand is a battery rack with a capacity of 36 kWh (initially 20 kWh were installed). The hot water runs in pipes that have been attached to the old building and then covered with the new building fabric, this means that they are de facto inside the building envelope (Figure 5.14.) The water is supplied to the radiators at temperatures in a range between 44 and 48°C.

Figure 5.14 Piping before being covered with the new insulation layer

Figure 5.15. Solar roof and heat storage

5.4. Case study further developments

The initial case study underwent an expansion process during the duration of this PhD, the number of refurbished homes increased from 10 to 27 and, consequently, the centralised heating system was revamped.

The new homes subject to refurbishment are the same type as the ones in the initial case study, specifically another block with 9 terraced houses (also in this case only 7 have been refurbished) and 10 more bungalows. In Figure 5.16 the buildings subjected to refurbishment are highlighted in blue and the centralised energy centre in red. clear that when the picture was taken not all the retrofit interventions were completed.

Figure 5.16. Final case study satellite view
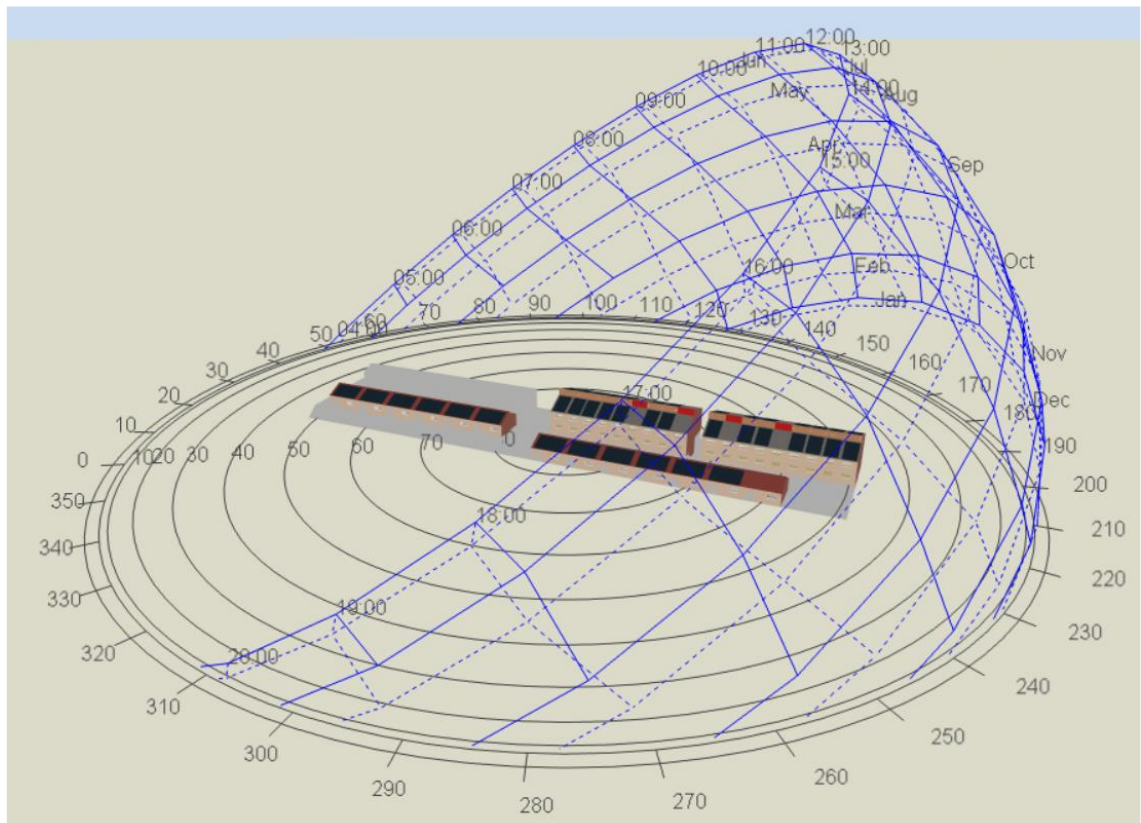
Figure 5.17 Site view from the DesignBuilder visualiser function with the sun path in the different months of the year
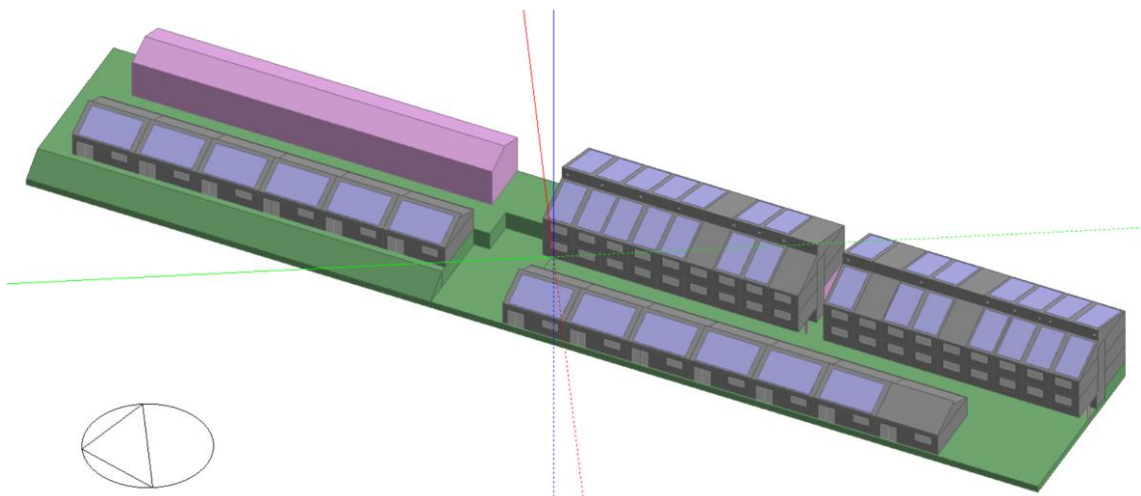
Figure 5.18 Site view from the DesignBuilder modelling tab

Figure 5.17 and Figure 5.18 show the DesignBuilder visualisation of the site, with 4 non refurbished properties within the two blocks and also one bungalow, where, even after the retrofit intervention, the PV has not been installed due to the shadowing produced by nearby trees.

As it was mentioned the initial centralised heating system was composed of two heat pumps for a total of 32.4 kW$_{th}$. After the expansion a more powerful system was required

to satisfy the increased heat demand. The new heating systems consist of 3 GSHPs with a thermal output of 41.4 kW$_{th}$ (with B0/W55 ΔT 8 K) each for a total combined power of 124.2 kW$_{th}$. The new GSHPs have a 4.4 CoP (B0/W35 ΔT 5 K EN 14511) or 3.2 CoP (B0/W55 ΔT 8 EN 14511) (British Standards Institution, 2018).

New boreholes set for a total of 19 (including the already existing 5) have been drilled (Figure 5.19) in order to provide a proper heat exchange surface for the bigger HP evaporator circuit. The heat storage system capacity has been increased too, and now has a total capacity of 12 m³ (12000 litres) while the EES has an enhanced capacity of 40 kWh.

Figure 5.19 Borehole drilling

Chapter 6: Simulation work

As described in Chapter 2: several different Building Performance Simulation tools are available. In this work two different BPS software have been used, DesignBuilder and IDA ICE. The latter as only been used in the initial phase of the research work which has been completed using only DesignBuilder/EnergyPlus and Dymola. The reasons for this decision are mainly three:

- Easier integration of EnergyPlus with Dymola to carry out the co-simulation process.
- Lack of capacity of IDA ICE to simulate photovoltaic plants with required accuracy or EES[6].
- A consistent difference in terms of simulation time has also been observed.

Nevertheless, the simulation work with IDA ICE has been part of the PhD and for completeness the results of the simulations will be presented in *APPENDIX I*

The first step during the generation of any energy model is to provide data on the building (or buildings) under analysis. The model creation phase can be divided in the following steps (Figure 6.1):

Location selection	Model creation (building geometry)	Type of building and activity selection	Building construction definition	Building systems definition
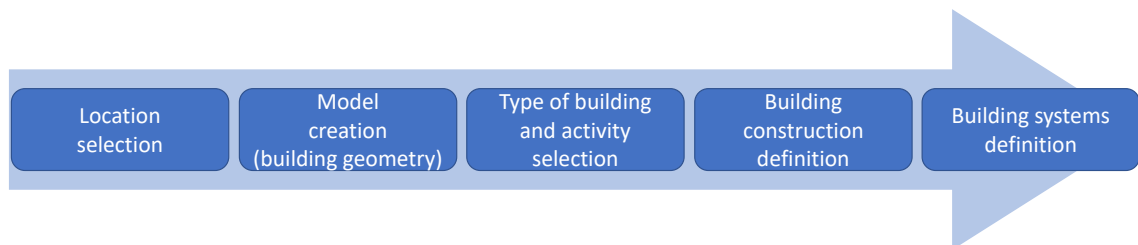
Figure 6.1 Model generation steps

6.1. DesignBuilder model

6.2. Model creation

The construction of the model in DesignBuilder followed the already discussed steps for the generation of an energy simulation model. It is important to note that different models of both pre and post-refurbishment case study have been developed:

---

[6] This is valid for the release available at the specific time in which the project was carried out, successive releases have not been investigated

1. A first set of models including only the main block, in addition to the pre-refurbishment model a set of three post-retrofitting models have been created analysing a number of scenarios that will be discussed in the results.
2. A second set of models including the entire initial case study (main block and 4 bungalows) with 10 refurbished homes (7 terraced houses from the main block plus 3 bungalows).
3. A final model had been created to include the entire 27 homes of the expanded case study.

The latest two, the model with 10 homes, and the one with 27 homes (both with the case study in post-refurbishment configuration) have been developed to be used in the co-simulation process.

6.2.1. Location selection

DesignBuilder offers several weather files for various locations around the world. These files (.epw format) contain the climate data for the chosen location; being the case study located in Sneinton the weather file for Nottingham/Watnall has been selected. The file comes from the International Weather for Energy Calculations (IWEC) database. The data is made up of hourly data collected over a period of up to 18 years (generally 1982-1999). The decision of using standardised weather data was due to the fact that the simulation work and the refurbishment work have been carried out in parallel for a long period, considering this, there was not availability for measured weather data. Furthermore the expansion of the case study caused the necessity of developing the model in other to take into account the new homes added to the case study as well as the new energy centre. Again the work on the case study and the model (and co-simulation model) development was carried out in parallel, considering the utilisation of the weather file provided by DesignBuilder in the first model the decision of carrying out the entire PhD using the same file was taken. Firstly for consistency reasons and also because the focus of the research was on the development of the co-simulation tool. Furthermore, in loco there was not a measuring system capable of providing all the data necessary to replace the file form the IWEC database. This means that measured weather data should have been obtained from third parties. However it is possible to make a comparison between

the weather data provided by DesignBuilder and measured data in terms of Heating Degree-Day[7] (HDD).

Table 6.1 HDD from measured data and from IWEC database

Month	HDD measured	HDD IWEC database
November	329	355
December	377	414
January	450	449
February	340	407

Table 6.1 includes a comparison between the HDD from the IWEC database used for the PhD work, and the HDD from measured data. Is possible to see how the IWEC database generally provides an higher number of HDD. This fact is reflected in the validation process in Chapter 7: , specifically, this is one of the reasons (among the others reported in the aforementioned chapter) which made necessary reducing the number of weekly heating hours in the model during the calibration/validation process.

6.2.2. Model creation (building geometry)

DesignBuilder is an extremely user friendly software when it comes to the definition of the building geometry, it offers the opportunity to import the building geometry from different software such as CAD (Computer Aided Design) and BIM (Building Information Modelling) software. In this case study however, no floor plans of the buildings were available, and dimensions and construction characteristics have been defined through site surveys. The data gathered from these surveys has been used to reproduce the case study in DesignBuilder manually drawing the building in three dimensions. The model has been created in order to have a modularity in the geometry and to make possible future scale ups of the model, this decision was taken at the very beginning of the PhD and, even if it led to a higher complexity in terms of geometry, it showed all its usefulness when the case study was expanded.

In the main block every single floor was built individually (Figure 6.2), consequently every single terraced house includes seven blocks, four blocks for the lived areas, one stairwell block and one block representing the roof/loft. The bungalow on the other hand

---

[7] Heating Degree-Day data is available on www.degreedays.net

have been divided in two blocks, one for the lived areas and one for the roof/loft. In Figure 6.3 the main block as represented in DesignBuilder.
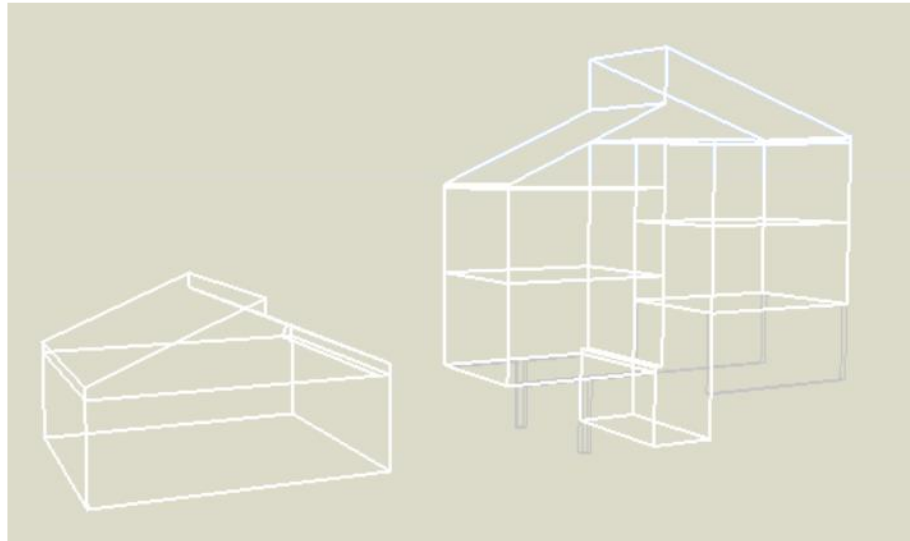
Figure 6.2 Block view of single bungalow and terraced house (part of the main block)
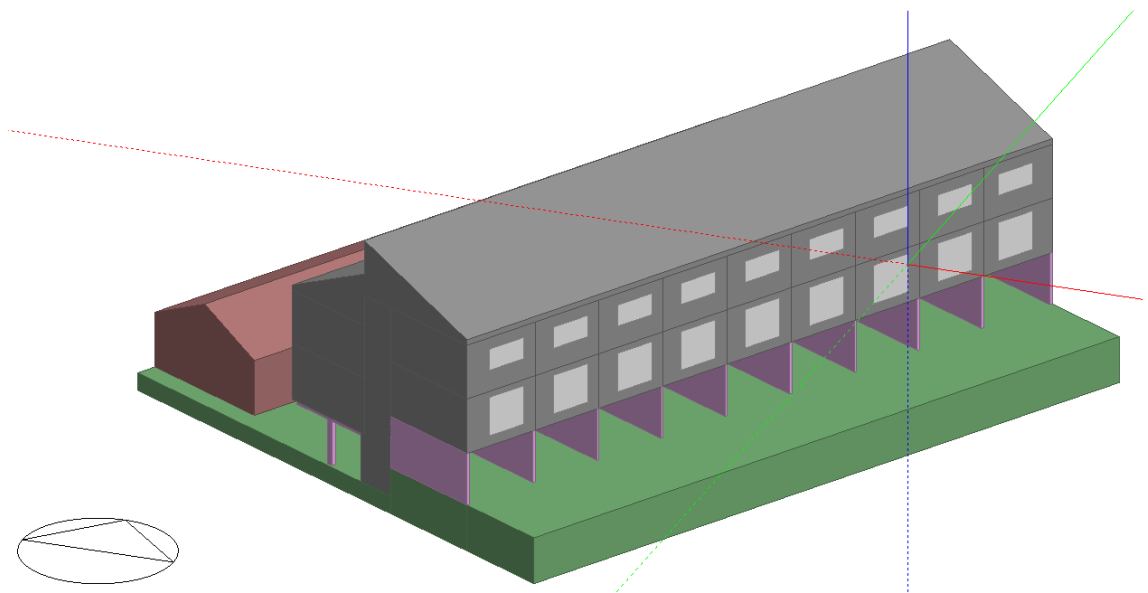
Figure 6.3 Back view of the pre-refurbished building in DesignBuilder

6.2.3. Type of building and activity selection

The building typology and activity are selected in DesignBuilder to define how energy is used within the building. The activity selection defines numerous parameters which have a considerable impact on the energy consumption, the more important are:

Table 6.2 Activity parameters

Occupation density	Defines the number of people in the room as (people/m²)
DHW consumption rate	Defines the consumption rate in the room as (l/m² per day)
Temperature setpoint	Defines target temperature (°C)
Equipment utilisation	Defines the energy use and relative heat emission (W/m²)
Target illuminance	Defines the target illuminance in (lux)

Every single room in the model has been identified accordingly to its final use, this changes the settings in the parameters listed in Table 6.2.

Table 6.3 Activity parameter for each of the modelled zones

Zone type	Occupation density (people/m²)	DHW cons. rate (l/m² - day)	Temp. setpoint (°C)	Target illuminance (lux)	Equipment utilisation (W/m²)
Kitchen	0.0237	1.05	19	300	30.28
Bedroom	0.0229	0.53	19	150[8]	3.58
Lounge	0.0188	0.72	21	300	3.90
Bathroom	0.0187	1.05	20	150	1.67
Toilet	0.0243	4.85	NA[9]	100	1.61
Stairs	0.0465	2.62	18	100	1.57
Circulation	0.0155	2.62	18	100	1.57

The values used to define the activity in the different rooms are shown in Table 6.3. Some of the values, like the energy consumption due to equipment's in the room, the DHW consumption rate and the occupation density were defined in the DesignBuilder library. On the other hand the target illuminance have been defined according to the indications provided by CIBSE (CIBSE, 2006). Temperature setpoints differ in the different models developed and will be shown in the relative paragraphs, values in Table 6.3 however

---

[8] 50 lux have been added to consider local illumination
[9] Toilets are no heated

represent the ones used in both the co-simulation models and have been defined during the surveys in the case study buildings.

A specification is needed when it comes to the DHW in the different rooms, it is possible to see how consumption is reported even in rooms in which no DHW is used, like for example the stairs, however, when using Detailed HVAC and the option "1-Simple HVAC Data" for the Detailed HVAC Activity Data), the DHW consumption rate in DesignBuilder is indicated as the DHW demand due to the activity carried out in the specific room, this explains why a zone defined as stairs or circulation zone still has a DHW consumption rate indicated even though no taps are present in there.

As mentioned in each room a target illuminance is indicated in the activity tab, this value is used to determine the energy consumption for lighting. Illuminance however is not the only value requested for this, other factors need to be defined, specifically the "Normalised power density", the type of light source (see Table 6.4) and the working schedule; another necessary value is the floor area of the room which is automatically calculated according to the geometry.

Table 6.4 Lighting parameters

Parameter	Unit	Value
Template		Fluorescent light
Normalised power density	W/m²-100lux	1.43
Luminaire type		Suspended
Radiant fraction		0.42
Visible fraction		0.18

Values in Table 6.4 are defined by DesignBuilder (Illuminating Engineering Society of North America, 1993) with the exception of the "normalised power density" which has been calculated to better reflect the properties of the bulbs.

Knowing the target illuminance is in fact possible to define how many lumens are necessary in each room, and considering the efficiency of the bulb in place (~70 lm/W) has been possible to define the "normalised power density". The calculation procedure is the following (values for the living room):

- Target illuminance = 300 lux
- Zone floor area = 16.11 m²
- Bulb efficiency = 70 lm/W

$$Watt\ per\ room = \frac{Target\ illuminance \cdot Floor\ area}{Bulb\ efficiency} = 4.29 \left(\frac{W}{m^2}\right) \qquad \text{Eq. 6-1}$$

$$Normalised\ power\ density = \frac{Watt\ per\ room}{\dfrac{Target\ illuminance}{100\ lux}} = 1.43 \left(\frac{W}{\dfrac{m^2}{100}\ lux}\right) \qquad \text{Eq. 6-2}$$

Lights are set to operate between 6:00-8:00 and 17:00-23:00.

6.2.4. Building construction definition

During the building construction definition phase all the properties of the building envelope and structure have been specified in DesignBuilder. All the opaque structures have been built to reflect the layers and material attributes listed in Chapter 5: .

In terms of air infiltration (air leakage) the result from the blower door test has been used, as stated in paragraph 5.2.3 the value is 8.74 m³/(m²hr)@50Pa. In the same paragraph in Table 5.6 are specified the ventilation values for each rooms, these values have been set as natural ventilation set points in the model.

The thermal bridges in the pre-refurbishment building have not been calculated, considering the very poor conditions of the insulation (which as mentioned in paragraph 5.2 was missing or ruined in many parts of the building) and the overall building envelope, would have been almost impossible define a reliable result. However where possible (for example in wooden frames filled with insulation) they have been considered. This approach puts the model in a conservative position, making sure that the performance of the not refurbished building are not over-estimated.

As mentioned Chapter 5: windows have a UPVC frame with double glazing, the U value calculated in DesignBuilder stands at 3.159 W/m²K.

6.2.5. Building systems definition.

A detailed HVAC system has been used in DesignBuilder to replicate the heating system present in the case study, as mentioned each terraced house and bungalow is fitted with a combi boiler which supplies both SH and DHW. In DesignBuilder the space heating system that represents the boiler and radiator system is divided in two parts, the "supply side" and the "demand side" (Figure 6.4).
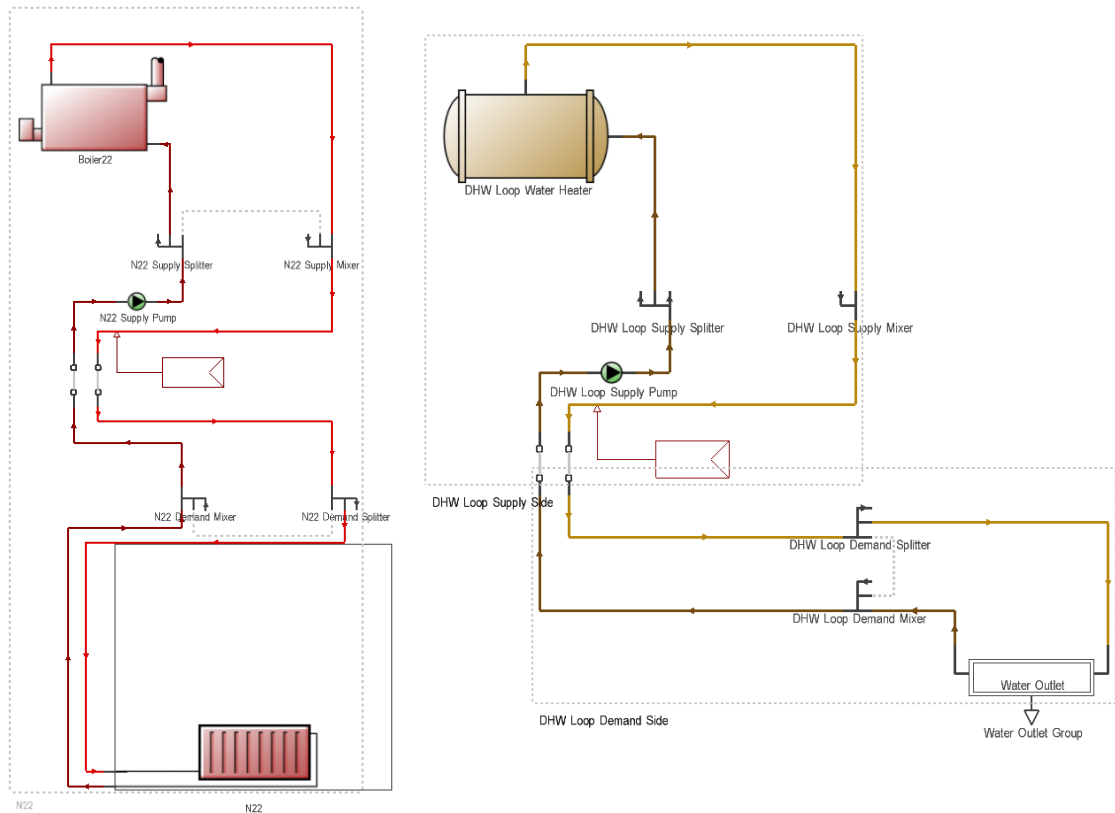
Figure 6.4 SH and DHW components in DesignBuilder

The first includes the boiler, the "set point manager", and the pump. Boiler efficiency is set 90.1% whereas the set point manager is set to operate following the schedule specified in the rooms, with a supply temperature for the SH water of 75°C. The "demand side" on the other hand includes the "zone group", here are specified all the rooms/homes served by the boiler (Figure 6.5)
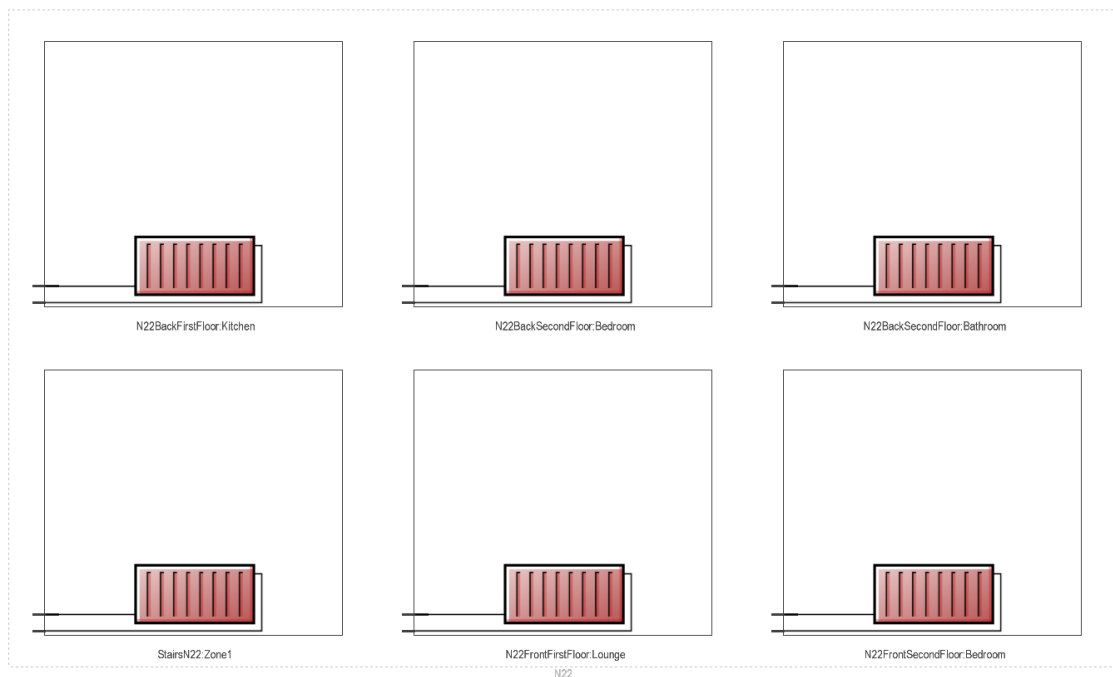
Figure 6.5 Zone group example

The DHW system is represented in a similar way, also in this case are present a supply and a demand side. The supply side includes the water heater, the set point manager (again the schedule follows the request from the rooms setpoints) and the pump. The temperature setpoint for the DHW is 55°C. In the demand side is present the "water outlet group" where, like in the zone group for the SH, the rooms served by DHW are specified. Again, as aforementioned in 6.2.3, it is important to underline that the DHW demand is calculated according to the activity that takes place in each specific room, stairs for example will contribute to the DHW demand even if no taps are present in there.

6.3. Post-refurbishment model

The initial model has been modified to reflect the retrofitting interventions applied to the case study. As aforementioned a number of models have been built. The first model includes only the 7 refurbished homes in the main block. The second model contains 10 refurbished homes (7 terraced houses from the main block plus 3 bungalows), a final model had been created to include the all 27 homes of the expanded case study. The latest two, the model with 10 refurbished homes, and the one with 27 refurbished homes have been developed to be used in the co-simulation process.

6.3.1. Building construction definition (first model, main block 7 refurbished homes)

The building fabric was subject to important improvements during the retrofitting, as mentioned in section 5.3.1 a completely new façade has been applied to both main block and bungalows. To represent this in the model some modification had to be made. Considering that the new insulated panels have been positioned on the external surface of the old façade some interventions on the build geometry were necessary, the dimension of the building have been changed to make sure that the internal volume of the building was not affected by the increased thickness of the walls. The software in fact takes into account the external dimension of the building (as for user choice) and an increase in the wall thickness would consequently lead to a reduction of the internal space, to avoid this the front and back facade of all the homes have been extruded by a length equal to the thickness of the new cladding. Same applies to the kitchen floor which have been extruded too to consider the additional insulation applied in the external surface.
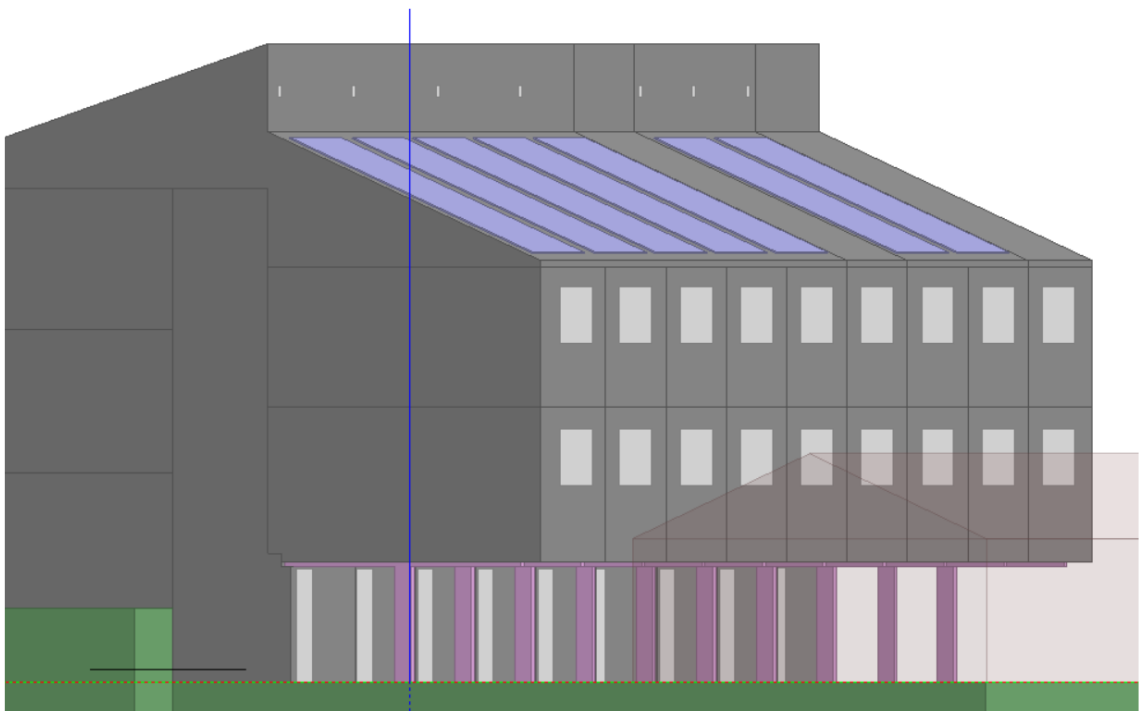
Figure 6.6 Main block refurbished with extruded surfaces and PV panels on the roof

The main block roof and end walls on the other hand did not require any intervention because the insulation has been applied on the loft and in the cavity within the walls themselves.

The new lounge rooms at ground level have been added, also in this case there were differences with the not refurbished houses in which the ground level is still an open air

storage, this have been represented in the model (Figure 6.7) to consider the thermal loss due to the air circulation in that area.
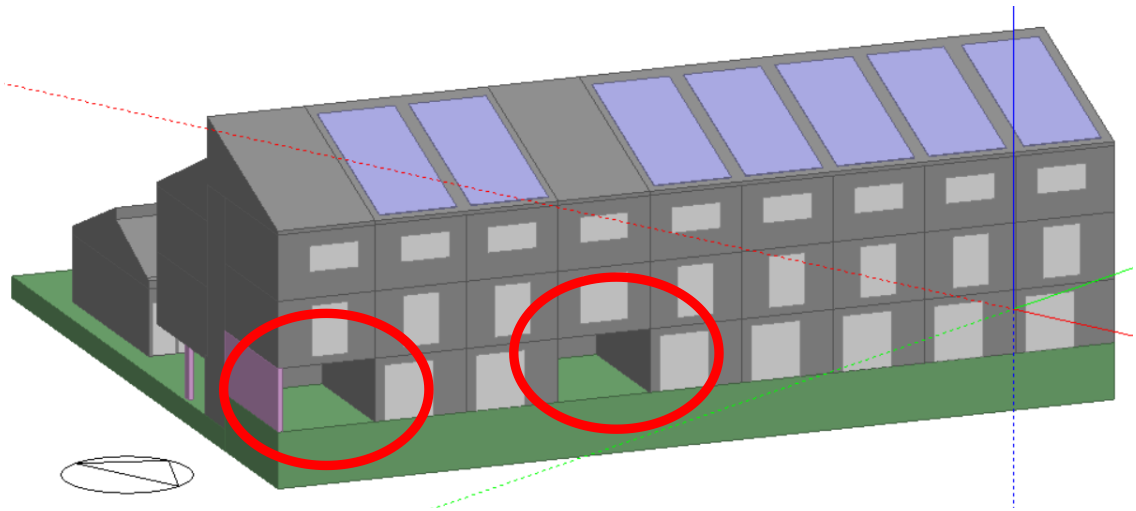
Figure 6.7 Main block retrofitted, the two non-retrofitted homes lack the new lounge room

Also the infiltration values was changed in order to reflect the new results of the blower door test, as said in paragraph 5.3.1 the infiltration rate after the refurbishment is equal to 6 m³/(m²hr)@50Pa.

6.3.2. Building systems definition.

6.3.2.1. New detailed HVAC system (first model, main block 7 refurbished homes)

In the model representing the post refurbishment building a new detailed HVAC system was implemented. As specified in 6.3 the first post refurbishment model has been developed including only the 7 retrofitted homes in the main block.
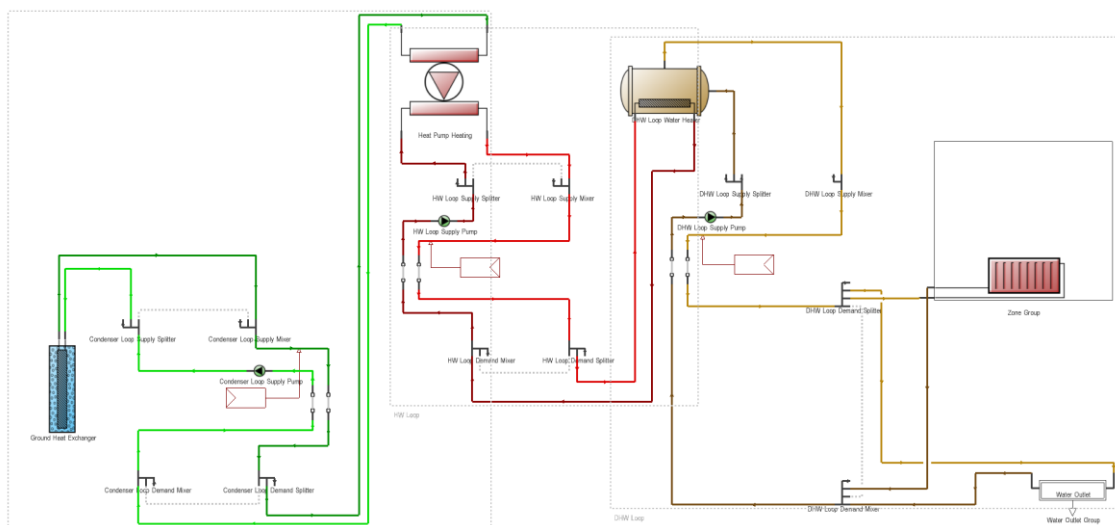
Figure 6.8 Detailed HVAC system with GSHP and thermal storage

The so called "demand side" of the system is unchanged, with the "zone group" including the radiators in the heated rooms and the "water outlet group" with the zones served by DHW. The supply part on the contrary has been modified to reflect the new heating system.

The individual boilers have been replaced by a centralised GSHP system with thermal storage (Figure 6.8). The three main components added to the HVAC system in the model are the condenser loop (Figure 6.9), the heat pump (Figure 6.10) and the thermal storage (Figure 6.11).

The condenser loop simulates the boreholes (ground heat exchanger) and relative systems. It is divided in a supply side that includes the boreholes, the pump and the set point manager, and a demand side connected to the HP. In the ground heat exchanger block all the geometry of the boreholes have been defined, as mentioned in paragraph 5.3.2 the system was initially served with 5 boreholes (radius 10 cm), each of them 130 m deep, the external diameter of the pipes in the boreholes is 40 mm.
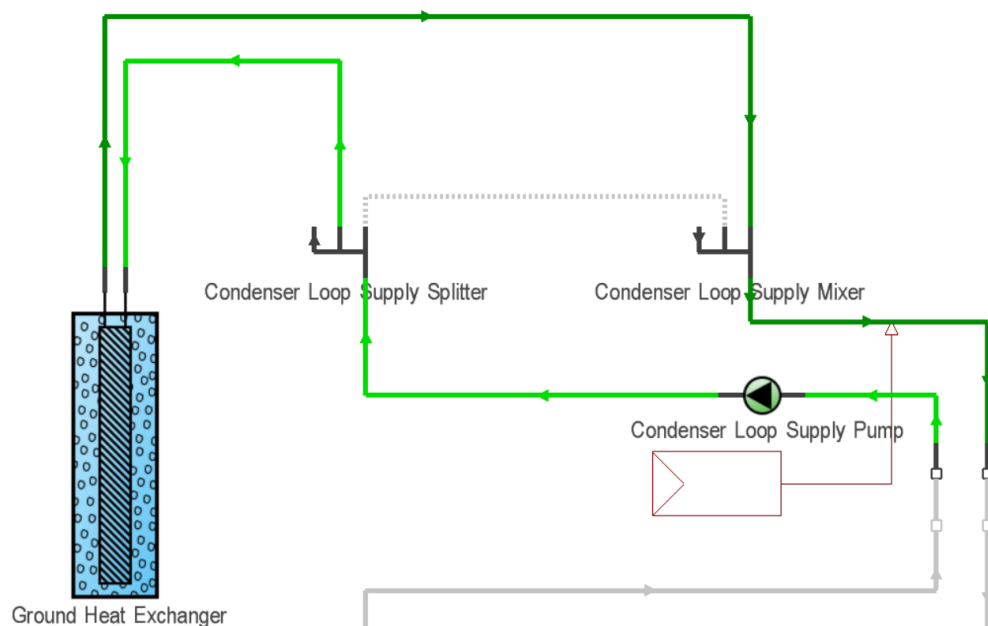
Figure 6.9 GSHP condenser loop

Similarly, to the other loops the heat pump loop is divided in supply and demand side (Figure 6.10). The first one is connected to the condenser loop and includes the heat pump, the setpoint manager and the supply pump. Design builder offers a wide range of heat pumps in the database and a model with performances very close to the system in the case study have been selected. The only parameters which slightly differ and have been adjusted are the rated heating capacity and the rated heating power consumption.

The two HPs present in the case study have been represented with a single HP having a heating capacity equal to the total capacity of the HPs in the energy centre, therefore the values set in DesignBuilder are respectively 32,4 kW for the rated heating capacity and 7.6 kW for the rated power consumption. The maximum output temperature has been set at 55°C in the setpoint manager. The outlet of the HP loop is connected to the storage loop (Figure 6.11).
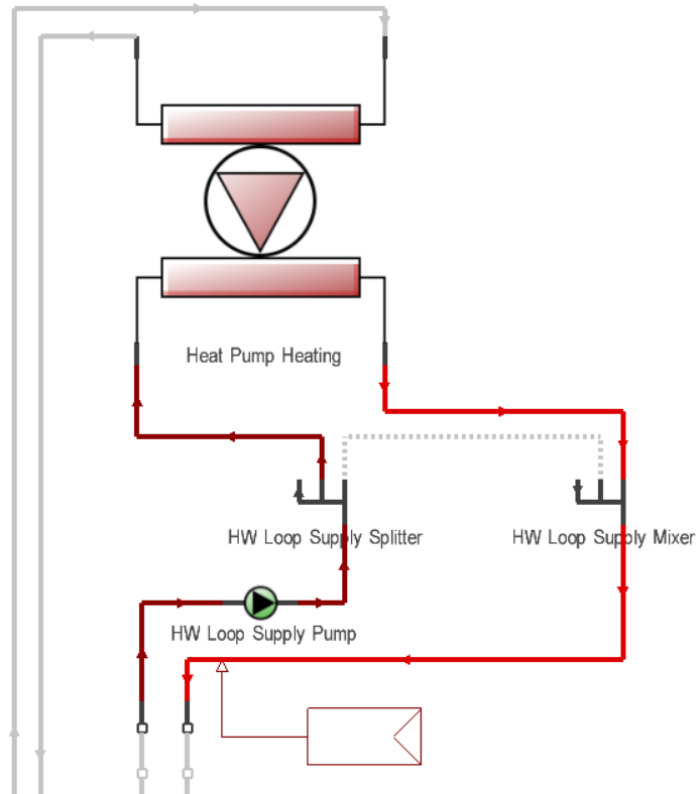
Figure 6.10 Heat pump loop
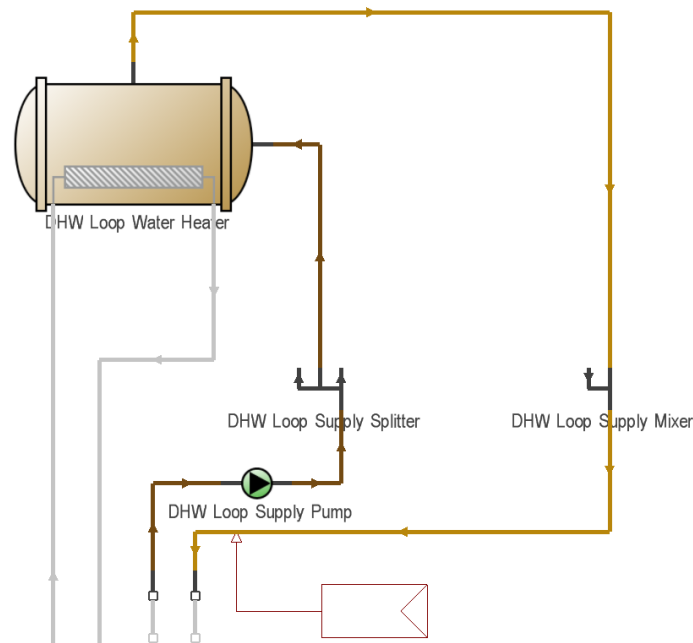
Figure 6.11 Thermal storage

In this part of the model the thermal storage is represented, and, even if named "DHW loop water heater" it supplies hot water to both the SH and DHW circuits with a setpoint of 48°C. The storage dimensions have been defined to match the thermal storage in the case study with a capacity of 4 m³. As indicated in Figure 6.11 the storage is heated by the HP via a heat exchanger.

6.3.2.2. Photovoltaic and electric storage system

An important part of the retrofitting intervention has been the installation of a photovoltaic plant on the roof of the buildings, DesignBuilder offers the opportunity to implement this kind of electricity generators building them directly on the roof surface. This allows the model to provide an excellent representation of the effective performance of the plant. The first step to introduce the PV system in the model is to add the photovoltaic solar collectors in the exact position in which they are in the real building, matching the dimensions with the actual modules.

This process is relatively straightforward, but in the case study each slope of the roofs has a different number of solar panels (Figure 6.12) this means that the surface covered by solar collectors is different in every slope.
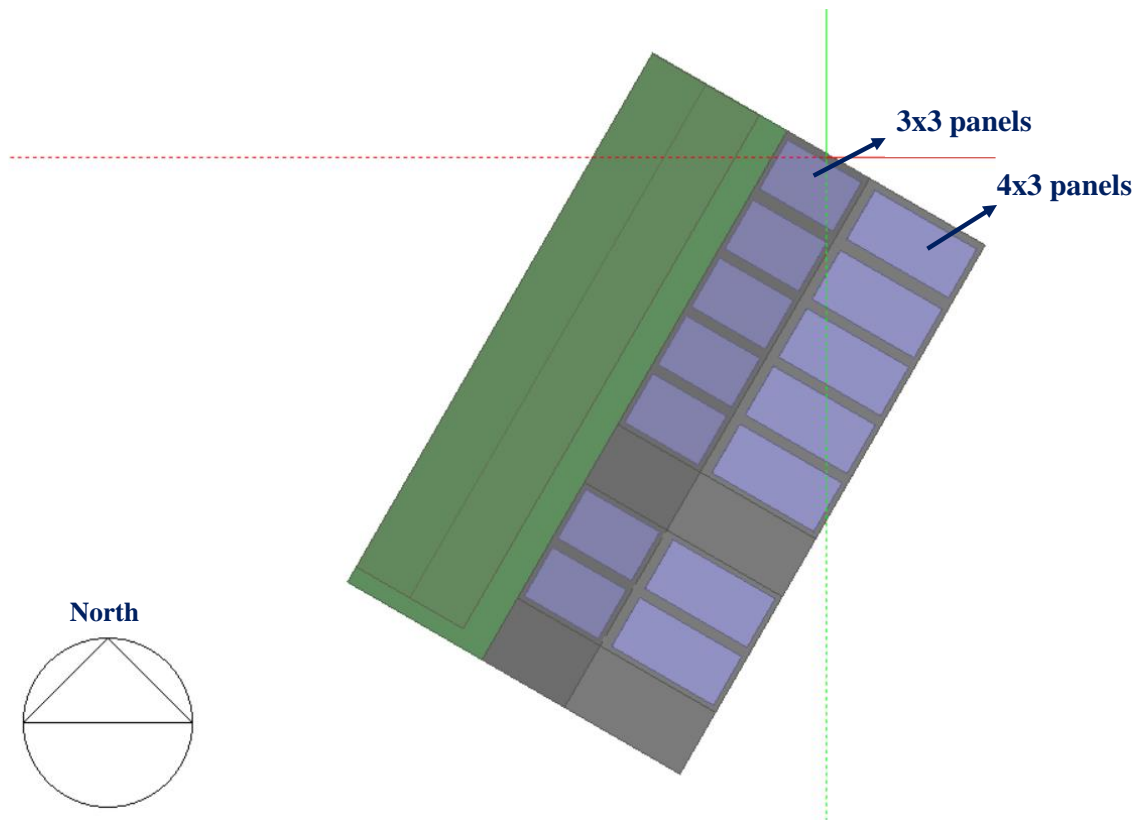
Figure 6.12 Plan view of the first 7 refurbished homes with PV panels

In the main building, on the roof of each terraced home 12 PV panels are present on the slope facing South-East whereas other 9 panels are on the slope facing North-West. This means that in the model a solar collector of 34.16 m² (19.52 m² facing South-East and 14.64 m² facing North-West) has been implemented on the roof of each refurbished terraced house. Once defined the solar collectors' geometry is necessary to define their properties in terms of performance. Several commercial PV panels are present in the DesignBuilder library, but to improve the accuracy of the model a new component has been added to the library with the properties of the Viridian solar PV panel (each of them has a peak power of 270 W) used in the case study. When the solar collectors' properties have been defined the next step is to activate the "on site energy generation" option. The next step is the definition of the number of "load centres" present in the system, one in this case study and then it is necessary to specify its layout. As mentioned in the previous chapter (section 5.3.2) within the retrofit intervention a PV plant has been installed on the roofs tighter with an EES (20 kWh capacity in this model). Considering this the layout "DC with inverter + DC storage" has been selected among the various layout present in DesignBuilder (DesignBuilder, 2016).
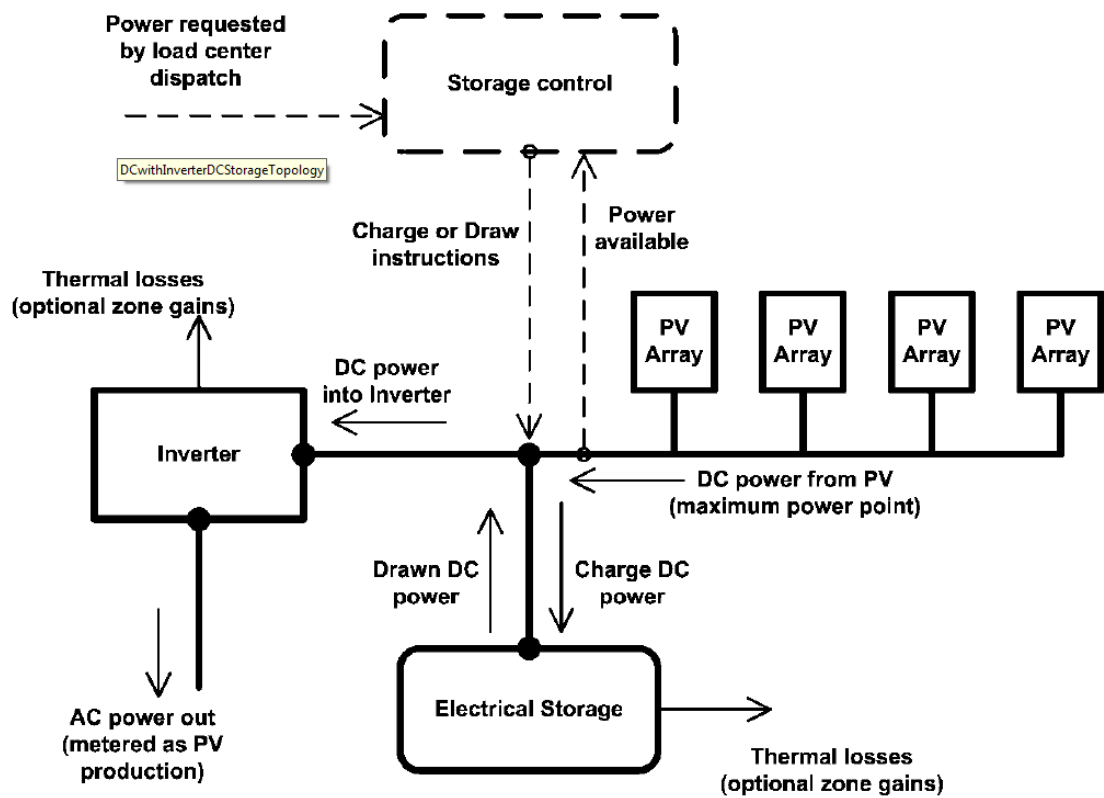
Figure 6.13 Direct current with inverter DC storage

As reported in (Figure 6.13) this system has the EES storage connected in DC with the PV array before the inverter.

6.3.3. Building construction definition (second model complete pilot cluster with 10 refurbished homes)

In this model the 3 retrofitted bungalows have been added, all the modifications listed in 6.2.4 have been applied to the bungalows too but in this case the roofs had to be modified because completely new structure has been added on top of the old one (see 5.3.1)
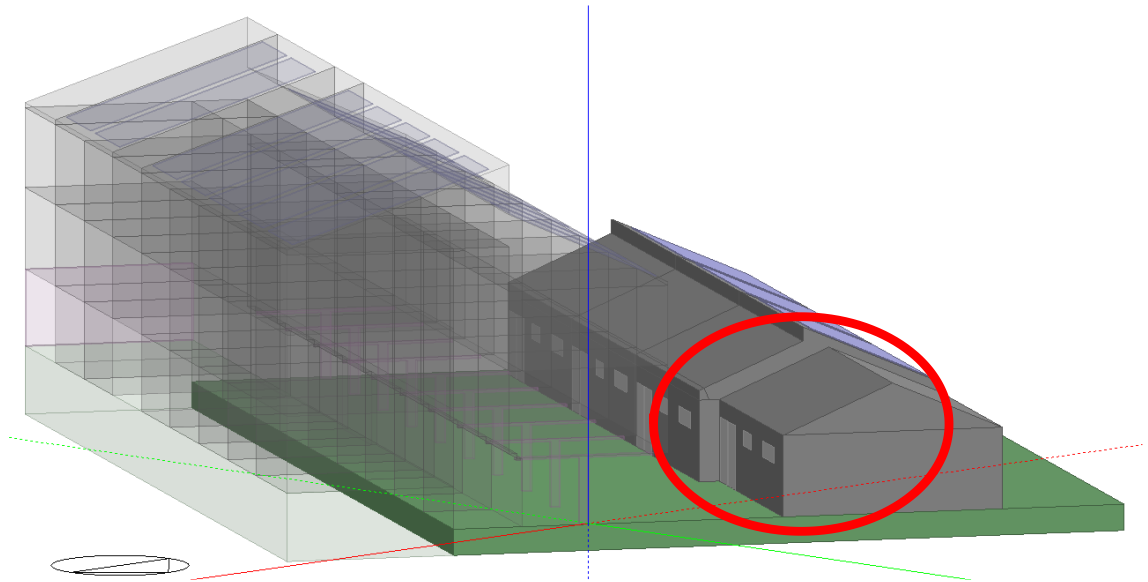
Figure 6.14 Side view of the bungalows with different dimensions

This intervention is clearly visible in Figure 6.14, one of the bungalows in fact was not subject to refurbishment and the difference in dimensions is consistent.

6.3.4. Building systems definition.

6.3.4.1. New detailed HVAC system (second model complete pilot cluster with 10 refurbished homes)

As said this model have been developed explicitly to be converted in FMU and used in the co-simulation with Dymola. This means that the entire energy centre will be simulated in Dymola, therefore the detailed HVAC system with GSHP and thermal storage in DesignBuilder has been replaced with two boilers that are going to be controlled by Dymola as explained in Chapter 4: . Because of this the detailed HVAC system in DesignBuilder looks similar to the one in the model of the not refurbished scenario, but in this case only two boilers are present, one dedicated to the SH and one for the DHW Figure 6.15.
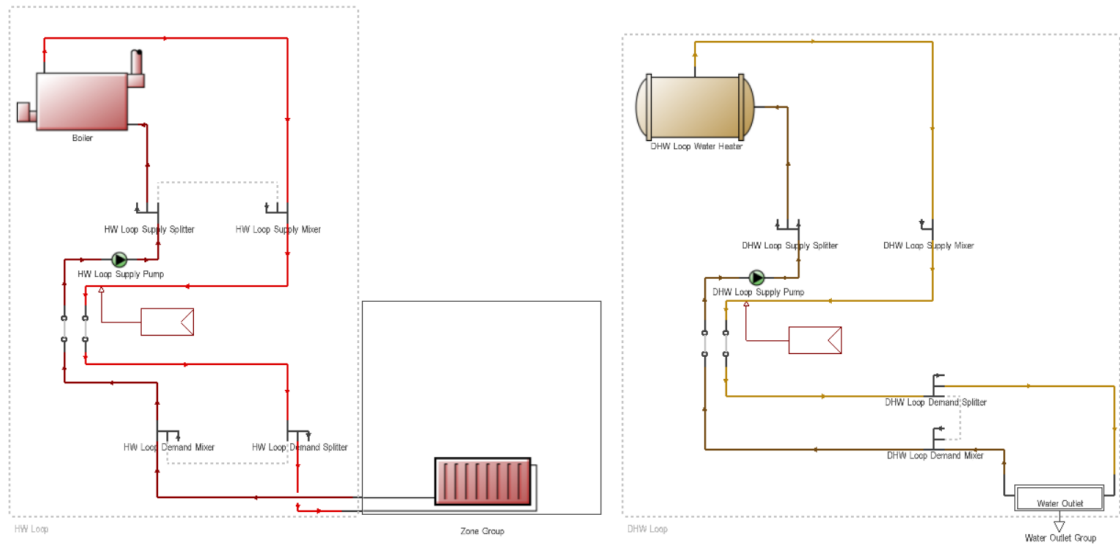
Figure 6.15 Fictitious boilers in the detailed HVAC system used for the FMU creation

The "zone group" and "water outlet" group in this model include all the heated zones in the ten homes in light of the fact that the system is centralized and serves all the buildings.

The power output of both systems is set at the maximum upper limit to ensure the immediate response to the input arriving from Dymola.

6.3.4.2. Photovoltaic and electric storage system

In this model the PV collectors on the bungalows have been added to the ones in the main building. As mentioned in 6.3.2.2 the main block has PV collectors on both the roof slopes, in the bungalows on the other hand PV panels are only on the slope facing North-West in groups of 16 per each bungalow. The area covered by PV on every roof is therefore 26.03 m² (Figure 6.16). Considering that the energy system (including the electric energy storage) will be simulated in Dymola the system layout was changed, from "DC with inverter + DC storage" to "DC with inverter". In this way no storage is simulated in DesignBuilder and "*the PV arrays produce DC power based on the availability of sunshine and do not respond to load requests made by the electric load centre*" (DesignBuilder, 2016), the PV energy production data is sent to Dymola.
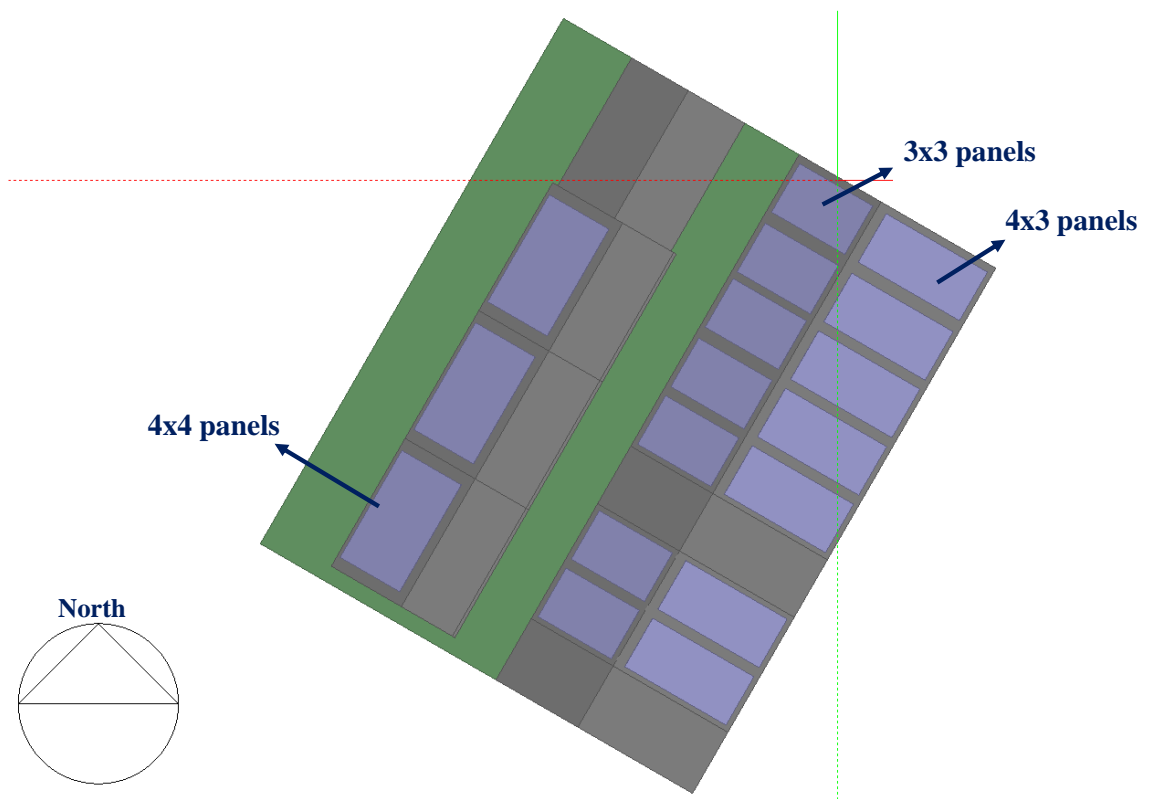
Figure 6.16 Plan view of the first 10 refurbished homes with PV panels

6.3.5. Building construction definition (third model expanded case study with 27 refurbished homes)

This third model has been generated to provide the FMU for the co-simulation of the expanded case study, all the considerations made in 6.3.3 for the model with 7 refurbished homes apply to this model where the retrofitted home are 27.
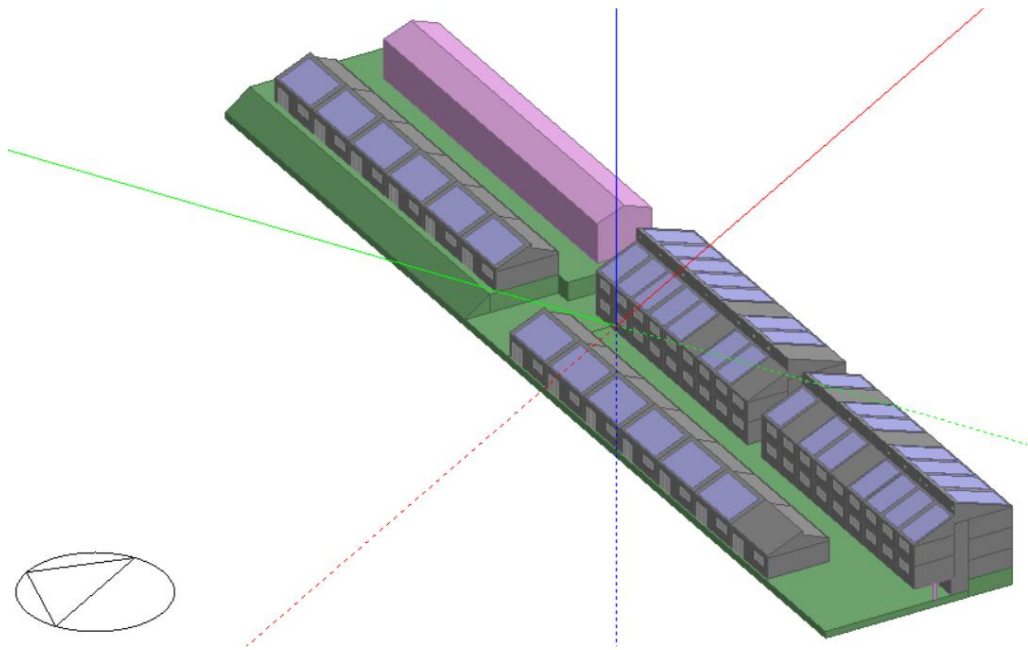
Figure 6.17 Axonometric view of the model representing the expanded case study

Figure 6.17 shows that also in the new refurbished block of buildings two terraced houses were not retrofitted (recognisable by the absence of PV on the roof), a new group of bungalows (at the North of the initial case study) have been renovated together with other three adjacent to the initial ones. Is important to underline that the bungalow not retrofitted in the initial case study has been renovated in this phase (the bungalow in the foreground without PV has been refurbished but because shadows due to vegetation near it the PV has not been installed). The HVAC system in this model is a simple evolution of the one in 6.3.3, the only modification applied is the inclusion of the new homes in the group zone and in the water outlet group.

6.4. DesignBuilder simulation results

6.4.1. Simulation results for the pre-refurbishment model

The simulation of the not refurbished buildings has been made to set a baseline in order to understand the benefits provided by the deep retrofitting work on the building envelope and the new energy system. As mentioned, the first model that was created included only the main building, with the bungalow structure included in the model (to keep into account shading etc..). The temperature setpoints have been set according to the SAP (BRE, 2014), with a setpoint of 21°C in the living area (the lounge in the model) and 18°C elsewhere. The heating periods also follow the SAP recommendations as shown in Table 6.5. The decision of using this temperature setpoints is due to the fact that before the refurbishment the houses where *de facto* not heated, occupants were living in fuel

Page | 89

poverty conditions and generally only one room was heated with a simple electric fan heater. Considering this and the lack of information about the consumption before the refurbishment it has been decided to use the SAP recommendation to give consistency to the model when evaluating the effect of the retrofitting on the heat demand of the building.

Table 6.5 Heating schedule

Day	Heating period
Weekday	07:00-09:00 and 16:00-23:00
Weekend	07:00-23:00

The results from the simulations in DesignBuilder for the pre-retrofitting block are reported in following tables:

Table 6.6 Energy consumption for space heating

				Space heating (kWh)					
					House				
Month	**A**	**B**	**C**	**D**	**E**	**F**	**G**	**H**	**I**
January	2200	1410	1435	1341	1435	1433	1433	1442	2151
February	1960	1250	1272	1184	1271	1269	1270	1279	1894
March	1499	920	923	861	923	925	926	941	1431
April	993	569	556	522	555	559	562	581	930
May	312	156	142	136	139	141	144	157	283
June	166	83	74	72	72	74	76	84	153
July	0	0	0	0	0	0	0	0	0
August	12	4	3	3	3	3	3	4	9
September	244	131	120	116	118	120	122	131	220
October	842	514	500	478	499	502	505	521	811
November	1611	1029	1035	972	1036	1036	1037	1048	1559
December	2089	1346	1366	1277	1366	1364	1365	1374	2043
TOTAL	11927	7412	7428	6961	7418	7425	7443	7561	11485

Table 6.7 Energy consumption in the different month for SH and DHW

Month	DHW [kWh]	Space heating [kWh]
	Overall energy consumption	
January	1337	14281
February	1209	12649
March	1362	9349
April	1308	5827
May	1248	1610
June	1197	854
July	1130	0
August	1135	44
September	1126	1321
October	1186	5172
November	1244	10362
December	1371	13591
TOTAL	14851	75061

Table 6.6 shows the energy used to provide space heating in each terraced house. As forecastable the two end terrace homes require more energy as the surface exposed to the external environment is consistently higher than the mid-terrace homes, furthermore, is possible to see how the house exposed to the south has a lower energy demand. Table 6.7 instead shows the energy consumption for SH and DHW during the different months, the fluctuation in the DHW energy demand is due to the different temperature of the water arriving from the mains.

6.4.2. Simulation numerical results for the first model of the pot-retrofitting case study (main block 7 refurbished homes)

Three different cases have been modelled for the post-refurbishment building:

- **Case 1** – seven of the nine homes have been refurbished, the heating is set to a target temperature of 20°C in each room and is constantly on.
- **Case 2** – seven of the nine homes have been refurbished, the temperature set point and the heating schedule follow the SAP recommendations like in the pre-refurbished building (see Table 6.5).

- **Case 3** – all the homes have been refurbished, the temperature set point and the heating schedule follow the SAP recommendations like in the pre-refurbished building (see Table 6.5).

The first two cases represent the actual condition of the case study, in which two out of nine terraced homes have not been refurbished, they differ however in terms of heating schedule and set point. Case 3 on the other hand has been modelled to analyse the impact of the two non-refurbished homes and define what energy performances could have been achieved with a full refurbishment of the block.

Results from these simulations have been compared to the outputs of the pre-refurbishment model, to have a clear image of the effectiveness of the retrofitting intervention on the building envelope the model have been compared in terms of heat demand of each house. Also, considering that 2 homes have not been upgraded a version of the pre-refurbishment model with only 7 heated homes was also run to provide a consistent reference.

Table 6.8 Heating demand per each home before the retrofitting

	Heating demand per house (kWh)									
	A	**B**	**C**	**D**	**E**	**F**	**G**	**H**	**I**	**TOT**
9 homes model	10894	6770	6784	6358	6775	6782	6799	6906	10490	68559
7 homes model	10918	6784	6805	6450	8624	0	8827	10597	0	59005

It is clearly visible from Table 6.8 the strong impact of two not heated homes which act as heat sink subtracting heat from the adjacent house (the partition wall is reinforced concreate with a high U-value). These results have been then analysed versus the ones from the different post-retrofitting models. Case 1 and 2 have been compared with the model with 7 heated homes while for Case 3 the comparison is against the model with all the 9 homes heated.

Table 6.9 Case 1 heat demand comparison

	A	B	C	D	E	F	G	H	I	TOT
			Heating demand per house (kWh)							
Case 1	7911	5225	5090	5298	8225	0	8853	11036	0	51639
% Diff	-27.5	-23.0	-25.2	-17.9	-4.6	0	0.3	4.1	0	-12.5

Table 6.10 Case 2 heat demand comparison

	A	B	C	D	E	F	G	H	I	TOT
			Heating demand per house (kWh)							
Case 2	4989	3141	3039	3214	5185	0	5593	7043	0	32204,0
% Diff	-54.3	-53.7	-55.3	-50.2	-39.9	0	-36.6	-33.5	0	-45.4

Table 6.11 Case 3 heat demand comparison

	A	B	C	D	E	F	G	H	I	TOT
			Heating demand per house (kWh)							
Case 3	5089	3199	3057	3037	3146	3115	3104	3184	4963	31894
% Diff	-53.3	-52.8	-54.9	-52.2	-53.6	-54.1	-54.3	-53.9	-52.7	-53.5

The data listed in Table 6.9, Table 6.10, and Table 6.11 highlight consistent differences between the different simulated cases.

6.5. Co-simulation modelling: pilot cluster 10 refurbished homes

In Figure 6.18 the co-simulation model of the pilot cluster is shown, with all the elements that were reported as schematic view in 4.1.2.

6.5.1. Overview

The working steps of the FMU have already been described in the aforementioned paragraph, but here is possible to see the connections between the different element in the real model therefore a better explanation of the fluid and signal loops will be given.

At the top part of the picture (Figure 6.18) the FMU block is visible, the signals leaving the block from the left side are the mass flow and return temperature in the SH loop,

whereas the signals leaving the FMU from the right side are the mass flow and mains temperature of the DHW loop. They represent the heat demand coming from the building and are connected to two "*fluid source*" blocks, which "generate" the water flow that goes in the two TES. The water is heated in the TES through a heat exchanger and sent to the "sink" blocks (visible on the sides of the FMU). A temperature sensor connected to the heated fluid before the sink (one for each branch) measures the water temperature and sends the signal back to the FMU (upper side). Here these signals define the temperature of the water that the two fictitious boilers in EnergyPlus send to the SH and DHW circuits.
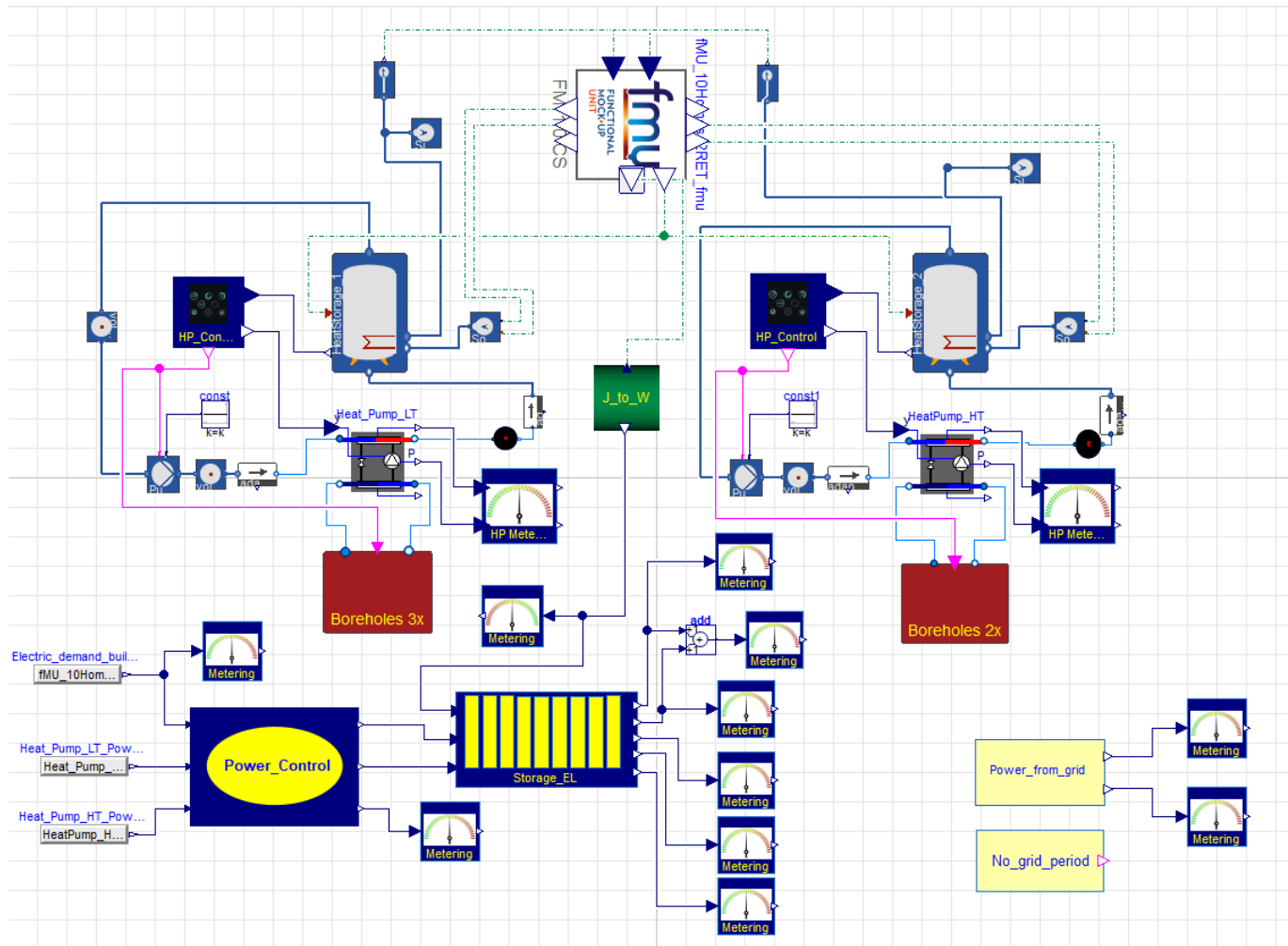
Figure 6.18 High level view of the co-simulation model of the pilot cluster in Dymola

Roughly in the middle of Figure 6.18 the two heat pumps are visible (the icon of the block is shown in Figure 6.19). The heat pump model was developed by (The Regents of the University of California (through Lawrence Berkeley National Laboratory), n.d.). Each heat pump as 4 flow ports. The two ports in the upper part, connected to the TES circuit, represent the inlet and outlet of the condenser. The connections on the lower part represent the inlet and outlet of the evaporator and are connected to the borehole circuit. The connection *y* on the top left is connected to the *HP_Control* block which will be later analyzed in more detail.
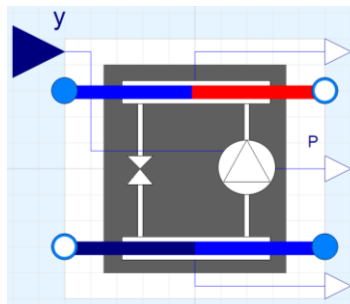
Figure 6.19 HP block in Dymola

In the circuit between TES and HPs are visible the two pumps which run the fluid in the loop. The two water pumps are controlled by *HP_Control* too. The red blocks visible below the HPs include the borehole loops visible in Figure 6.20. The flow arriving from the HP is split in two (in this case) separate lines of equal properties and sent into the borehole. Exiting the boreholes the two flow lines mix in a T joint before entering the pump, which runs the fluid in the loop. The control signal (purple line) which operates the pump arrives again from the *HP_Control* block.
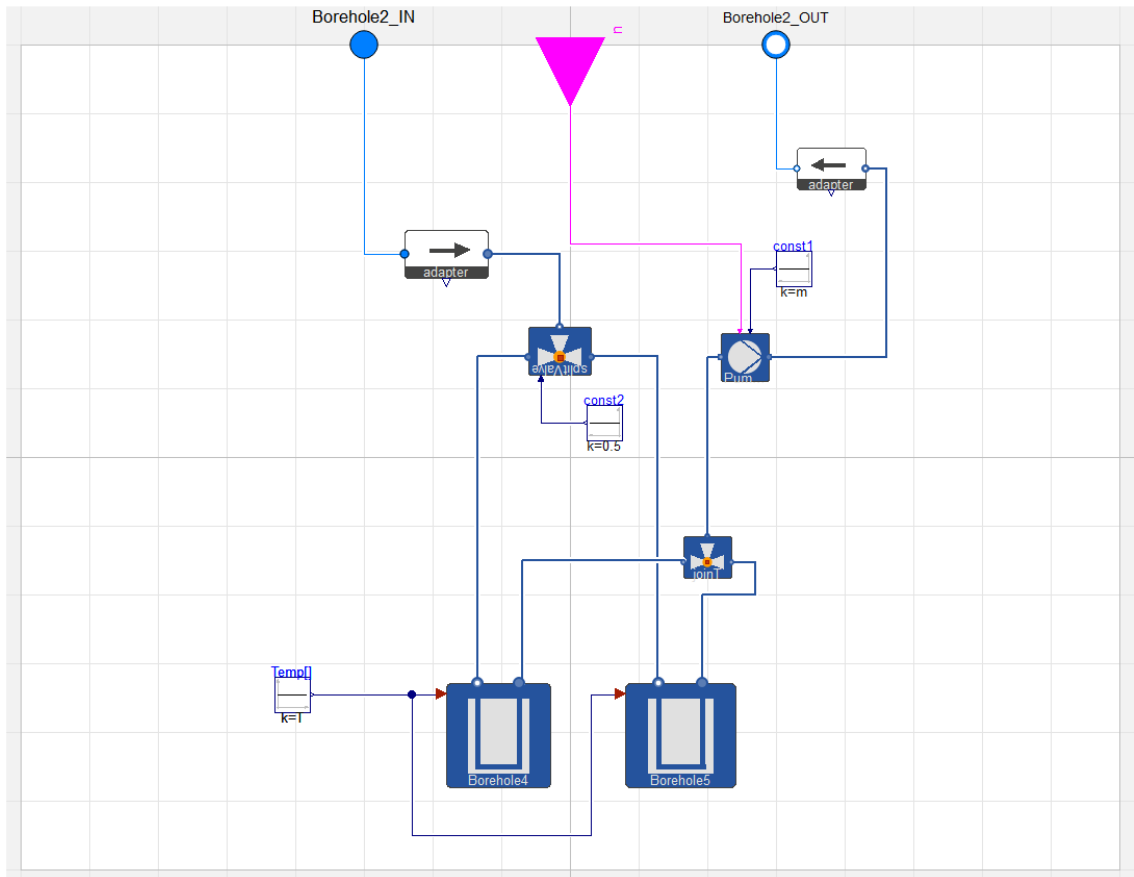
Figure 6.20 Boreholes loop

The core of this research is however the control and the optimisation of hybrid heating system; therefore, the remaining elements will be described in detail in the following paragraph.

6.5.2. Control system and simulated scenarios

The most important components, which allow the control of the energy system are:

- *HP_Control*
- *Power_Control*
- *Storage_EL*
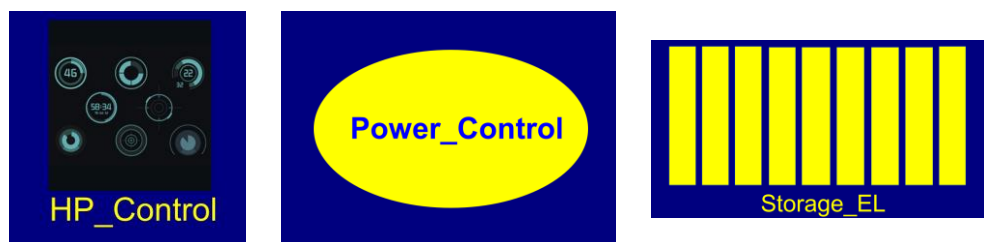
Figure 6.21 Icons of the main control blocks in the co-simulation model in Dymola

Before analysing in detail the control components (whose blocks are visible in Figure 6.21), it is important to underline that using the co-simulation tool, three distinct scenarios with different control schemes have been simulated to define the most efficient control strategy considering the pre-existent design and operative constrains.

- **Scenario 1** – In this simulation both the heat pumps and building appliances (including lighting) have access to the battery circuit 24/7. The electricity produced by the PV plant is first used (direct self-consumption) to satisfy the total demand (HPs and appliances). The eventual surplus is stored in the battery and used when no PV power is available to integrate and reduce the energy bought from the grid. HPs control is set on OFF between 4-7pm, during this period the 10 homes rely only on the thermal storages to satisfy both space heating and domestic hot water demand.

- **Scenario 2** – In this scenario, the electricity demand from HPs has the priority between 00:00 and 16:00, in this time window the domestic appliances have no access to the battery circuit, the eventual PV power surplus not used by the HPs is send to the battery to be stored. In these hours, if the HPs demand is satisfied and the battery is full, then the PV energy can be used by the homes appliances to reduce the electricity bought from the grid (i.e., increase the self-consumption of PV energy). After 16:00 appliances have access to the battery circuit, to reduce the energy bought from the grid between 4 and 7pm. Like in Scenario 1 HPs are off between 4-7pm with the heat storage providing space heating and DHW.

- **Scenario 3** – Control strategy is equivalent to the one in Scenario 2, but, starting from day 105 (mid-April) and until day 273 (last day of September), appliances have full access to the battery circuit. The aim is by differentiating the energy used in different periods of the year to increase the amount of self-consumed energy during the summer period when the PV production is high. In this case, like in the previous two, the HPs are off between 4 and 7pm.

Modifying the three control elements listed at the beginning of the paragraph is possible to change the power flow and the energy management in order to simulate the desired scenario. In the following paragraphs each component will be described individually.

6.5.2.1. HP_Control

The *HP_Control* block gives, as suggested by the name, the possibility to define the control logic of the HPs.
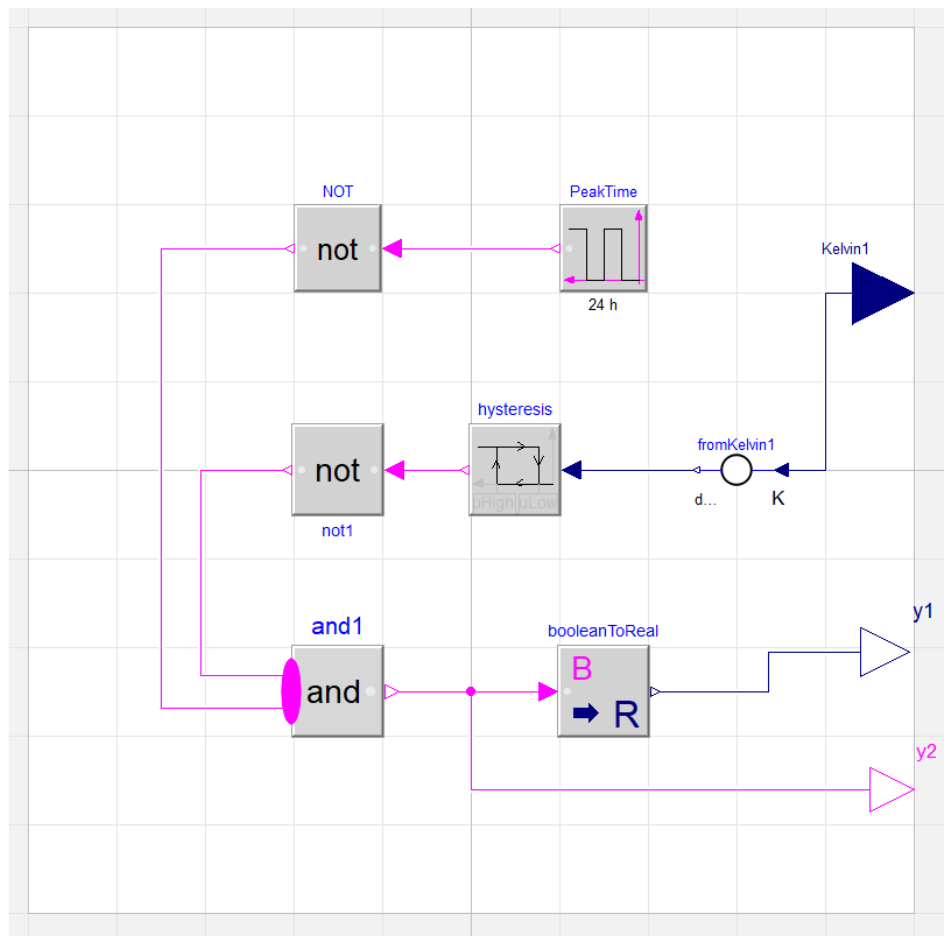
Figure 6.22 Heat pump control system

The control system operates the HPs according to the hour of the day, and the temperature in the thermal storage. The input port *Kelvin1* receives the temperature value from the TES, the signal is then converted from Kelvin to Celsius degrees and sent to the *hysteresis* control. In this element is possible to define the operating range of the HPs. The control connected to the HPs dedicated at the SH have a high limit of 45°C whereas the lower limit is 40°C . The *hysteresis* control (which has a Boolean output i.e., true or false) combined with the following *not1*[10] block, will therefore send a signal which turns on the HPs when the temperature in the tank is below the lower limit and vice versa the signal will be switch off the HPs when the tank temperature reaches the higher limit. The same logic applies to the control of the HP which provides the DHW, in this case the higher set

---

[10] "not" blocks turn a Boolean signal **true** in **false** and vice versa

point is 53°C, while the lower one is 48°C. As mentioned, the logic behind the control system is a function of the TES temperature, but also of the hour of the day. The *PeakTime* block in fact, sends a signal which turns off the HPs between 4 and 7pm. The two signals (the one depending on the temperature and the one depending on the time) are combined in the *and1* block. The Boolean output of this block will be true when both the inputs it is receiving are true. If one of them is false, the output will be false too. This means that during the peak time the HPs will always be off and in the remaining hours will be operated according to the TES temperature. The *HP_Control* block has two outputs, one (*y1*) is a real output (i.e., 1 or 0) and is responsible for switching on and off the HPs, whereas *y2* is a Boolean signal which has authority on the pumps both in the circuits between HPs and TESs and the circuits between HPs and boreholes.

6.5.2.2. Power_Control and Storage_EL

The *Power_Control* has been built in order to manage the power flows direct to the *Storage_EL* block. These two components work in symbiosis giving the opportunity to develop different control strategies for the energy management.

Storage_EL layout does not change in the different scenarios (Figure 6.27), different parts of the block are used (or not) depending on the simulated scenario. On the contrary the internal layout of the *Power_Control* block changes according to the scenario (Figure 6.23, Figure 6.24, Figure 6.26), for this reason, and because of the work *Power_Control* and *Storage_EL* do jointly, the best way to understand how they operate is to analyse them together in the different scenarios' configurations.

Before this it is important to observe that block has four separate inputs, *u1*, *u2*, *u3,* and *u4* (optional). Input *u1* and *u2* are connected to the power demand of the HPs whereas *u3* receives from the FMU the electric energy demand of the building (appliances and lighting). In Figure 6.23, Figure 6.24 and Figure 6.26, also the *u4* is present, it can be connected to a zero constant or to an additional HP (this is the case of the extended case study model in which 3 HPs are present).
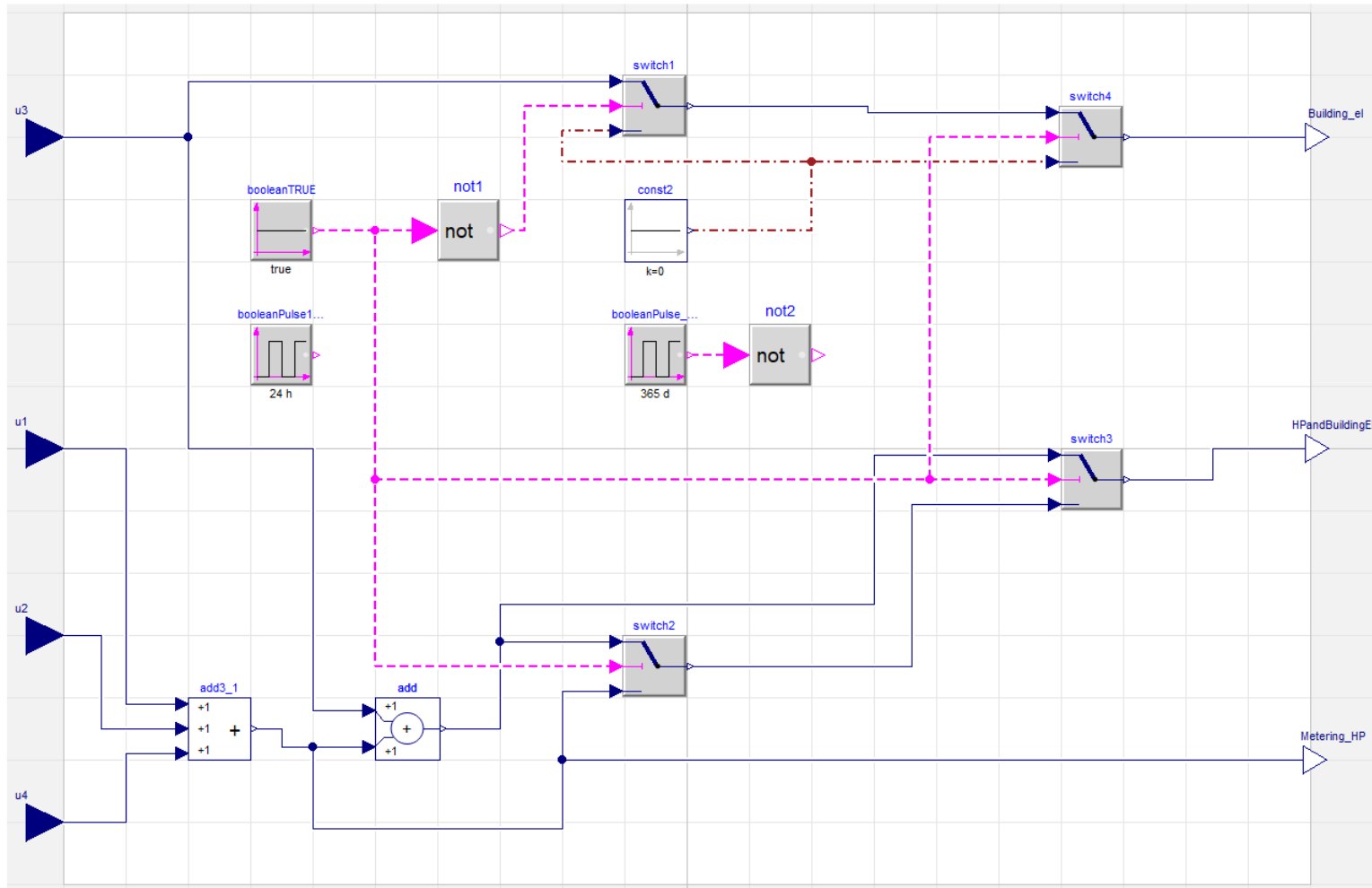
Figure 6.23 Control logic set for Scenario 1

Scenario 1 (*Power_Control* layout as in Figure 6.23)

As explained at the beginning of paragraph 6.5.2 in this simulation both HPs and building appliances have continuous access to the battery circuit. As a consequence, the power demand must always be sent to the output named *HPandBuildingEL* which is connected to the input *To_Battery_circuit* in *Storage_EL* block. The signals arriving from the HPs are combined in the block *add3_1* and then added to the signal arriving from *u3*. As *switch3* is connected to the Boolean controller named *booleanTRUE* it will always stay in the position which sends the signal from the block *add* directly to the *HPandBuildingEL* output. In this configuration *switch2* is de facto bypassed (the leaving signal goes to *switch3* which as just mentioned is set to always make pass the output from *add*). *Switch1* on the other hand is receiving a constant false signal from the block *not1* this means this means that the signal "zero" arriving from *const2* will pass i.e., no power demand is arriving to the output *Building_el* (which is connected to the input called *From_building_00_16* in *Storage_EL)*

The combined power demand arriving in *Storage_EL* through the input *To_Battery_circuit* is then compared with the signal from *PV_Power* (this signal is provided by the FMU in Joules, converted in Watts in the specific block visible in Figure 6.18, and then sent to the *PV_Power* input port). The power flow in *Storage_EL* will take different (virtual) ways according to the result of the comparison, the two cases will be described below.

*Case 1 (**Combined power demand > PV power available**)* – If the combined power demand is bigger than the PV power available, the latter will be completely self-consumed to satisfy the demand. If the battery[11] (Figure 6.25) State Of Charge (SOC) is above 20% it will be used to further cover the power demand. If the sum of the self-consumed PV power and the power discharged from the battery is not enough to cover the entire combined demand, the difference will be calculated as power coming from the grid (in the block *Power_from_grid* visible in the bottom right corner of Figure 6.18) and metered as such.

---

[11] developed by (The Regents of the University of California (through Lawrence Berkeley National Laboratory), n.d.)
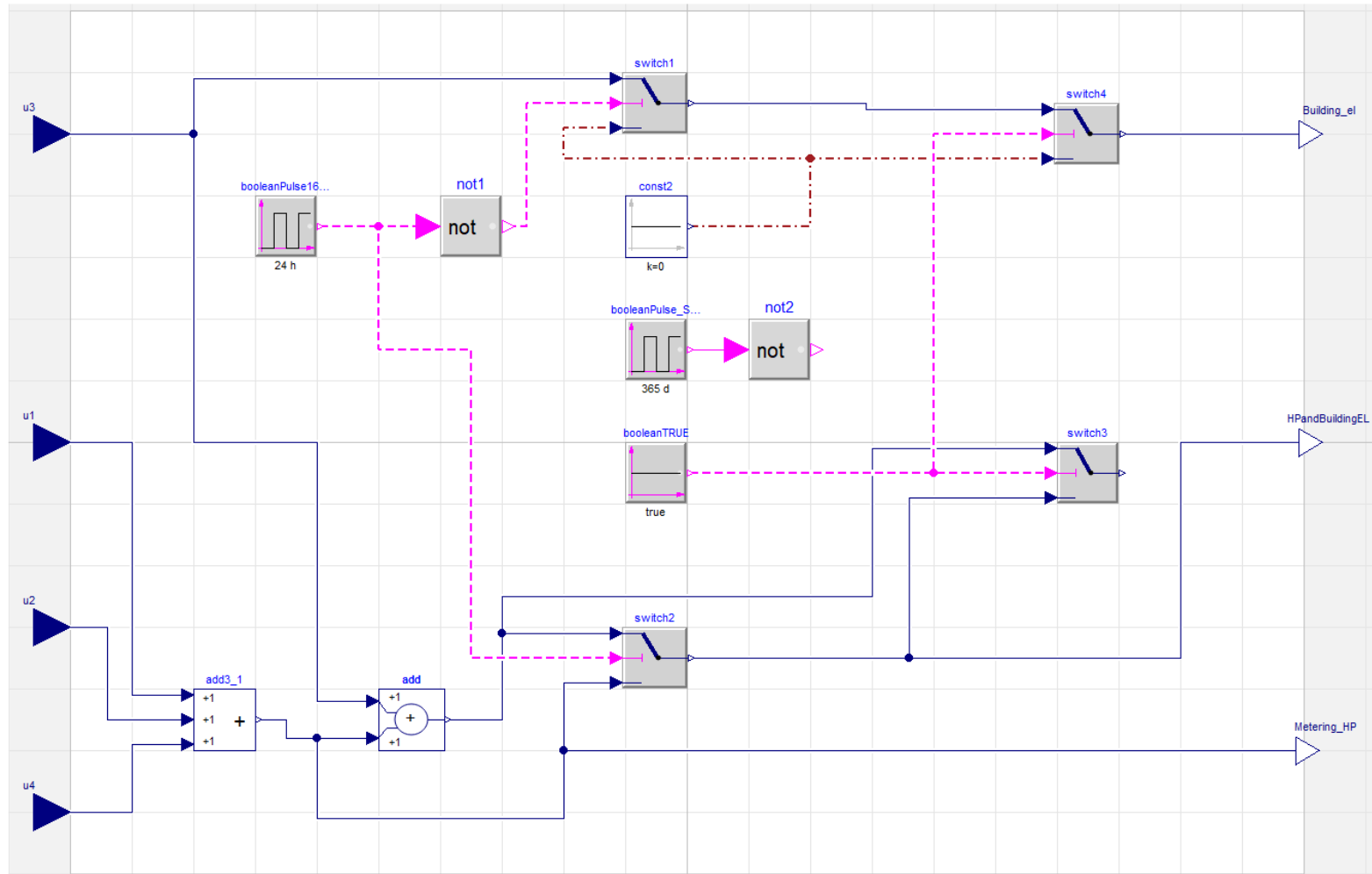
Figure 6.24 Control logic set for Scenario 2

Case 2 (Combined power demand < PV power available) – If the combined power demand is smaller than the PV power available, the first will be completely covered by the photovoltaic production. The remaining part of solar power will be used to charge the battery, if the SOC is below 99%, otherwise it will be sent to the grid. It is important to underline, that (unlike in the other scenarios) being the signal from *From_building_00_16* always equal to zero all the self-consumption will be metered from the output *Selfcon_Power_16_24* independently from the time of the day (the reason for the presence of two outputs for the self-consumed PV power will be clarified while analysing the control in Scenario 2).

In order to facilitate the understanding of the control logic flow charts representing each of the three scenarios have been produced and they are shown in Figure 6.28, Figure 6.29 and Figure 6.30

Scenario 2 (*Power_Control* layout as in Figure 6.24)

As aforementioned in Scenario 2 the HPs have the priority in terms of PV power utilisation between 00:00 and 16:00 (with specific exception as already described) and the surplus is stored. After 16:00 the power demand from the building has full access to the battery circuit. This control strategy implies a change in the layout of the *Power_Control* block. A Boolean control named *booleanPulse16_24* manages *swtitch1* (through *not1*) and *switch2*. The control transmits a signal true between 16:00 and 24:00 to the block *not1*, which changes the signal into false before sending it to *swtitch1*. In this way the power demand coming from the building will reach the output port *Building_el* (connected to the port *From_building_00_16* in *Storage_EL)* only in the time window 00:00 to 16:00 (during the other hours the value will be zero). On the other hand, *switch2* will send directly to *HPandBuildingEL* (*switch3* is disconnected in this specific configuration) the power demand coming from the HPs in the hours between 00:00 and 16:00, and the combined power demand (HPs plus building) in the remaining hours of each day.

The logic control in *Storage_EL* explained in Case1, and Case2 in the Scenario 1 section remain valid. There are however differences due to the different power flows arriving to the input ports. In Scenario 1 in fact the power demand arriving from the input *From_building_00_16* is always zero. In this scenario on the other hand there's power (the building demand) "flowing" through that port from midnight to 4pm. As mentioned, "if the HPs demand is satisfied and the battery is full then the PV energy can be used by

the homes appliances to reduce the electricity bought from the grid". To do this the signal provided by *From_building_00_16* is subtracted (in *add5*) the signal leaving the block *add3* (which represent all the power that has not been self-consumed or used to charge the battery).

If the value of the signal leaving *add5* is greater than zero, then the power signal arriving from *From_building_00_16* goes through the blocks *Self_3* and *Self_4* being metered as self-consumed. The difference between the two values (i.e., the signal leaving *add5*) is sent to the grid.

On the contrary if the value leaving *add5* is smaller than 0 (i.e., the power demand from the building is higher than the remaining available power from *add3*) no power will be sent to the grid, the entire power arriving from *add3* will be self-consumed, and the portion of power demand not covered will be calculated as power coming from the grid and metered as such.

After 4pm the signal provided by *From_building_00_16* will be zero, and all the electric demand (from building and HPs) will run through the port *To_Battery_circuit* following the logic described for Scenario 1.

Scenario 3 (*Power_Control* layout as in Figure 6.26)

This scenario is a combination of Scenario 1 and 2 developed to make a better use of the EES and at the same time improve the direct self-consumption of the photovoltaic energy. In this scenario the power control works following the logic of Scenario 2 between January 1st and April 15th, starting from April 16th until the last day of September the control strategy is the same as Scenario 1, from that day on, the working scheme goes back to the one of Scenario 2.

To achieve this kind of control the layout of the *Power_Control* control block has been changed as shown in Figure 6.26. The controls for *switch1* and *switch2* are the same used for Scenario 2, *switch3* (which in this scenario is not bypassed like in Scenario 2 but connected to *HPandBuildingEL*) and *switch4* on the other hand are not connected to *booleanTRUE* but to *booleanPulse_SUMMER*[12]. The latter sends a false signal from day 0 until day 105, and from day 273 until the last day of the year. In the window between days 105 and 273 the signal is true. This means that in the initial (days 0 – 105) and final part of the year (days 273 – 365) *switch4* and *switch2* will stay in a position which allows

---

[12] Signal from *booleanPulse_SUMMER* arrives at *swtich4* after passing the block *and2*

the power flows to be controlled by *booleanPulse16_24* (exactly like in Scenario 2). In the central part of the year (days 105 – 273) *switch4* will be locked on the second input (i.e., the zero coming from *const2*) sending no power demand to the *Building_el* port. In the same time window *Switch2* is locked on the input arriving from the block *add* meaning that for the entire period the sum of the power demand from the HPs and from the building will be sent to the *HPandBuildingEL* output. This replicate exactly the logic in Scenario 1. Concerning *Storage_EL* no changes have been made and it will work like described for Scenario 1 and 2 according to the time of the year.
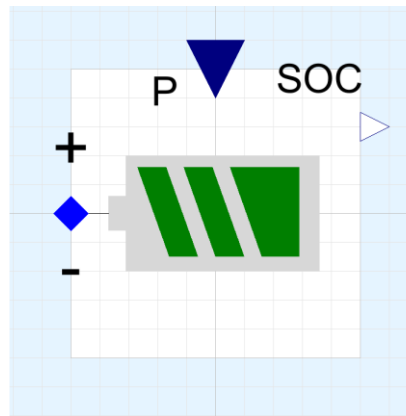
Figure 6.25 Electric energy storage with power port P and SOC output
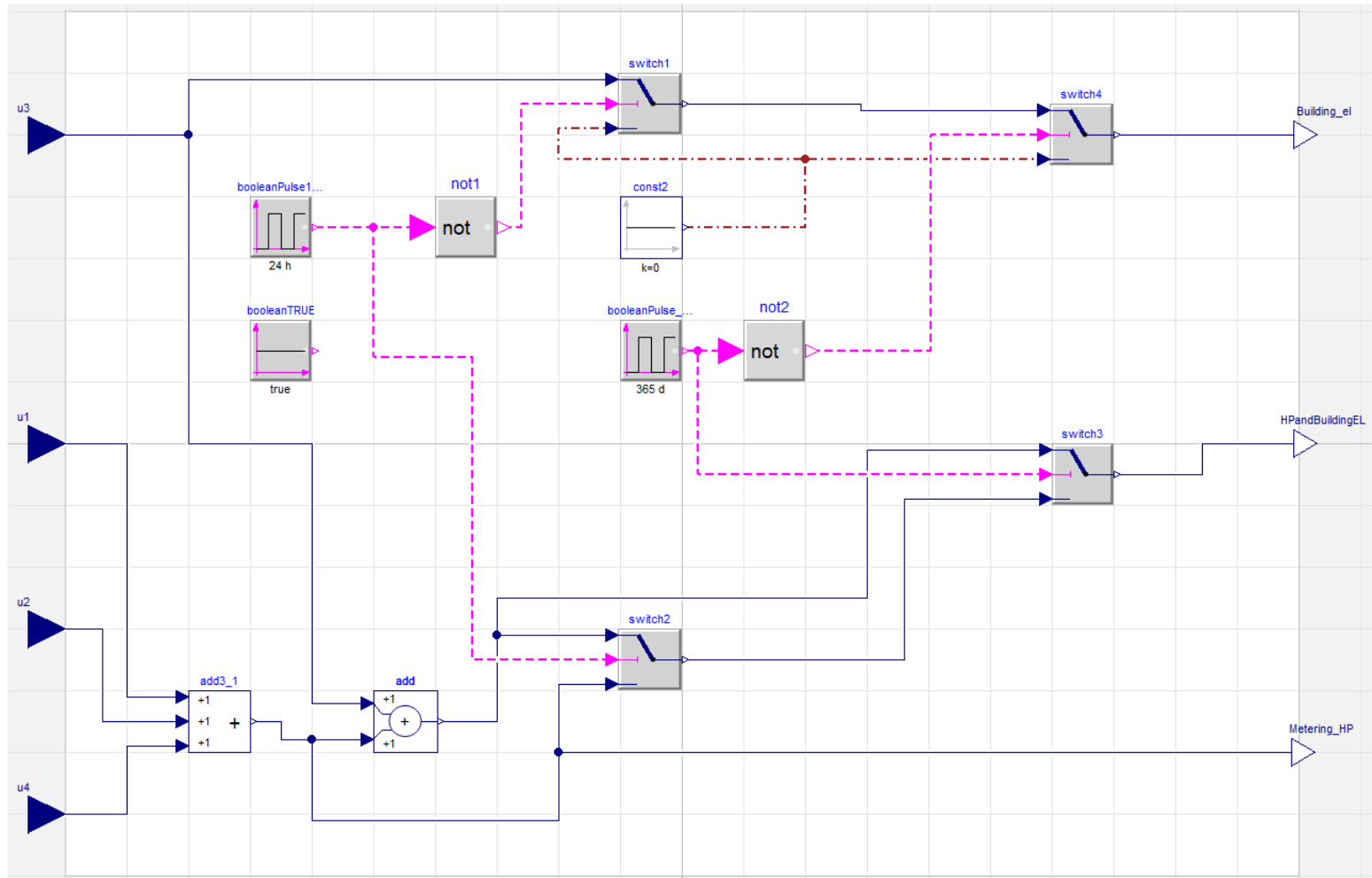
Figure 6.26 Control logic set for Scenario 3
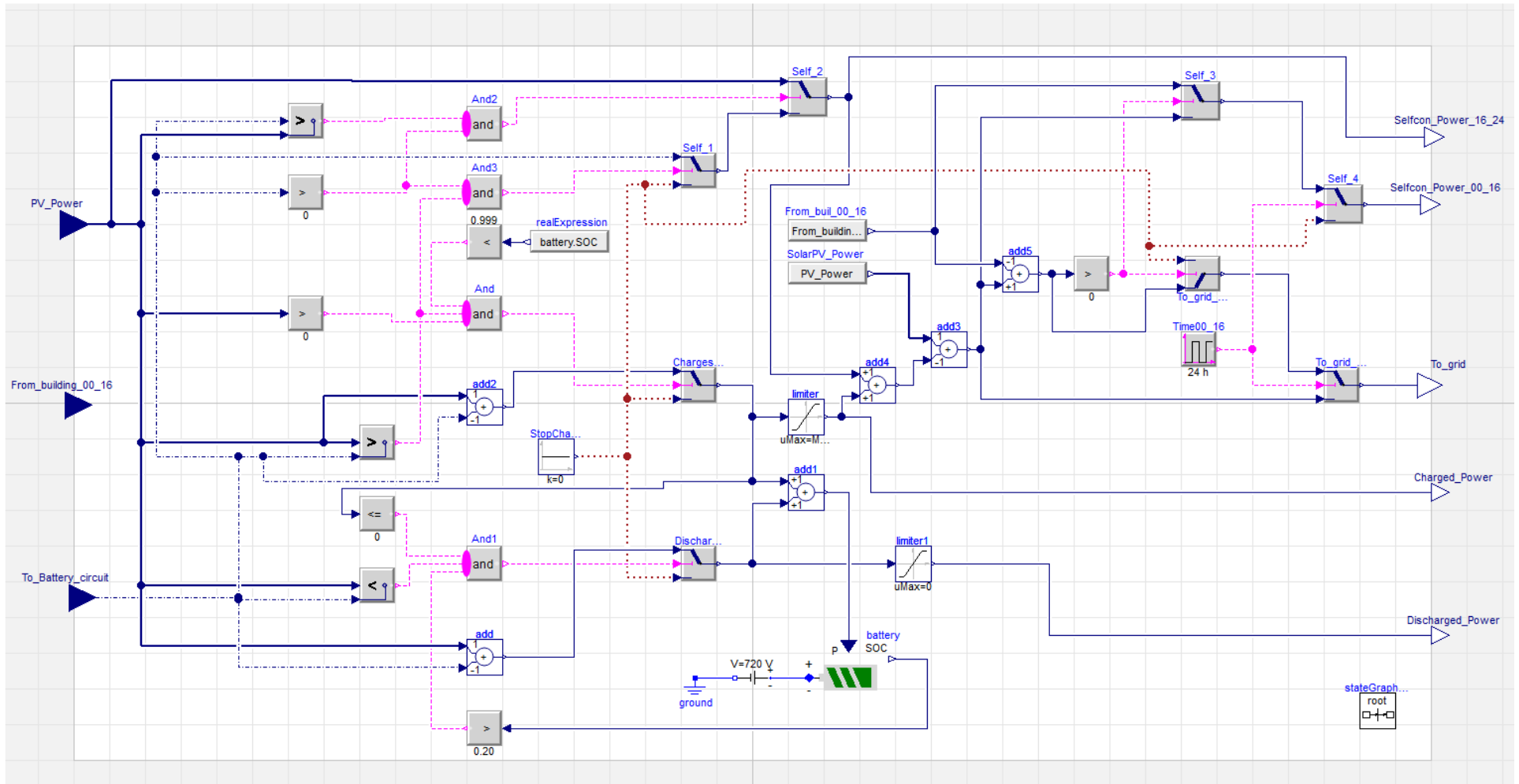
Figure 6.27 Storage_EL block control loop

Figure 6.28 Scenario 1 PV energy control logic.

The flowchart contains the following elements:

Scenario 1*

$P_D = P_{HPs} + P_{build.}$

$P_D > PV$

YES → Battery SOC>20%

    YES → PV completely self-consumed, The battery helps covering the demand, if still not enough power will come from the grid

    NO → PV completely self-consumed, The battery cannot discharge, all the difference between P_D and PV comes from the grid

NO → Battery SOC<99%

    YES → PV covers all the demand and charges the battery.

    NO → PV covers all the demand, battery is full, excess production goes to the grid

*HPs and building electric appliances demand always combined

Scenario 2*

00:00<Time**<16:00

YES → PV > P_{HPs}

YES → Battery SOC<99%

YES → PV completely self-consumed, The battery cannot discharge, all the difference between P_{HPs} and PV comes from the grid

NO → PV covers all P_{HPs}, the battery is full, PV is used to cover also P_{build}. If still there is excess power from the PV is then sent to the grid

NO → Battery SOC>20%

YES → PV completely self-consumed, The battery helps covering the demand, if still not enough power will come from the grid

NO → PV completely self-consumed, The battery cannot discharge, all the difference between P_{HPs} and PV comes from the grid

NO → Control logic like in Scenario 1

*HPs have the priority in terms of PV power utilisation between 00:00 and 16:00
** Time of the day

Figure 6.29 Scenario 2 PV energy control logic.
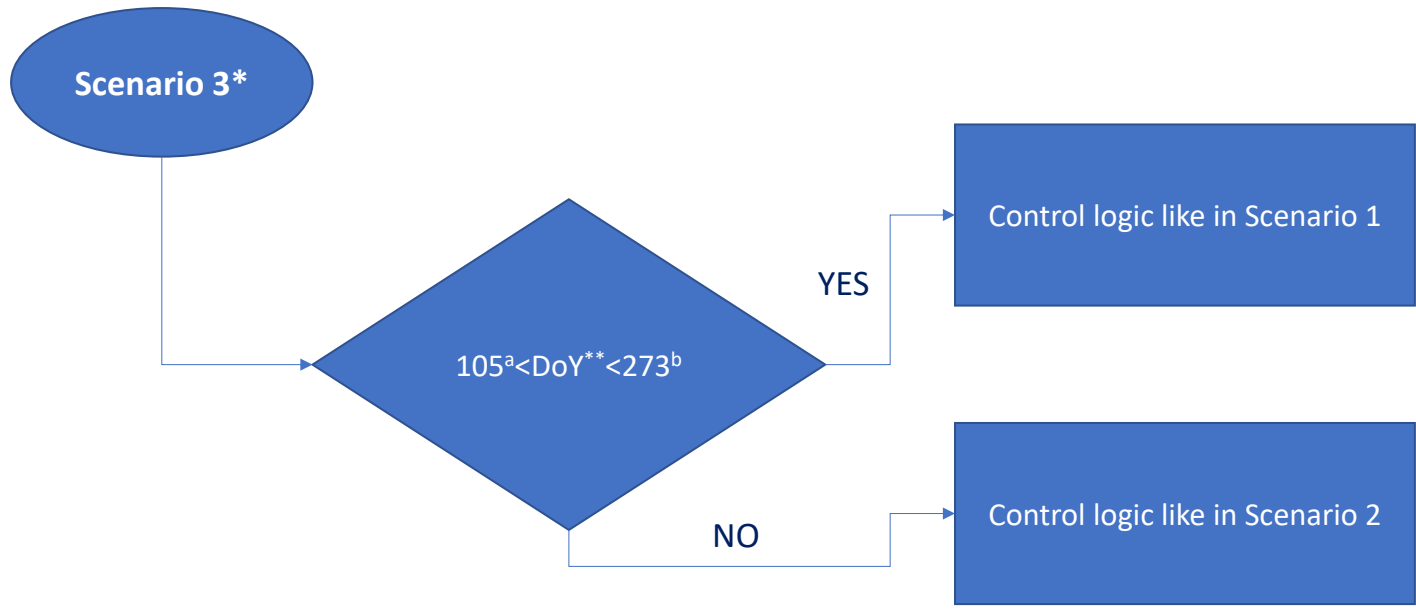
Figure 6.30 Scenario 3 PV energy control logic.

In the flow charts PV indicates the photovoltaic power production, P_{HPs} the power demand from the heat pumps, $P_{build.}$ the power demand from building appliances. P_D is the power demand as sum of P_{HPs} and $P_{build.}$

6.6. Co-simulation numerical results for pilot cluster (10 refurbished homes)

6.6.1. Heating demand pre and post-refurbishment

Before presenting the results from the co-simulation model for the different scenarios a brief overview of the energy performance pre and post-refurbishment in the pilot cluster will be introduced.

As mentioned in 6.2.3 the temperature setpoint is different in different models, in the models representing only the main block the set point and the heating schedules follows the SAP recommendations (6.4.1) in all the co-simulation models on the other hand the target temperature is the one indicated in Table 6.3 and the heating schedule is the one in Table 6.5.

The heat demand in the 7 homes in the main block before the refurbishment varies between 12999 kWh$_{th}$/year and 8291 kWh$_{th}$/year, depending on the home position (with mid-terrace homes having the lower SH demand) and between 11827 kWh$_{th}$/year and 9928 kWh$_{th}$/year in the three bungalows.

The floor area of each home in the main block is 88 m², whereas each bungalow has an internal area of 47.5 m². Considering this the space heating energy demand can be expressed in terms of kWh$_{th}$/m²year, the resulting value vary between 147.8 kWh$_{th}$/m²year and 94.3 kWh$_{th}$/m²year for the terraced homes, with an average of 119.3 kWh$_{th}$/m²year. The bungalows heat demand goes from a maximum of 235.1 kWh$_{th}$/m²year in the end-terrace bungalow and a minimum of 208.6 kWh$_{th}$/m²year in the mid-terrace, the average heat demand for the bungalows is 224 kWh$_{th}$/m²year.

After the refurbishment the heat demand drops to an average of 5737 kWh$_{th}$/year in the terraced homes and 4406 kWh$_{th}$/year in the bungalows. In terms of kWh$_{th}$/m²year the value is 55.14 kWh$_{th}$/m²year for the terraced houses in the block and 92.61 kWh$_{th}$/m²year for the bungalows. As mentioned in paragraph 5.3.1 a new room was added to each of the terraced homes, increasing the internal surface to 104 m². The total reduction in heat demand is around 45% in the terraced houses and close to 59% in the bungalows, but unlike the pre-refurbishment building this heat will now be supplied by an HP system.

6.6.2. Energy production and utilisation results

The following charts (Figure 6.31 to Figure 6.33) show the energy details of the different scenarios, whereas Table 6.12 provides numeric data about the energy production and consumption:
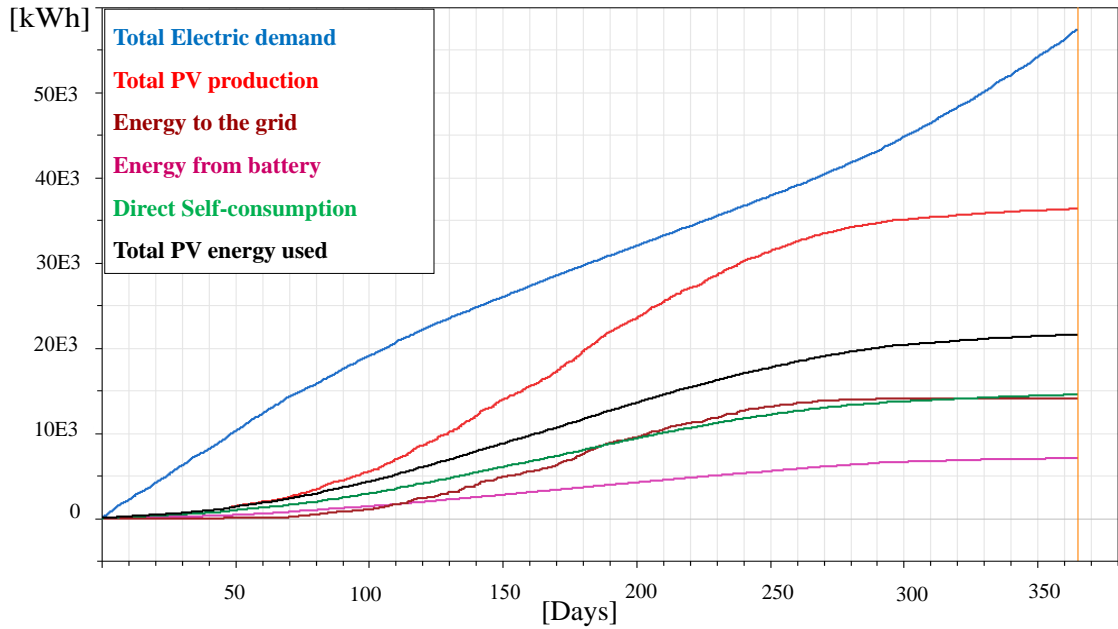
Figure 6.31 Scenario 1 Energy details (pilot cluster model)
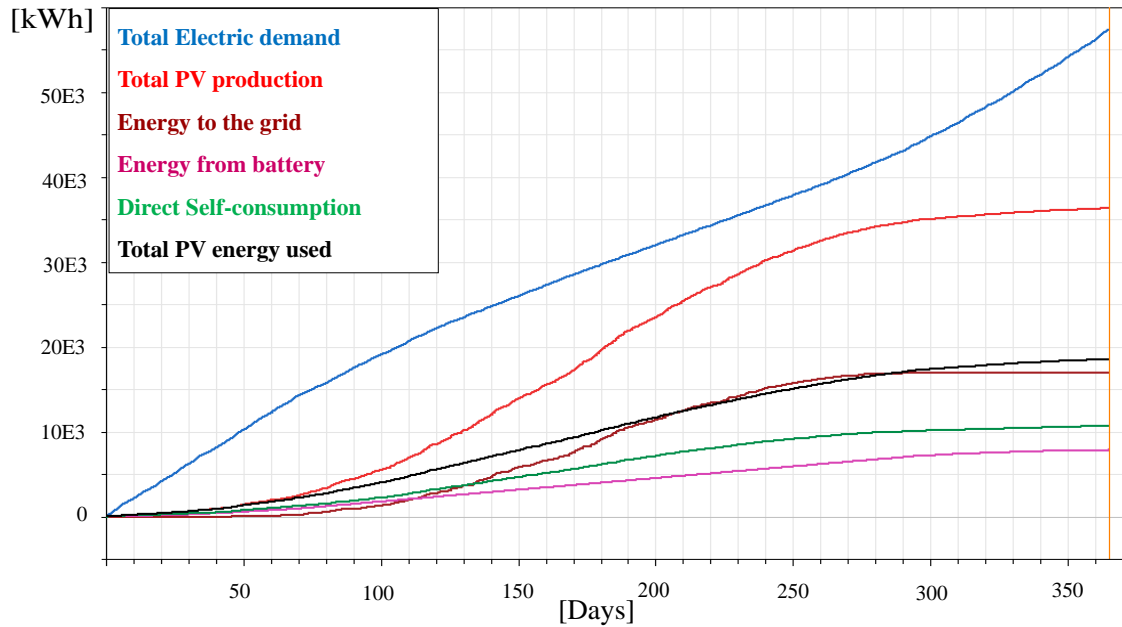
Figure 6.32. Scenario 2 Energy details (pilot cluster model)
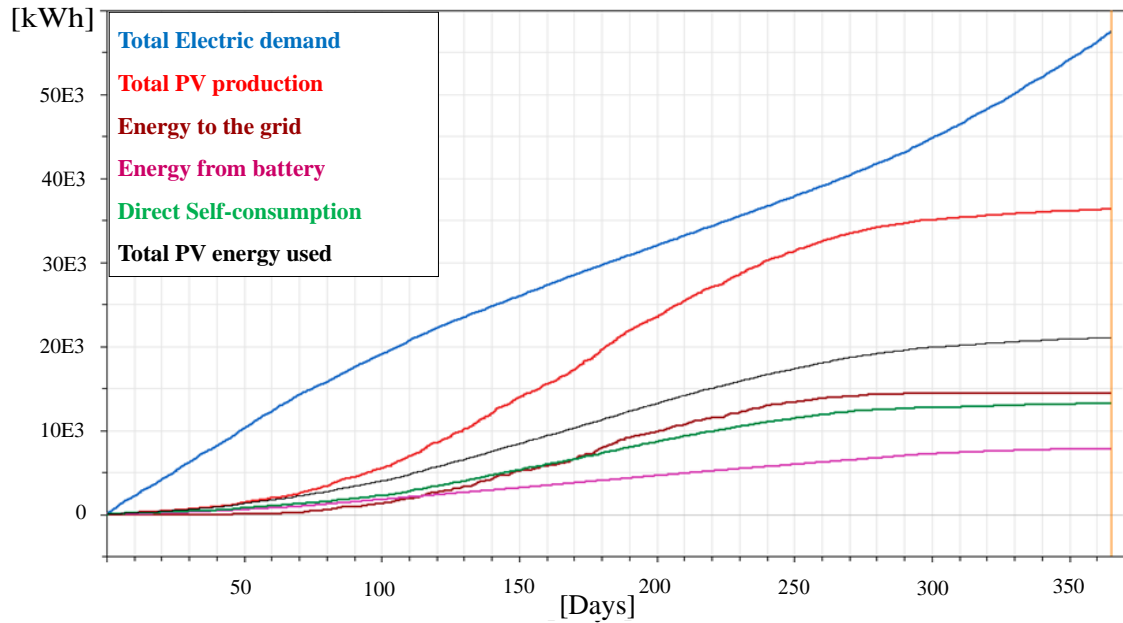
Figure 6.33. Scenario 3 Energy details (pilot cluster model)

Table 6.12 Energy utilization details in the three scenarios (pilot cluster model)

	SCENARIO 1 [kWh]	SCENARIO 2 [kWh]	SCENARIO 3 [kWh]
Tot. Elec. Demand	57448	57448	57448
PV Production	36357	36357	36357
Total PV Used	21582	18569	21107
Direct Self-cons.	14549	10713	13267
Energy from battery	7033	7856	7840
Energy to the grid	14064	16991	14455
Share of PV used	59.4%	51.1%	58.1%

Important, to define the behaviour of the system and define the most effective control scheme, is to compare the total amount of electricity bought between 16:00 and 19:00 when the price is at its maximum, these values are displayed in Figure 6.34 and Table 6.13.
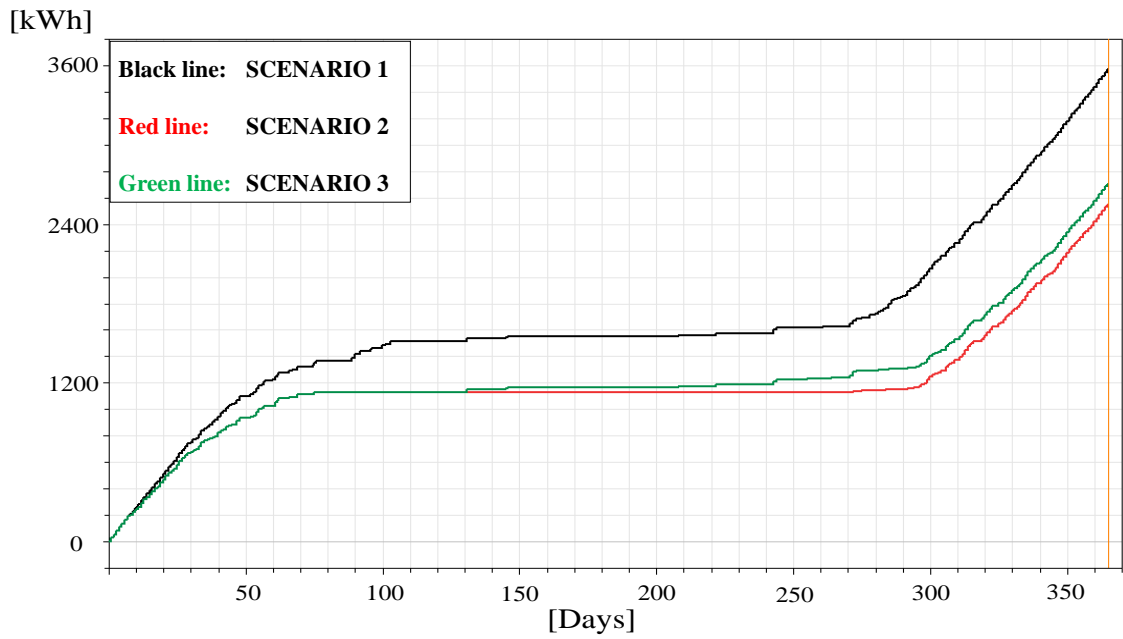
Figure 6.34 Energy bought from the grid between 4 and 7pm (pilot cluster model)

Table 6.13 Pilot case study, energy from grid 4-7pm (pilot cluster model)

	SCENARIO 1 [kWh]	SCENARIO 2 [kWh]	SCENARIO 3 [kWh]
Energy bought from grid between 4 and 7pm	3569	2543	2698

6.7. Co-simulation modelling: expanded case study 27 refurbished homes

When the case study was expanded going from 10 refurbished homes to 27 refurbished homes the co-simulation model had to be modified to replicate these changes. Thanks to its the modularity however the model is relatively easy to scale up and modify.

As first thing the FMU had to be replaced with a new one representing the new, bigger, case study, this process has been explained in paragraph 6.3.5.
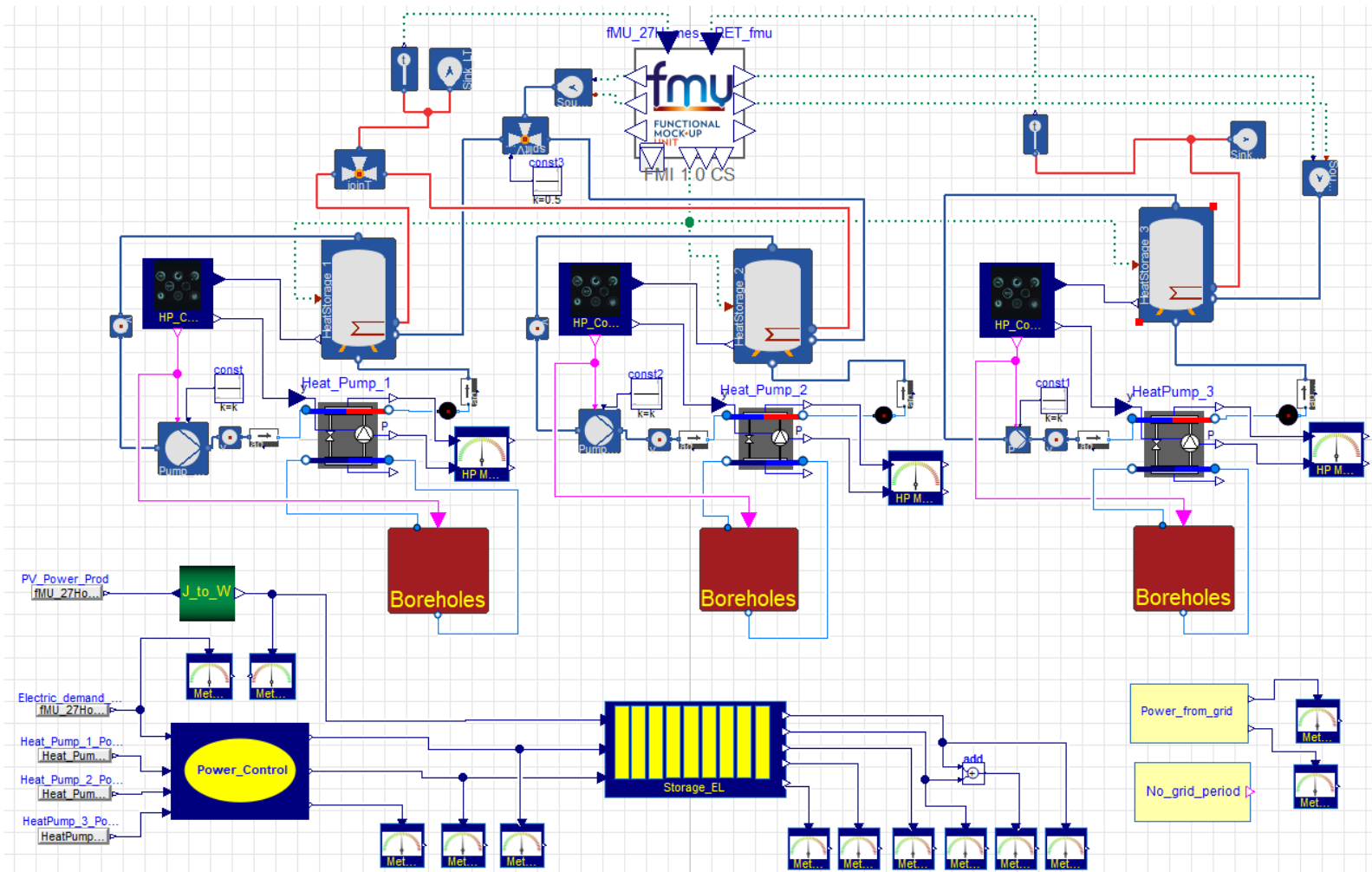
Figure 6.35 High level view of the co-simulation model of the extended case study in Dymola

Reflecting the interventions in the case study an additional HP circuit was added duplicating one of the two already present. The properties of several components had to be updated to reflect the interventions on the real energy centre, the most important changes regard:

- HPs technical specifications (as specified in paragraph 4.4)
- Thermal storage size (three tanks of 4 m³ each)
- Electric energy storage capacity (from 36 to 40 kWh)
- Boreholes number (from 5 to 19)

All the changes have been applied very easily just changing the specifications of the components (for example the volume of each tank). Only the *Boreholes* block required some additional work, mainly to build a system more flexible and easier to scale than the one in Figure 6.20. The first approach was a simple expansion of the initial configuration, and it is shown in Figure 6.36.
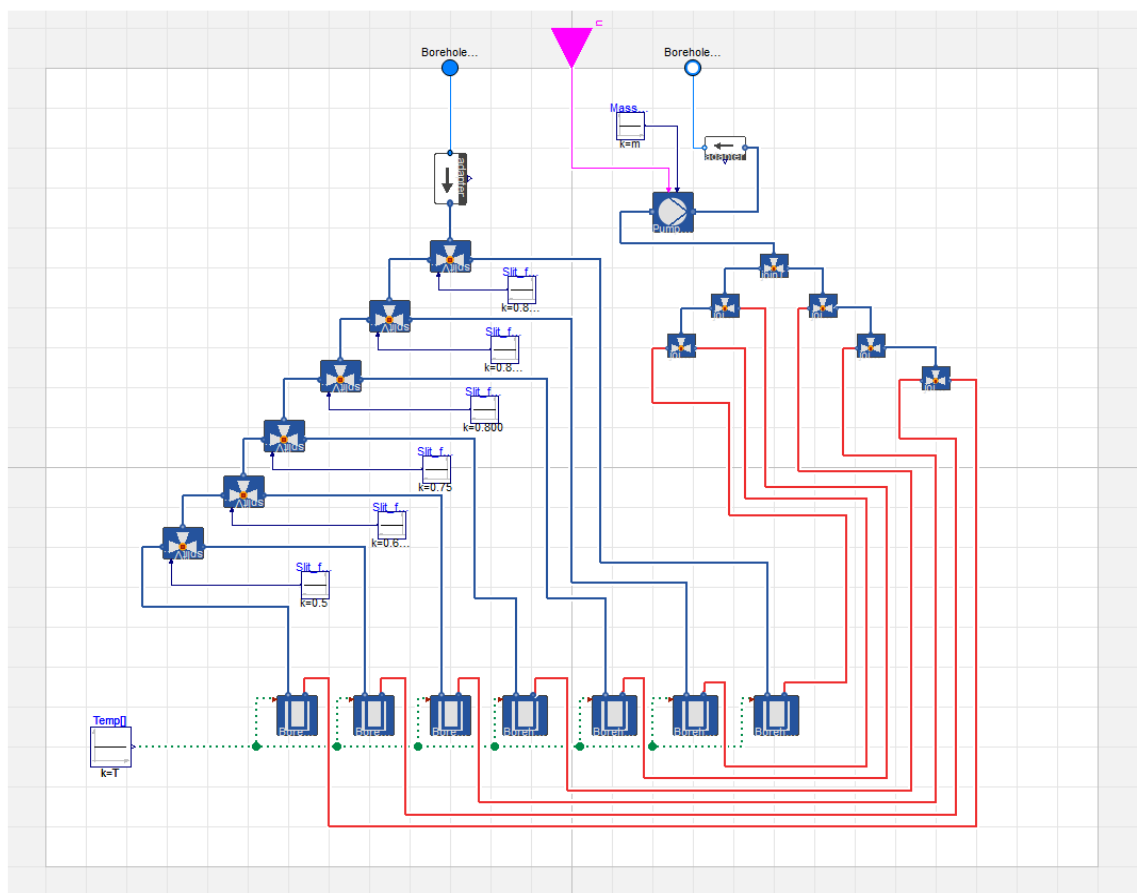
Figure 6.36 Boreholes block layout with 7 boreholes inside

It is visible how complex was the system in terms of connections (which makes the use of the component more open to errors), furthermore the split factor in each split valve had to be calculated by the user according to the number of boreholes, introducing again an error-prone process, especially considering that each value had to be inserted manually. Considering this, the increased computational time, and the difficulty of scaling the system, another block called *Boreholes_NEW* was developed (Figure 6.37).
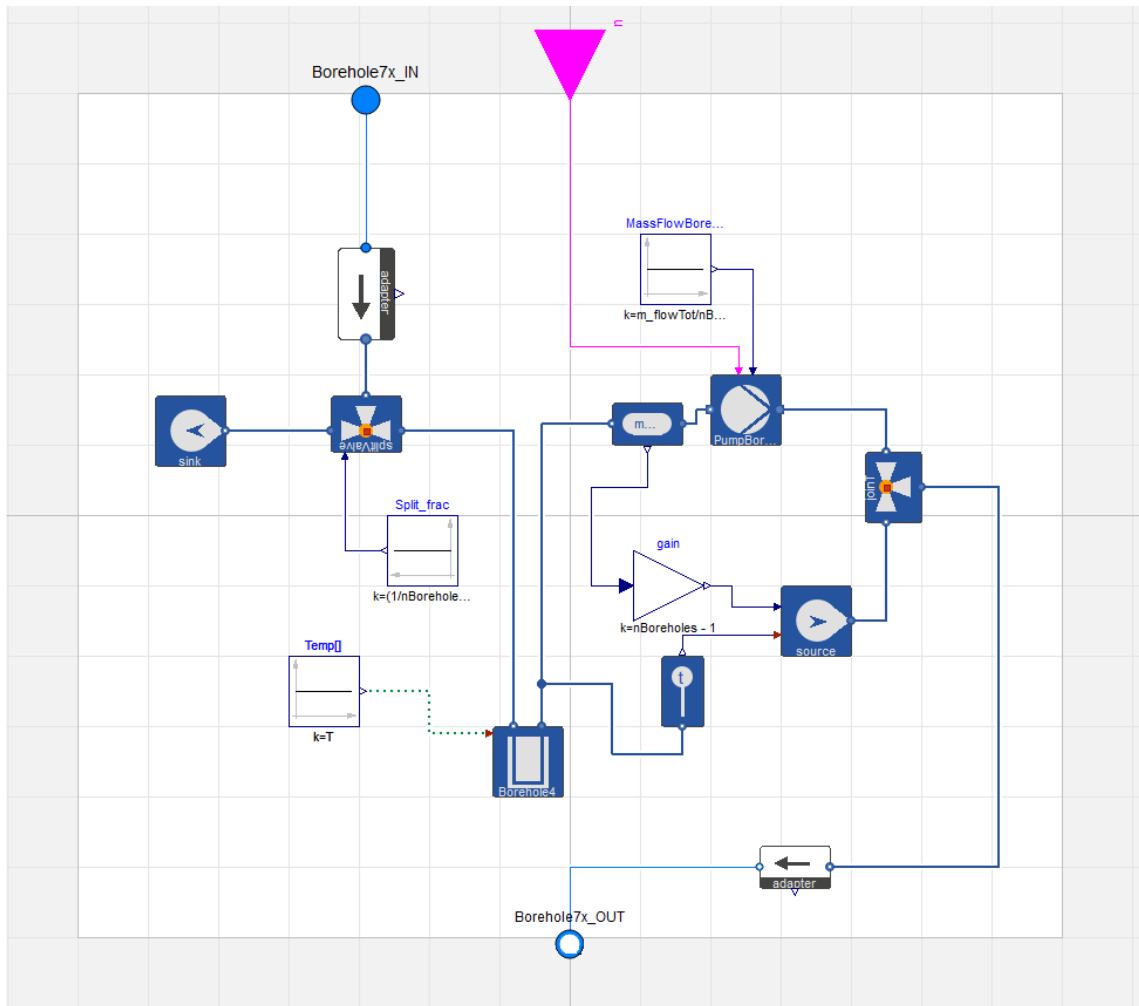
Figure 6.37 Scalable Boreholes block

In the model the different boreholes present into the *Boreholes* block do not interfere with each other and the fluid temperature at the out port of every single borehole is the same (as long as the mass flow through them is the same). In the light of this, in *Boreholes_NEW* a single borehole is present, the total mass flow arriving from the HP is split so that the mass flow reaching the borehole is equal the ratio between the total mass flow and the number of boreholes. To do so the split factor provided to the valve by the block *Split_frac* is equal to the following equation:

$$k = \left(\frac{1}{nBoreholes} \right) \cdot (nBoreholes - 1) \qquad \text{Eq. 6-3}$$

Where nBoreholes is the number of boreholes that the user wants to simulate. The secondary branch of the *splitValve* is connected to a fluid sink to preserve the mass balance. The mass flow of the fluid leaving the borehole is multiplied in order to restore the initial mass flow and sent to the output *Borehole7x_OUT*. Concerning the fluid temperature, it will be the one fluid leaving the single borehole. Comparative simulations were run to ensure that the output values from the old block *Boreholes* and from *Boreholes_NEW* do not differ. The two blocks provide identical results but the newer one is much faster in terms of computational time, more flexible, versatile, and user friendly considering that only requires to insert the value of the total mass flow and the number of boreholes that the block has to represent.

6.8. Co-simulation numerical results for the expanded case study (27 refurbished homes)

6.8.1. Heating demand pre and post-refurbishment

Like for the pilot cluster also for the expanded case study an overview of the heat demand pre and post-refurbishment will be provided. In the expanded case study 14 out of 27 refurbished homes are terraced homes, the remaining 13 dwellings are bungalows. The heat demand before the refurbishment of the 14 terraced houses vary between 14972 kWh_{th}/year and 8218 kWh_{th}/year, again depending on the home position, in the bungalows on the other hand the heat demand is in a range between 11170 kWh_{th}/year and 9635 kWh_{th}/year.

In terms of kWh_{th}/m²year, the results vary between 170.2 kWh_{th}/m²year and 93.4 kWh_{th}/m²year for the terraced houses, with an average of 121.4 kWh_{th}/m²year. The bungalows heat demand goes from a maximum of 234.8 kWh_{th}/m²year and a minimum of 202.6 kWh_{th}/m²year, the average heat demand for the bungalows is 210.4 kWh_{th}/m²year.

After the refurbishment, the heat demand drops to an average of 6060 kWh_{th}/year in the two blocks and 4221.6 kWh_{th}/year in the bungalows. In terms of kWh_{th}/m²year the value is 58.2 kWh_{th}/m²year for the terraced homes and 88.7 kWh_{th}/m²year for the bungalows. These values are equivalent to 43.2% reduction of the heat demand in the terraced houses and almost 58% in the bungalows,

6.8.2. Energy production and utilisation results

The charts represented in Figure 6.38, Figure 6.39 and, Figure 6.40 display the details in terms of energy utilisation between the different scenarios. These details are shown in numerical terms in Table 6.14.
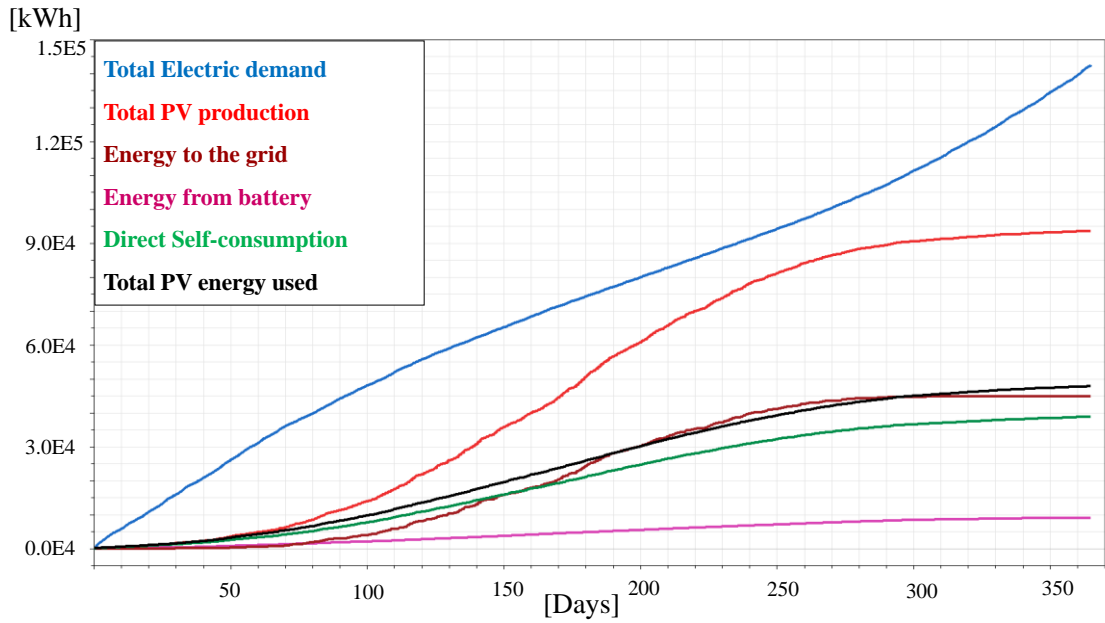
Figure 6.38 Scenario 1 Energy details (expanded case study model)
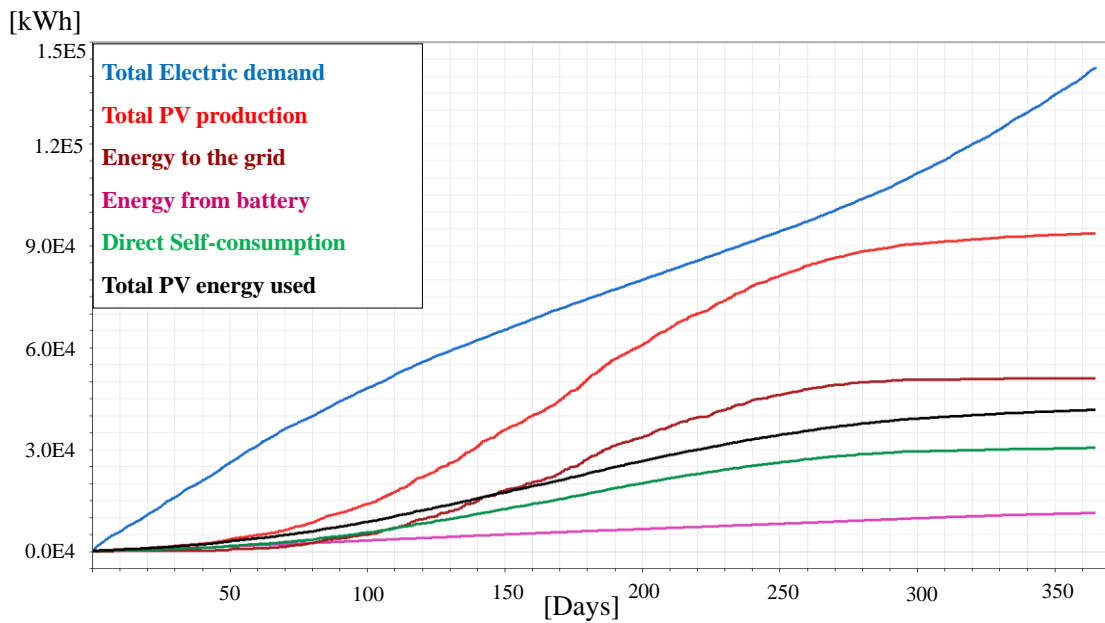
Figure 6.39 Scenario 2 Energy details (expanded case study model)
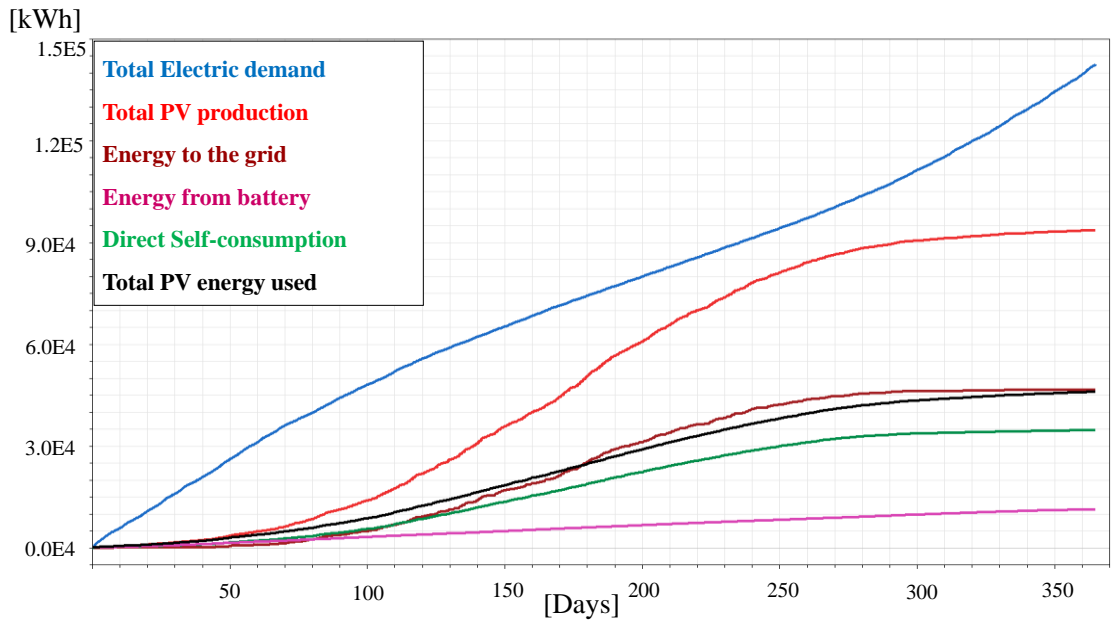
Figure 6.40 Scenario 3 Energy details (expanded case study model)

Table 6.14 Energy utilization details in the three scenarios (expanded case study model)

	SCENARIO 1 [kWh]	SCENARIO 2 [kWh]	SCENARIO 3 [kWh]
Tot. Elec. Demand	142533	142533	142533
PV Production	93640	93640	93640
Total PV Used	47844	41651	45998
Direct Self-cons.	38840	30449	34723
Energy from battery	9005	11201	11275
Energy to the grid	44881	50844	46488
Share of PV used	51.1%	44.5%	49.1%

Figure 6.41 and Table 6.15 summarise the data regarding the electric energy bought from the grid during the cost peak time.
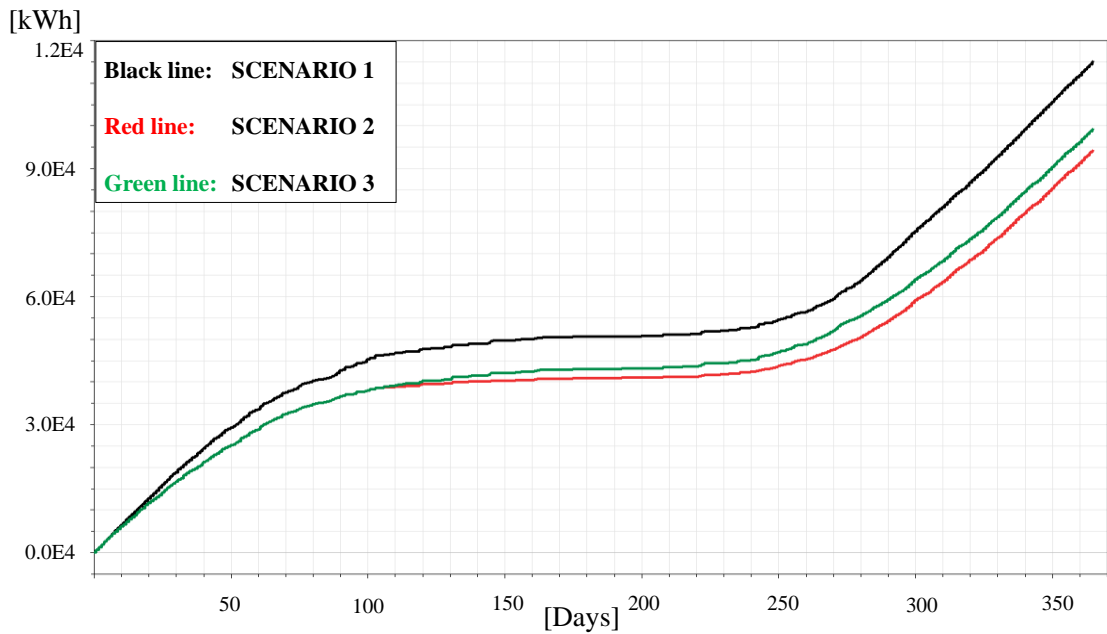
Figure 6.41 Electricity bought from the grid during peak time (expanded case study model)

Table 6.15 Expanded case study, energy from grid 4-7pm

	SCENARIO 1 [kWh]	SCENARIO 2 [kWh]	SCENARIO 3 [kWh]
Energy bought from grid between 4 and 7pm	11508	9426	9923

6.8.3. Test with 72 kWh battery, numerical results

A further analysis has been carried out to understand the effect of a bigger EES on the system. The 36 kWh battery of the pilot cluster has been replaced in the expanded case study with a 40 kWh one, a rise in storage capacity not in line with the augmented PV power installed and increased electricity demand. On these bases a model with a 72kWh battery (twice the size of the one in the pilot cluster) has been created looking for potential benefits.
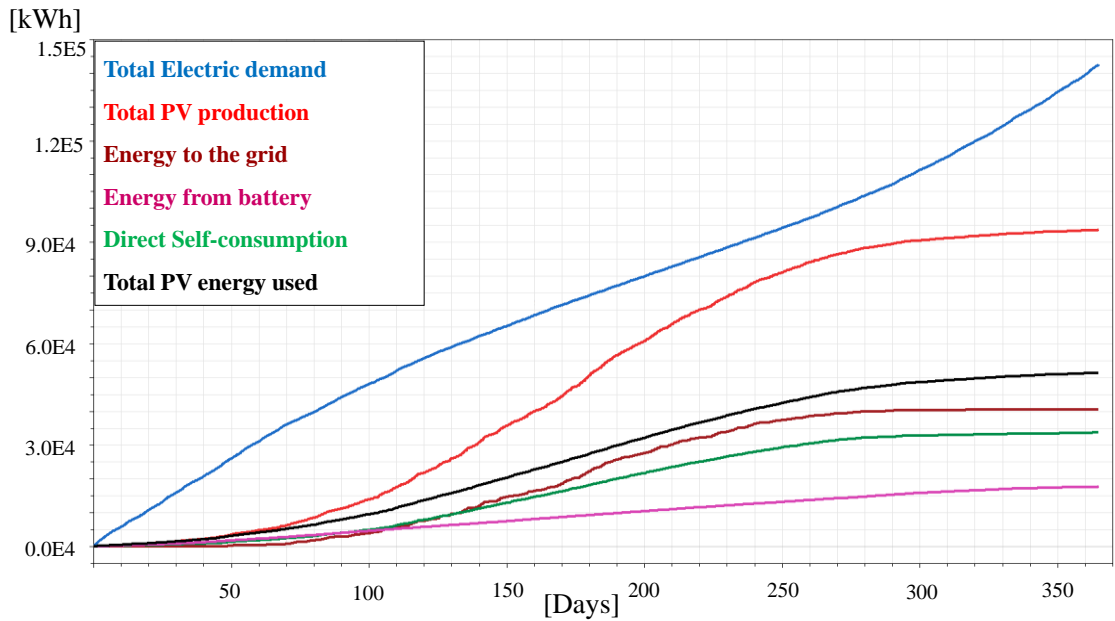
Figure 6.42 Scenario 3 Energy details with 72 kWh storage (expanded case study model)

Figure 6.42 Table 6.16 summarise the details about the energy utilisation in the model with a 72kWh battery, whereas Figure 6.43 in clearly showed the reduction in the amount of electricity bought from the grid during the peak hours.

Table 6.16 Energy utilisation breakdown with different battery capacity

	SCENARIO 3 (40 kWh battery) [kWh]	SCENARIO 3 (72 kWh battery) [kWh]	Δ
Tot. Elec. Demand	142533	142533	-
PV Production	93640	93640	-
Total PV Used	45998	51372	5374
Direct Self-cons.	34723	33687	-1036
Energy from battery	11275	17686	6411
Energy from the grid	96535	91161	-5374
Energy from the grid peak time	9923	6729	-3194
Energy to the grid	46488	40466	-6022
Share of PV used	49.1%	54.9%	+5.8%
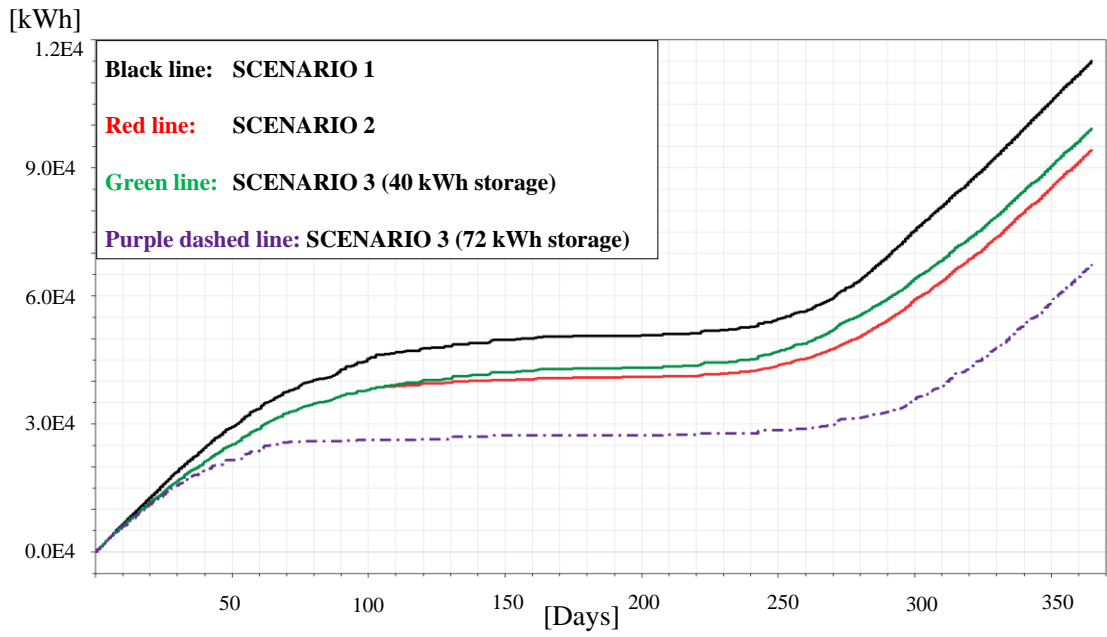
Figure 6.43 Electricity bought from the grid during peak time (expanded case study model with 72 kWh storage)

Chapter 7: Model validation

The model has been validated comparing heat demand metered in the case study with the one obtained by the co-simulation model. Before presenting the data is necessary to point out some particularities of the case study and some modification that have proved to be necessary in order to calibrate the model. It must be taken into account that the occupancy level considered in DesignBuilder for the various homes comes from the National Calculation Methodologies (NCMs), this means that the values are averaged and not representative of a particular case study, where a number of homes can be occupied by single, retired, elderly people and distort the expected energy consumption. To compensate this discrepancy and calibrate the model two homes in the pilot cluster model and four in expanded case study model have been modelled with different temperature setpoints (the maximum temperature has been set at 18°C in both bathrooms and bedrooms) and with a reduced number of heating hours (63 hours per week instead of 77). The new set point has been set taking into account the values suggested by SAP, the author decided this in order to have a valid reference, lower values in fact would have been arbitrary. The decision of reducing the heating hours on the other hand has been taken to simulate the behaviour of elderly people which showed the propensity to use the heating for less time. Furthermore, this reduction partially compensates the difference in Degree-day (as seen in 6.2.1) between the actual weather and the input standardised weather. In order to define the amount of heating hours SAP was again taken as reference, 63 hours per week of heating represents in fact the extension to the weekend of the heating pattern suggested for the workdays. The values of the heat demand measured in this case study have been calculated as an averaged value not considering two homes (one bungalow and one in the main block) that show completely unpredictable energy consumption and huge gaps in the metering. This process has been necessary because the co-simulation tool provides the total value (for the whole cluster or district) of the energy demand and not the value for every single house. In order to have a consistent comparison the average value of the energy demand from the homes in the main block (excluded one as already said) have been calculated and then multiplied for the total number of homes in the main block, compensating the unreliable data from one house. Same process have been applied to the bungalows. The reason for the unpredictable data is probably due to the previous circumstances in which residents used to live. For example, elderly people that spent many years in conditions of fuel poverty show the tendency to reduce the

temperature settings in their home for "comfort" reasons (especially in the bedrooms) and in some cases to completely switch off the heating or close the radiators in some rooms without following any kind of pattern, leading to unpredictable results.

Analysing the heat consumption (comprehensive of SH and DHW demand) from 10 homes in November (2018), December (2018), January and February (2019) demonstrate a very close correlation between the metered data and the simulated one (Figure 7.1), with a difference between the two values of 1.74%, 0.3%, 2.25% and 2.13% in November, December, January, and February respectively, these values stay within the allowable difference (Rahman, Rasul and Khan, 2010). The importance of the calibration process appears clearly showed in Figure 7.2, the simulated results in fact, were showing a very weak correlation with the measured data, the percentage difference between simulated and measured data was, in fact, of 5.56%, 3.97%, 5.45% and 5.98% in November, December, January, and February respectively.
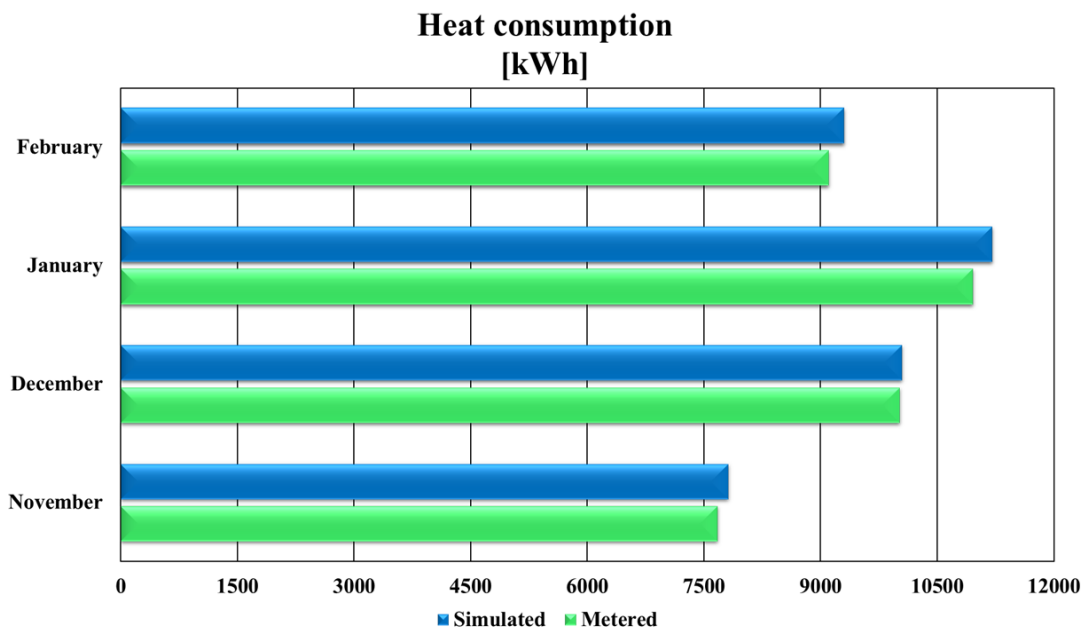
Figure 7.1 Comparison between metered and simulated heat demand in the calibrated model
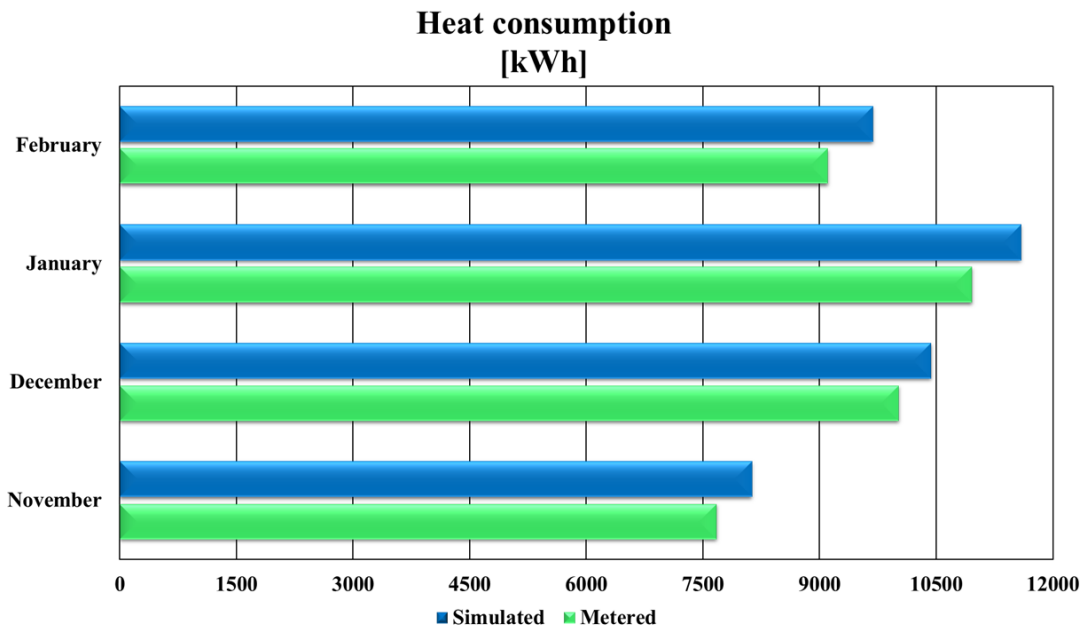
Figure 7.2 Comparison between metered and simulated heat demand in the not calibrated model

Analysing the results of the simulation accordingly to the methods suggested by ASHRAE-14 (ANSI/ASHRAE, 2002; Ruiz and Bandera, 2017) it is possible to calculate both the Normalized mean bias error (NMBE) and the Coefficient of variation of the root mean square error (CVRMSE), respectively calculated as:

$$NMBE = \sum\nolimits^{n} \frac{(y_i - \hat{y}_i)}{(n-p) \cdot \bar{y}} \cdot 100 \qquad \text{Eq. 7-1}$$

And

$$CVRMSE = 100 \cdot \left[\sum (y_i - \hat{y}_i)^2 / (n-p) \right]^{\frac{1}{2}} \Big/ \bar{y} \qquad \text{Eq. 7-2}$$

Where:

n = number of data points

p = 0 (NMBE) (Ruiz and Bandera, 2017)

p = 1 (CVRMSE) (Ruiz and Bandera, 2017)

y_i = measured data

$\hat{y}_i$ = simulated data

$\bar{y}$ = arithmetic mean of the sample of n observations

Calculating the NMBE and CVRMSE before the calibration is possible to see how the NMBE exceeds the limits set by ASHRAE-14 (Table 7.1).

Table 7.1 NMBE and CVRMSE values from the pre-calibration model and limits

	Calculated	Objective
NMBE	**-5,50%**	-5%<NMBE<5%
CVRMSE	6,44%	<15%

On the other hand, using the results from the calibrated model both NMBE and CVRMSE are well within the limits set by ASHRAE-14 (Table 7.2), confirming the validity of the model.

Table 7.2 NMBE and CVRMSE values from the calibrated model and limits

	Calculated	Objective
NMBE	-1,63%	-5%<NMBE<5%
CVRMSE	2,13%	<15%

Chapter 8: Discussion of the results and conclusion

8.1. Results discussions for the first model of the post-retrofitting case study (main block 7 refurbished homes)

As mentioned in 6.4.2 three different cases have been simulated for the first model which includes the only the homes in the main block. In this chapter results from the simulations will be discussed.

In **Case 1** (Table 6.9) the energy demand reduction is the lower among the 3 simulated cases, this is due to the higher average temperature in the houses and to the continuous operation of the heating system. At general level, the reduction is around 12.5% but is clearly visible how the heat demand increases in the terraced houses adjacent to the not refurbished and not heated ones. The reduction in heat demand decreases from 27.5% to 4.6%. In two houses the heat demand is even higher than the one in the pre-refurbishment building. The benefits of the refurbished building envelope are in fact cancelled by the increased average temperature setpoint, higher number of heated hours and adjacency with two "cold" homes.

Case 2 (Table 6.10) represents the comparison between the original building and the actual refurbished case study in which two terraced homes are neither refurbished nor heated. The heating in this case follows the same set points of the pre-refurbishment building as for Table 6.5. The reduction in heat demand is consistent, 45.4% considering the entire block. The decrease however is much higher in the terraced homes that are not influenced by the two not refurbished houses, with the heat demand dropping as much as 55.3%. The homes in contact with the two cold houses still show a reduced heat demand compared to the pre-refurbished situation, but the decrease in heat demand is, in this case, around 36.7% (averaged value for the three homes adjacent to the not retrofitted ones). The heat sink effect due to the cold houses is well represented in Figure 8.1 The chart shows the average monthly temperature in the lounge rooms of house I and F. It is clearly visible how the lounge in terraced home F has an average temperature roughly 3°C higher in winter months compared to the lounge in house I. The latter in fact shares only one wall with a heated home, while home F is surrounded by heated areas. As the partition between the terraced homes is a simple reinforced concrete wall the heat flow through it is high. De facto house F is partially heated by the surrounding homes, same happens to house I but in smaller terms as there is only one shared wall.

Temperature comparison
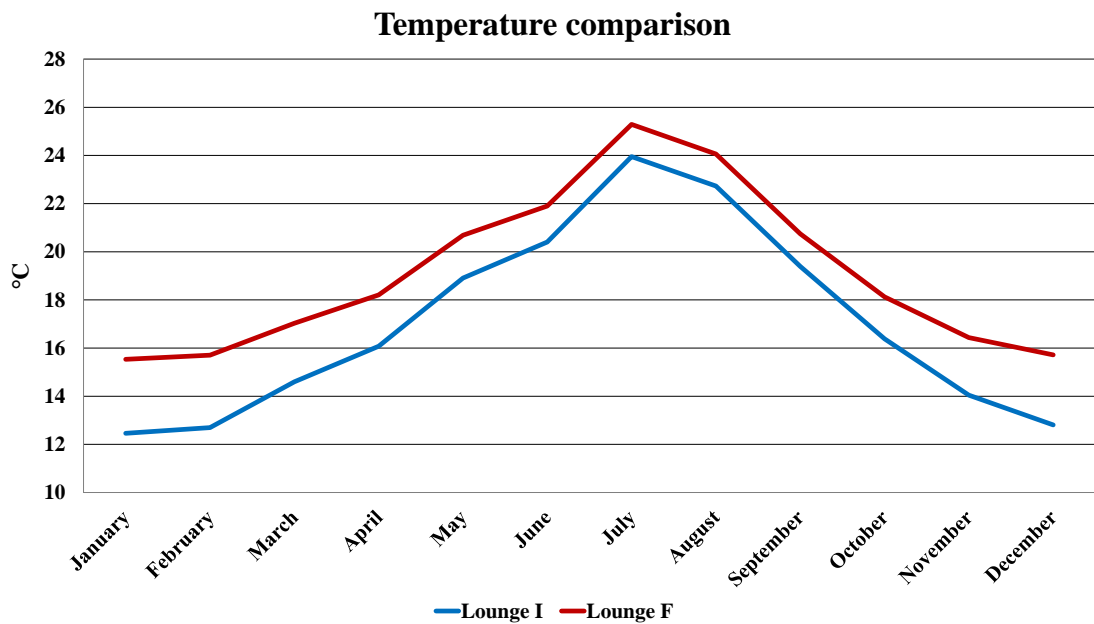
Figure 8.1 Temperature comparison in the lounge of two not-refurbished buildings

Case 3 (Table 6.11) has been modelled with the purpose of analyse the potential effect of a full block refurbishment. The results are significant, the heat demand drops by 53.5% in the entire block[13]. This analysis shows that the total energy demand is lower than in case 2 (even if only by roughly 310 kWh) with two more homes heated and comfortable, highlighting the detrimental effect of the non-refurbished dwellings.

In this model, under the hypothesis of using the PV energy only to cover the GSHP consumption, an analysis of the impact of the retrofitting on the GHGs emission has been carried out. The simulation shows that the PV plant can produce a total of about 24200 kWh of electricity distributed during whole year as in Table 8.1. A mismatch between HP demand and PV production is (as expected) present.

---

[13] It is important to underline again that Case 3 has been compared with the results of the pre-refurbished model in which all the 9 homes in the block are heated, case 1 and 2 have been compared with the model including only 7 heated homes.

Table 8.1 Photovoltaic energy production and electricity for SH and DHW (Case 2)

Month	Production (kWh)	Electricity for SH and DHW (kWh)
January	460.5	3008.6
February	860.9	2703.9
March	1717.0	1916.1
April	2692.4	1098.3
May	3234.3	467.9
June	3226.9	414.9
July	3085.6	374.6
August	3059.1	378.8
September	2923.4	466.4
October	2074.4	1022.6
November	517.9	2131.8
December	319.1	2959.3
Total	24171.7	16943.3

A visual representation of the mismatch between PV production and GSHP energy consumption is shown in Figure 8.2
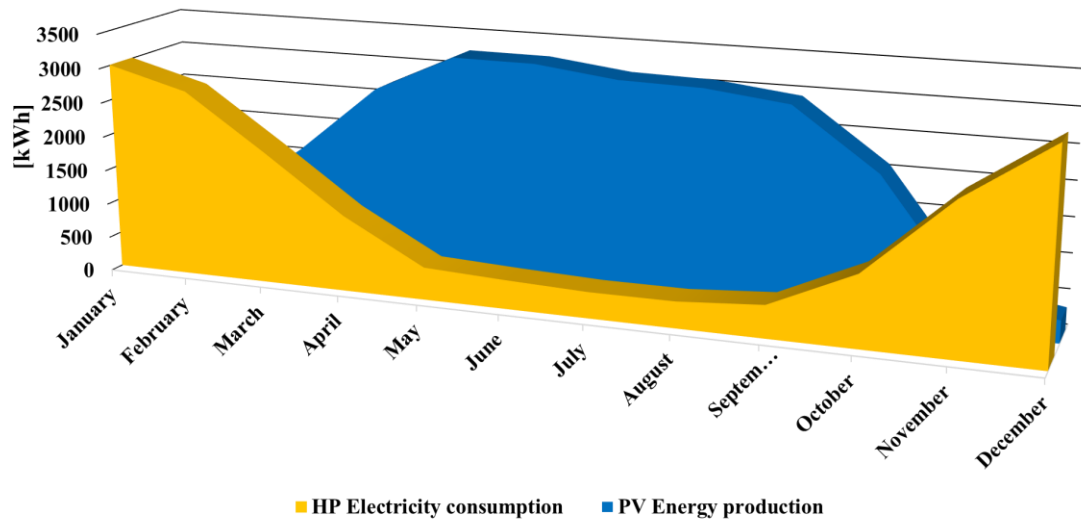
Figure 8.2 Yearly distribution of PV energy production and electricity usage for SH and DHW

In Table 8.2 it is reported the amount of electricity that, due to the aforementioned mismatch, must be bought from the grid to cover the HP demand.

Table 8.2 Electricity from the grid used for SH and DHW production

Month	Case 1 (kWh)	Case 2 (kWh)	Case 3 (kWh)
January	3674.0	2548.1	2639.1
February	2831.0	1843.0	1921.7
March	1150.4	199.2	268.0
April	0	0	0
May	0	0	0
June	0	0	0
July	0	0	0
August	0	0	0
September	0	0	0
October	495.6	0	0
November	2633.4	1613.9	1720.7
December	3712.7	2640.1	2748.3
Total	14497.2	8844.3	9297.8

The comparison in terms of GHGs emissions before the refurbishment and after (in all the three cases) has been carried out using the emission factor provided by the Department for Business, Energy & Industrial Strategy (BEIS) has been used (BEIS, 2020).

Table 8.3 Emission factor for natural gas and electricity

Fuel (energy vector)	Emission factor $\left[\dfrac{kg_{CO2e}}{kWh}\right]$
Natural gas	0.20374
Electricity	0.25319[14]

Greenhouse gas emissions are expressed in terms of "kilograms of carbon dioxide equivalent" as defined by BEIS, in this way is possible to consider not only the CO_2 emissions, but also the emissions of other gasses (like CH_4) which have a role too in terms of greenhouse effect.

Table 8.4 shows the emissions in the different cases and the relative reduction in comparison to the pre-refurbishment situation.

Table 8.4 Emission comparison

	CO_2 Emissions [kgCO₂e]		Emissions Variation
	Natural gas	Electricity	
Pre-Ref. 9 homes	18318.7	-	-
Pre-Ref 7 homes	15873.8	-	-
Case 1	-	3670.5	-76,9%
Case2	-	2239.3	-85.9%
Case 3	-	2354.1	-87.1%

The emissions listed for Case 1, Case 2 and 3 are the ones related to the electricity that must be bought from the grid when the PV production is not enough to cover the demand from the GSHP. Results show that the reduction in GHGs emissions is considerable in all the simulated cases and again highlights the negative impact of the two not refurbished terraced homes on the overall performance of the system.

---

[14] The electricity emission factor includes generation, transmission and distribution factors

8.2. Results discussions for the pilot cluster (10 refurbished homes) co-simulation model

As shown in Figure 6.31, Figure 6.32, Figure 6.33, and Table 6.12 the energy consumption and the energy source change consistently accordingly to the different control scheme. Scenario 1 presents the best results in terms of PV energy utilisation, direct self-consumption and the lowest value in terms of PV energy send to the grid. On the other hand, Scenario 2 seems to offer the worst performances, if indeed, the values in terms of total PV energy used and direct self-consumption are the lowest within the three analysed scenarios, the amount of energy sold to the grid in the highest. An exception is represented by the utilization of energy stored in the battery (i.e., a better use of the battery). Evaluating the first two scenarios it is clear that Scenario 1 directly self-consume about 4000 kWh/year more than Scenario 2 and that the difference concerning total PV energy used is above 3000 kWh/year. In terms of percentage the share of PV energy self-consumed and not sent to the grid stands at 59% for Scenario 1 and just 51% for Scenario 2. Based on these data the control strategy in Scenario 1 seems to offer the best performance in terms of how the small cluster of 10 homes is capable to utilise the PV energy generated by the photovoltaic plant. Scenario 3 offers values not very dissimilar from Scenario 1, where the share of self-used PV energy differs by just one percentage point, and the control strategy in Scenario 3 makes a better use of the battery.

Self-consumed energy and share of PV energy sent to the grid are not the only important parameters that must be taken into account. It is important to also consider the amount of energy bought during the hours of peak price of electricity. In this case Scenario 1 performs in a much worst way compared to Scenario 2 and 3, with about 1000 kWh more consumed between 4-7pm. Scenario 2 and 3 present similar results with just 100 kWh difference. Doing a direct comparison between Scenario 1 and 3 appears clear that sacrificing just 400 kWh in one year, in terms of total PV energy used by the complex, it is possible to save around 1000 kWh in the hours in which the transmission cost increases by a factor 10. These peak price hours have the highest impact on the energy bill of the community.

After these evaluations is possible to state that the control scheme in Scenario 3 offers the better performances with an amount of PV energy self-consumption very close to the maximum shown in Scenario 1 but with a consistent reduction of the energy bought from the grid during peak price time between 4-7pm.

The model also offers the opportunity to analyse the behaviour of the different control strategies in terms of GHGs emissions.

Table 8.5 Energy utilization details for pre-refurbishment and the three Scenarios (pilot cluster model)

Energy consumption	Unit	Pre-Ref	SCENARIO 1	SCENARIO 2	SCENARIO 3
Gas For SH+DHW	[kWh$_{th}$]	126878	-	-	-
Electricity For SH+DHW	[kWh$_{el}$]	0	17747	17747	17747
Electricity For Appl. and Lights	[kWh$_{el}$]	35998	39700	39700	39700
Total Electricity Consumption	[kWh$_{el}$]	35998	57448	57448	57448
Total PV Self-consumption	[kWh$_{el}$]	0	21582	18569	21107
Electricity from grid (TOT - PV)	[kWh$_{el}$]	35998	35866	38878	36341

Table 8.6. Greenhouse gas emissions (pilot cluster model)

CO$_2$ Emissions [kgCO$_2$e]	Pre-Ref.	SCENARIO 1	SCENARIO 2	SCENARIO 3
Emissions from gas	25850	-	-	-
Emissions from Elec.	9114	9081	9844	9201
Total emissions	34965	9081	9844	9201
Emissions Variation		-74,0%	-71,8%	-73,7%

Table 8.5 shows the values for the energy consumption in the different scenarios, energy consumption is divided accordingly to utilization. The value "Elec. from the grid (TOT-PV)" represents the energy imported from grid calculated as the difference between the total electricity consumption and the PV energy self-consumed. Also in this model to define the GHGs emission before the refurbishment and in the three post-refurbishment scenarios the emission factors provided by BEIS have been used (BEIS, 2020).

Table 8.7 Emission factors

Fuel (energy vector)	Emission factor $\left[\frac{kg_{CO2e}}{kWh}\right]$
Natural gas	0.20374
Electricity	0.25319[15]

Once the energy consumption has been broken down according to the energy source (or, in case of the electricity, energy vector) it is possible to calculate the amount of GHGs emitted. Before the retrofitting gas was used to provide SH and DHW, on the contrary, after the refurbishment the entire energy demand of the buildings is satisfied with electricity provided by the PV plant and the electric grid. This, combined with the reduction of energy demand achieved with the retrofit, allows to cut the GHGs emission.

In Table 8.6 is possible to see how the GHGs reduction changes in the different scenarios, again control strategy plays an important role, scenario 1 indeed shows a 74% emission reduction, 2 percentage points better than scenario 2. The difference between scenario 1 and 3 is, on the other hand, is very small (0.3%) showing that with a similar benefit in terms of environmental impact is possible to reduce the electricity consumption during the peak price time.

Considering the difference in energy source in the pre and post refurbished heating system, and to have a deeper understanding of the effectiveness of the intervention, an analysis of the primary energy use has been carried out. Primary energy can be defined as "*energy from renewable and non-renewable sources which has not undergone any conversion or transformation process*" (European Commission, 2018d).

Calculations for defining the primary energy use in the different scenarios have been carried out following the indications provided in (BRE, 2019) and are listed in Table 8.8.

---

[15] The electricity emission factor includes both generation and transmission and distribution factors

Table 8.8 Primary energy demand and variation in the pilot cluster

Energy consumption	Unit	Pre-Ref	SCENARIO 1	SCENARIO 2	SCENARIO 3
Primary energy from gas consumption	[kWh]	143372	-	-	-
Primary energy from electricity consumption	[kWh]	54033	53834	58356	54548
Exported to the grid	[kWh]	-	17969	19478	18207
Total primary energy	[kWh]	197406	35866	38878	36341
Variation in primary energy demand	[kWh]		-81.8%	-80.3%	-81.6%

Data highlights remarkable savings when the comparison is at primary energy level. The demand reduction is above 80% in all the co-simulated scenarios, with a very close result for Scenario 1 and 3.

It is also worth to be noted that the consistency of the data exchange between Dymola and EnergyPlus has been monitored. In Figure 8.3 it is possible to see the water temperature value in both Dymola (signal sent to the FMU) and EnergyPlus where it represents the temperature of the water sent from the boiler to the SH system. The values are perfectly identical meaning that the SH in in EnergyPlus is running according to the temperature values defined in Dymola.

Figure 8.3 Temperature signals from Dymola and boiler
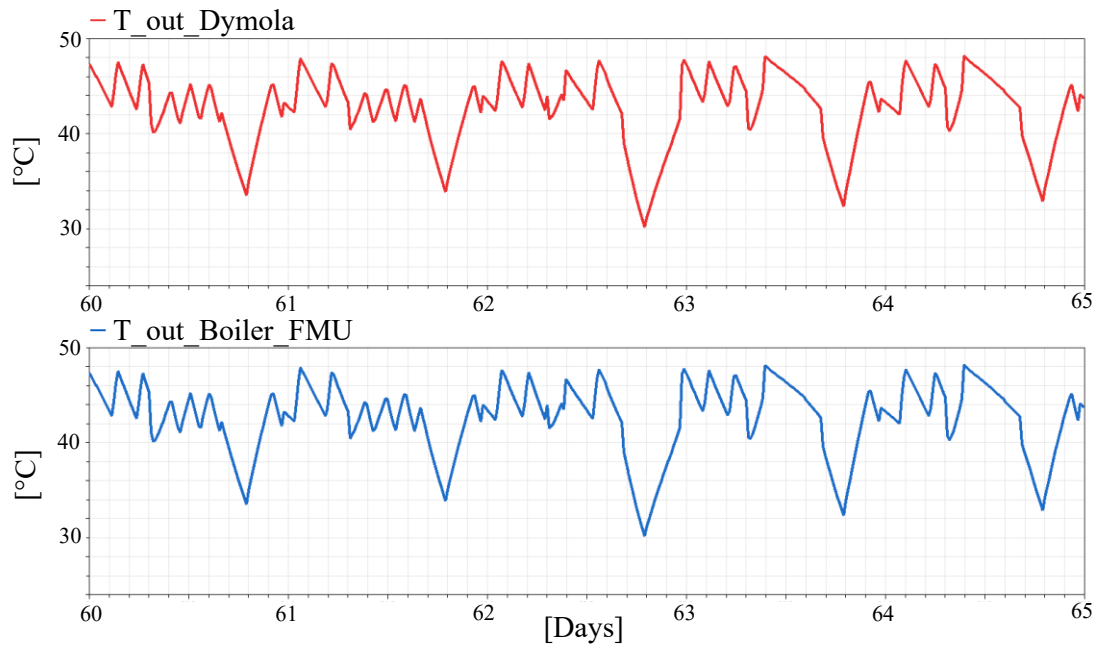
The room temperature in different houses was also monitored, again as control method to ensure that the data exchange between the two software was correct and that the rooms were effectively heated at the desired temperature. The temperature values for two rooms in different homes are represented in Figure 8.4
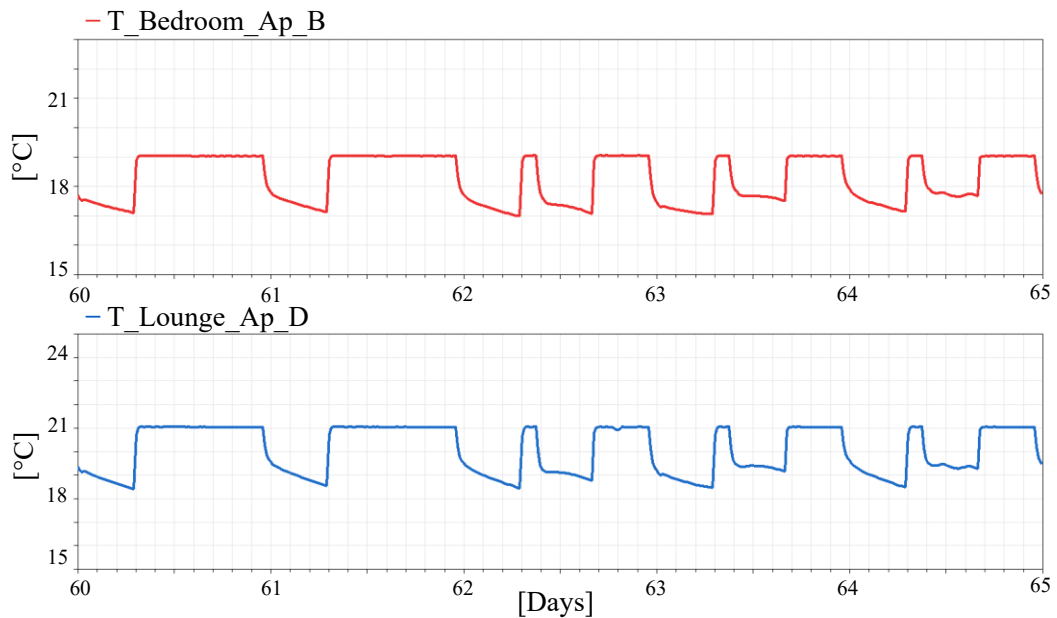
Figure 8.4 Temperature values calculated in EnergyPlus

8.3. Results discussions for the expanded case study co-simulation model

Like for the pilot cluster the results for the co-simulation model with 27 refurbished homes show how energy utilisation is massively affected by the control strategy, clear differences are illustrated in Figure 6.38, Figure 6.39 and Figure 6.40. Table 6.14 summarises the details for the energy consumption in the different simulated scenarios.

The general consumption pattern is similar to the one seen in the co-simulation of the pilot cluster, also in this case in fact Scenario 1 shows the best performance concerning energy direct self-consumption and PV energy send to the grid. Again, Scenario 2 shows the lowest value of direct self-consumed energy and the highest value of photovoltaic electricity sent to the grid. On the other hand, the utilisation of energy coming from the EES is higher than in Scenario 1, with around 2200 kWh more of stored energy utilised.

Focusing on the results from the first two scenarios it is possible to observe that Scenario 1 directly self-consume roughly 8400 kWh/year more than Scenario 2 with the difference in terms of total PV energy used standing at 6100 kWh/year. Comparting the share of PV energy self-consumed and not sent to the grid Scenario 1 shows again a better performance with 51.1% of the photovoltaic energy used in loco, whereas for Scenarios 2 this value is around 44.5%. Results are congruent with what showed also in the pilot cluster simulation but with lower percentages of PV energy used. This is mostly due to two facts, firstly the energy demand has grown slightly more than the PV production (the roof area is limited and one of the bungalows even if refurbished does not have a PV roof because of nearby trees), and most importantly the battery capacity went from 36 kWh to 40 kWh limiting the amount of storable energy and consequently the capacity of utilising the PV energy in loco.

As seen Scenario 1 and Scenario 2 provide quite different results in terms of PV energy utilisation. On the other hand, Scenario 3 shows results not dissimilar from Scenario 1, the amount of directly self-consumed energy is higher in Scenario 1, but this is partially compensated by the better use of the battery guaranteed by the control strategy in Scenario 3. This means that the two scenarios differ in terms of share of self-consumed PV energy by just 2 percentage points.

Again, to have a full picture of the performances of the three control logics, it is important also to consider the volume of energy arriving from the grid during the hours of peak price of electricity. Figure 6.41 and Table 6.15 clearly highlight how the control strategy

in Scenario 1 (which presents the best results in terms of self-consumed PV energy) brings to the higher grid electricity consumption during the peak time, with more than 11000 kWh bought from the grid in those peak hours. On the other hand, Scenario 2 and 3 present similar results with respectively 9426 and 9923 kWh coming from the grid when the electricity price it is at its maximum. Comparing Scenario 1 and 3 is possible to notice that even if the first guarantees around 1800 kWh more of self-consumed energy it also makes necessary buying almost 1600 kWh from the grid in the hours in which the transmission cost increases by a factor 10.

Considering this it is clear that again Scenario 3 has a total self-consumed energy very close to the best value shown in Scenario 1 (just a 2% difference in terms of share) but with a consistent reduction of the energy bought from the grid during the peak price time.

The analysis of the GHGs emissions has been carried out for this co-simulation model too. Table 8.9 includes a detailed report of the energy utilization in the expanded case study before the retrofitting intervention and in the three co-simulated scenarios, whereas in Table 8.10 the data about the GHGs emissions are listed.

Table 8.9 Energy utilization details pre-refurbishment and for the three Scenarios (expanded case study model)

Energy consumption	Unit	Pre-Ref	SCENARIO 1	SCENARIO 2	SCENARIO 3
Gas For SH+DHW	[kWh$_{th}$]	334179	-	-	-
Electricity For SH+DHW	[kWh$_{el}$]	-	46312	46312	46312
Electricity For Appl. and Lights	[kWh$_{el}$]	88627	96221	96221	96221
Total Electricity Consumption	[kWh$_{el}$]	88627	142533	142533	142533
Total PV Self-consumption	[kWh$_{el}$]	-	47844	41651	45998
Electricity from grid (TOT - PV)	[kWh$_{el}$]	88627	94689	100882	96535

Table 8.10 Greenhouse gas emissions (expanded case study model)

CO_2 Emissions [$kgCO_2e$]	Pre-Ref.	SCENARIO 1	SCENARIO 2	SCENARIO 3
Emissions from gas	68086	-	-	-
Emissions from Elec.	22439	23974	25542	24442
Total emissions	90525	23974	25542	24442
Emissions Variation	-	-73.5%	-71.8%	-73.0%

Results show a behaviour similar to the ones from the pilot cluster co-simulation. Concerning the emissions reduction, it is possible to notice that the number are marginally lower, this is a consequence of the already discussed reduction in PV energy used.

Just like in the previous model the difference between Scenario 1 and 3 is very small (0.5%) highlighting that the control logic in Scenario 3 can reduce the energy acquired by the grid during the peak time while delivering environmental benefits almost equals to the ones in Scenario 1.

Also for this co-simulation model a primary energy analysis has been conducted, results in Table 8.11 show results in line with the pilot co-simulation model. In this case too the drop in terms of primary energy demand is significant and above 80% for all the simulated scenarios.

Table 8.11 Primary energy demand and variation in the extended case study

Energy consumption	Unit	Pre-Ref	SCENARIO 1	SCENARIO 2	SCENARIO 3
Primary energy from gas consumption	[kWh]	377623	-	-	-
Primary energy from electricity consumption	[kWh]	133029	142128	151425	144898
Exported to the grid	[kWh]	-	47439	50542	48364
Total primary energy	[kWh]	510652	94689	100882	96535
Variation in primary energy demand	[kWh]		-81.5%	-80.2%	-81.1%

8.4. Results discussions for expanded case study co-simulation model with a 72 kWh battery

Table 6.16 highlights how an EES with twice the capacity of the original one would increase the share of the PV energy used by 5.8 points, reducing the annual import of electricity from the grid by more than 5300 kWh, roughly 3200 of which during the peak time (Figure 6.43). As stated by the Energy Networks Association "there is a business model for electricity storage only if is the stored electric energy is used at times of higher price/cost periods. This allows users to benefit from the difference in the price of energy between peak and off-peak and avoid peak transmission and distribution costs. A number of potential business models for electricity storage exist that will become more attractive as costs continue to fall and changes to the regulatory regime occurs" (Energy Networks Association, 2017). This topic, however, falls outside the perimeter of this research, yet the developed tool will be able to analyse complex multi-source hybrid energy systems with great accuracy while demonstrating to have high modularity and an ease of scaling up.

8.5. Conclusions and contribution to knowledge

The aim of the research is to optimise the management of complex domestic, multi-element energy generation and storage systems, through both active strategies to manage electrical and thermal energy and passive strategies to optimise the building fabric.

To achieve this the following objective were set:

- Build a model to investigate the existing building structures and plants using building performance simulation tools like DesignBuilder and IDA ICE, and other modelling software like Dymola/Modelica.
- Compare and validate the results of simulated model with monitored data from the case study.
- Investigate the performances of the whole energy system (PV, GSHP, thermal and electric storage) in the case study.
- Develop and optimize new operation management procedures in order to find the most efficient way to run the system and meanwhile guarantee the maximum energy saving for that specific configuration.

A deep retrofitting intervention, following the 2050 Homes approach, has been performed on a set of 27 (initially 10) residential properties in Nottingham. The building envelope has been improved from the point of view of both thermal insulation and air tightness. The old heating system based on individual combi-boilers has been replaced by a centralized hybrid energy system including GSHPs, PV roofs, EES, and TES, creating a micro, low temperature, district heating network. Several simulation models have been developed to assess the energy performance of the whole system before and after the refurbishment.

In the first phase of the research four models (two in DesignBuilder and two in IDA ICE) have been built to simulate the pre-refurbishment conditions and define the energy consumption. Six different models (three in DesignBuilder and three in IDA ICE) of the post-refurbishment situation have been built to analyse different scenarios from the point of view of refurbishing extension and heating system running scheme.

These models include only the 9 homes in the main block of the pilot cluster and have been simulated under the following scenarios:

- **Case 1** – seven of the nine homes have been refurbished, the heating is set to a target temperature of 20°C in each room and is constantly on.
- **Case 2** – seven of the nine homes have been refurbished, the temperature set point and the schedule follow the SAP recommendations like in the pre-refurbished building
- **Case 3** – all the homes have been refurbished, the temperature set point and the schedule follow the SAP recommendations like in the pre-refurbished building

The simulations results display how the refurbishment of the envelope, and the installation of a micro district heating network can guarantee a reduction in heat demand of about 45%. On the other hand, it is evident the negative effect of the two not refurbished terraced houses which act as a heat sink for the surrounding homes. By refurbishing all the houses is possible to further reduce the overall heat demand (around 53.5%) while heating two more homes.

In the second phase of the work a co-simulation model of the entire pilot cluster (10 refurbished homes) has been developed. The co-simulation model gives the opportunity to analyse in much more detail the energy flows in the system and to study different control strategies to optimise the energy utilisation.

In terms of reduction of the energy demand the co-simulation model demonstrates that the refurbishment is capable to deliver a 45% reduction in energy demand in the terraced houses and a 59% reduction in the retrofitted bungalows.

The most important result however is that the 2050 Homes development can reduce the carbon emissions in the pilot cluster by 72-74% depending on the control strategy and the primary energy demand by 80-82% (again depending on the control strategy). A proper management of the energy system can also reduce consistently (-24.4%) the amount of energy arriving from the grid during the hours in which the electricity price is at its peak, while at the same time almost the 60% of the PV energy produced is used locally.

During the PhD the case study of 10 homes have been expanded to a total of 27 homes with a new energy centre including more powerful GSHPs, bigger TES and bigger EES.

This can be indicated as third phase of the research work, thanks to its modularity the initial co-simulation model has been upgraded to represent the new, expanded, case study.

Results for the expanded case study display a reduction in energy demand between 43% in the terraced homes and roughly 58% in the bungalows. Carbon emissions drops also in this case by more than 70% (range between 71.8 and 73.5%). The reduction in primary energy demand varies between 80.2 and 81.5%.

Like in the case study with 10 homes also in this case the control system which manages the PV energy flow, as well as the battery utilisation, plays a key role. It allows an increase in PV energy utilisation comprised between 6.6% and 4.6% (compared to the worst performing scenario) while delivering a 13.78% reduction in terms of electricity bought from the grid during the peak time.

This approach to retrofitting shows a big potential, especially because of his modularity and the possibility to scale up the system creating micro energy grids able to offset the heat demand of micro districts with a combination of passive and active retrofitting measures. The co-simulation tool demonstrates to be capable of compensating the shortcomings of the BPS tools and provides an opportunity to develop specific and detailed control strategies for complex hybrid energy systems. The tool is flexible thanks to the modular architecture and can be easily scaled up in case of need being capable to simulate districts of different dimensions under a number of different scenarios.

8.5.1. Contribution to knowledge

The author claims the following contribution to knowledge:

- Precise building energy models have been developed on existing building using building performance simulation tools (DesignBuilder/EnergyPlus, IDA ICE) to analyse the energy consumption of these buildings.

- Innovative co-simulation models have been built with FMU block coupling a building energy performance simulation program (EnergyPlus/DesignBuilder) with energy system modelling platform Dymola/Modelica.

- By implementing the FMU block a two-way interaction has been achieved between the building performance simulation tool (EnergyPlus), which simulates the energy demand of the buildings and the specialised platform (Dymola/Modelica) to do a detailed modelling of the hybrid energy system.

- The co-simulation models have been validated with real data of energy consumption.

- Using the co-simulation models the performance of the whole hybrid energy systems (PV, GSHP, thermal and electric storage) was analysed.

- Three different operating settings / procedures have investigated to find the most efficient way to operate the hybrid energy system with the best/highest environmental impact.

- The control system integrated in the model proved to be capable of increasing the amount of PV energy used in loco, while, at the same time, drastically reducing the use of electricity from the grid when the price is at its peak . All this by managing the PV energy usage, the building appliances access to the EES, and the battery control strategy.

- Using the co-simulation tool the impact of different electrical battery configurations on the performance of the whole hybrid system was analysed.

8.6. Future work

The developed tool has enormous potential, some improvements could be applied to streamline the utilisation, for example by using partial models for the control system to take advantage of inheritance and reusability. A further development that could be applied to the co-simulation model is the implementation of the optimisation library now available on Dymola. This tool can provide multi-objective optimization indicating the

best settings for the control system accordingly to the desired targets. This would require modifications to the co-simulation tool, with interventions on the Modelica code and on the structure of the tool itself which has not been possible to carry out in this PhD research. However, this represents the ideal continuation of this PhD.

Further acknowledgments and copyright

Bibliography

Papers presented by the author:

➤ Cucca. G. and Ianakiev. A. . (2020). Assessment and optimisation of energy consumption in building communities using an innovative co-simulation tool. *Journal of Building Engineering*: 101681. ISSN 2352-7102

Conference attended and presentations:

➤ Cucca. G. and Ianakiev. A. . (2019). "Co-simulation tool for hybrid energy system optimisation". 5th International Conference on Smart Energy Systems Copenhagen. 10-11 September 2019

➤ Cucca. G. et al. (2018). "Energy models for deep retrofitted homes using Energiesprong approach". 4th International Conference on Smart Energy Systems and 4th Generation District Heating Aalborg. 13-14 November 2018

➤ Cucca. G. et al. (2018). "Energy simulation tools for buildings with deep retrofitting interventions". 13th SDEWES Conference on Sustainable Development of Energy. Water and Environment Systems. Palermo 30th September – 4th October 2018

References

Abanda, F. H. and Byers, L. (2016) 'An investigation of the impact of building orientation on energy consumption in a domestic building using emerging BIM (Building Information Modelling)', *Energy*, 97, pp. 517–527. doi: 10.1016/j.energy.2015.12.135.

Al-Homoud, M. S. (2005) 'Performance characteristics and practical applications of common building thermal insulation materials', *Building and Environment*, 40(3), pp. 353–366. doi: 10.1016/j.buildenv.2004.05.013.

Allen, M. R. *et al.* (2018) *IPCC: Framing and Context*, *Global warming of 1.5°C. An IPCC Special Report*.

Amirifard, F., Sharif, S. A. and Nasiri, F. (2019) 'Application of passive measures for energy conservation in buildings–a review', *Advances in Building Energy Research*, 13(2), pp. 282–315. doi: 10.1080/17512549.2018.1488617.

Andarini, R. (2014) 'The role of building thermal simulation for energy efficient building design', *Energy Procedia*, 47, pp. 217–226. doi: 10.1016/j.egypro.2014.01.217.

Andrea, S. *et al.* (2008) *Global Sensitivity Analysis: The Primer*. Chichester,WestSussexPO198SQ,England: John Wiley & Sons, Inc. doi: 10.1002/9780470725184.

ANSI/ASHRAE (2002) *ASHRAE Guideline 14-2002 Measurement of Energy and Demand Savings*, *Ashrae*.

Arabzadeh Saheli, M., Lari, K. and Kasaeian Ziarati, S. B. (2019) 'Techno-economic feasibility of a standalone hybrid energy system for semi equatorial climates: a case study', *International Journal of Green Energy*, 16(14), pp. 1131–1143. doi: 10.1080/15435075.2019.1653880.

Asadi, I. *et al.* (2018) 'Thermal conductivity of concrete – A review', *Journal of Building Engineering*, 20(July), pp. 81–93. doi: 10.1016/j.jobe.2018.07.002.

Asaee, S., Ugursal, V. and Beausoleil-Morrison, I. (2016) 'Retrofit measures to approach net energy status for the canadian housing stock: air to water heat pump + PV', in *eSim 2016 Building Performance Simulation Conference*.

Ascione, F. *et al.* (2015) 'A new methodology for cost-optimal analysis by means of the multi-objective optimization of building energy performance', *Energy and Buildings*, 88,

pp. 78–90. doi: 10.1016/j.enbuild.2014.11.058.

Ascione, F., De Masi, R. F., *et al.* (2016) 'Optimization of building envelope design for nZEBs in Mediterranean climate: Performance analysis of residential case study', *Applied Energy*, 183, pp. 938–957. doi: 10.1016/j.apenergy.2016.09.027.

Ascione, F., Bianco, N., *et al.* (2016) 'Simulation-based model predictive control by the multi-objective optimization of building energy performance and thermal comfort', *Energy and Buildings*, 111, pp. 131–144. doi: 10.1016/j.enbuild.2015.11.033.

Ascione, F., Bianco, N., De Stasio, C., *et al.* (2017) 'Artificial neural networks to predict energy performance and retrofit scenarios for any member of a building category: A novel approach', *Energy*, 118, pp. 999–1017. doi: 10.1016/j.energy.2016.10.126.

Ascione, F., Bianco, N., De Masi, R. F., *et al.* (2017) 'Energy retrofit of educational buildings: Transient energy simulations, model calibration and multi-objective optimization towards nearly zero-energy performance', *Energy and Buildings*, 144, pp. 303–319. doi: 10.1016/j.enbuild.2017.03.056.

Augenbroe, G. (2002) 'Trends in building simulation', *Building and Environment*, 37(8–9), pp. 891–902. doi: 10.1016/S0360-1323(02)00041-0.

Becchio, C. *et al.* (2015) 'Cost optimality assessment of a single family house: Building and technical systems solutions for the nZEB target', *Energy and Buildings*, 90, pp. 173–187. doi: 10.1016/j.enbuild.2014.12.050.

BEIS (2020) 'Conversion factors 2020: condensed set (for most users)', *Greenhouse gas reporting: conversion factors 2020 - GOV.UK*, pp. 1–4. Available at: https://www.gov.uk/government/publications/greenhouse-gas-reporting-conversion-factors-2020.

Borkowski, E. *et al.* (2016) 'Optimisation Of The Simulation Of Advanced Control Strategies For Adaptive Building Skins'.

Branco, F., Tadeu, A. and Simoes, N. (2004) 'Heat conduction across double brick walls via BEM', *Building and Environment*, 39(1), pp. 51–58. doi: 10.1016/j.buildenv.2003.08.005.

BRE (2014) 'The Government's Standard Assessment Procedure for Energy Rating of Dwellings 2012 edition'. Garston, Watford, WD25 9XX. Available at: https://www.bre.co.uk/filelibrary/SAP/2012/SAP-2012_9-92.pdf.

BRE (2019) 'Briefing Note – Derivation and use of Primary Energy factors in SAP (v1.3)', (May 2018), p. 4. Available at: https://www.bregroup.com/sap/.

British Standards Institution (2018) *BS EN 14511-4:2018 Air conditioners, liquid chilling packages and heat pumps for space heating and cooling and process chillers, with electrically driven compressors*.

Bruck, D. *et al.* (2002) 'Dymola for multi-engineering modelling and simulation', *2nd International Modelica Conference, Proceedings*, 6, pp. 55-1-55–8. doi: 10.1109/VPPC.2006.364294.

Cabonare, N. *et al.* (2019) 'Comfort-oriented control strategies for decentralized ventilation using co-simulation Comfort-oriented control strategies for decentralized ventilation using co-simulation'. doi: 10.1088/1757-899X/609/3/032018.

Çağlar, F. Z., Gedik, G. Z. and Gökdemir, H. (2020) 'The impact of transparency ratio on thermal comfort: A field study on educational building', *Civil Engineering and Architecture*, 8(5), pp. 890–897. doi: 10.13189/cea.2020.080516.

Chen, X. *et al.* (2020) 'Multi-criteria assessment approach for a residential building retrofit in Norway', *Energy and Buildings*, 215. doi: 10.1016/j.enbuild.2019.109668.

CIBSE (2006) *CIBSE Guide A: Environmental Design*. doi: 10.1016/B978-0-240-81224-3.00016-9.

CIBSE (2015) *CIBSE Guide B2: Ventilation and ductwork*. Edited by E. Palmer.

CIBSE (2016) *CIBSE Guide B1: Heating*.

Coakley, D., Raftery, P. and Keane, M. (2014) 'A review of methods to match building energy simulation models to measured data', *Renewable and Sustainable Energy Reviews*, 37, pp. 123–141. doi: 10.1016/j.rser.2014.05.007.

Committee on Climate Change (2019a) 'Net Zero Technical report', (May).

Committee on Climate Change (2019b) 'Net Zero The UK ' s contribution to stopping global warming', (May).

Crawley, D. B. *et al.* (2001) 'EnergyPlus: Creating a new-generation building energy simulation program', *Energy and Buildings*, 33(4), pp. 319–331. doi: 10.1016/S0378-7788(00)00114-6.

Danielski, I., Fröling, M. and Joelsson, A. (2012) 'The impact of the shape factor on final

energy demand in residential buildings in nordic climates', *World Renewable Energy Forum, WREF 2012, Including World Renewable Energy Congress XII and Colorado Renewable Energy Society (CRES) Annual Conferen*, 6, pp. 4260–4264.

Dassault Systèmes (no date) *Dymola*. Available at: https://www.3ds.com/products-services/catia/products/dymola/ (Accessed: 25 June 2021).

Dassault Systèmes AB (2017) *Dymola Dynamic Modeling Laboratory*.

DesignBuilder (2016) *DesignBuilder Help - Capabilities*. Available at: http://www.designbuilder.co.uk/helpv4.7/#_Capabilities.htm%3FTocPath%3DGetting%2520Started%7C_____2 (Accessed: 9 April 2021).

DesignBuilder Software Ltd (2017) *DesignBuilder Software Ltd - Tutorials*. Available at: https://www.designbuilder.co.uk/training/online-learning/tutorials (Accessed: 29 June 2021).

DesignBuilder Software Ltd - About Us (2019). Available at: https://designbuilder.co.uk/about-us (Accessed: 6 July 2021).

Dodoo, A., Gustavsson, L. and Sathre, R. (2011) 'Primary energy implications of ventilation heat recovery in residential buildings', *Energy and Buildings*, 43(7), pp. 1566–1572. doi: 10.1016/j.enbuild.2011.02.019.

Duffy, M. J. *et al.* (2009) 'TRNSYS - features and functionalitity for building simulation 2009 conference', *IBPSA 2009 - International Building Performance Simulation Association 2009*, pp. 1950–1954.

Dylewski, R. and Adamczyk, J. (2011) 'Economic and environmental benefits of thermal insulation of building external walls', *Building and Environment*, 46(12), pp. 2615–2623. doi: 10.1016/j.buildenv.2011.06.023.

Energiesprong Foundation (no date) *Energiesprong*. Available at: https://energiesprong.org/ (Accessed: 29 June 2021).

Energy Networks Association (2017) 'Energy Networks Association Electricity storage guide for communities and independent developers'.

'EnergyPlus Essentials' (2021). Available at: https://energyplus.net/sites/all/modules/custom/nrel_custom/pdfs/pdfs_v9.5.0/EnergyPlusEssentials.pdf (Accessed: 25 June 2021).

EQUA Simulation AB (2016a) 'IDA ICE - Getting Started', (February), pp. 4–6.

EQUA Simulation AB (2016b) 'IDA Indoor Climate and Energy'. Available at: https://www.equa.se/en/ida-ice (Accessed: 22 May 2021).

European Commission (2018a) '2050 long-term strategy | Climate Action', *2050 Long-Term Strategy*. Available at: https://ec.europa.eu/clima/policies/strategies/2050_en (Accessed: 23 June 2021).

European Commission (2018b) 'A Clean Planet for all. A European long-term strategic vision for a prosperous, modern, competitive and climate neutral economy', *Com(2018) 773*, p. 114. Available at: https://eur-lex.europa.eu/legal-content/EN/TXT/PDF/?uri=CELEX:52018DC0773&from=EN.

European Commission (2018c) 'DIRECTIVE (EU) 2018/2002 OF THE EUROPEAN PARLIAMENT AND OF THE COUNCIL', *Official Journal of the European Union*, 2018(December), pp. 210–230.

European Commission (2018d) 'DIRECTIVE (EU) 2018/844 OF THE EUROPEAN PARLIAMENT AND OF THE COUNCIL of 30 May 2018', *Official Journal of the European Union*, 2018(May 2010), pp. 75–91.

EuropeanCouncil (2018) *2030 climate & energy framework | Climate Action*, *2030 Climate & energy framework*. Available at: https://ec.europa.eu/clima/policies/strategies/2030_en (Accessed: 29 June 2021).

Favoino, F. *et al.* (2016) 'Optimal control and performance of photovoltachromic switchable glazing for building integration in temperate climates', *Applied Energy*, 178, pp. 943–961. doi: 10.1016/j.apenergy.2016.06.107.

Ferrara, M., Monetti, V. and Fabrizio, E. (2018) 'Cost-optimal analysis for nearly zero energy buildings design and optimization: A critical review', *Energies*, 11(6). doi: 10.3390/en11061478.

Foucquier, A. *et al.* (2013) 'State of the art in building modelling and energy performances prediction: A review', *Renewable and Sustainable Energy Reviews*, 23, pp. 272–288. doi: 10.1016/j.rser.2013.03.004.

Fumo, N. (2014) 'A review on the basics of building energy estimation', *Renewable and Sustainable Energy Reviews*, 31, pp. 53–60. doi: 10.1016/j.rser.2013.11.040.

Galadanci, A. S. *et al.* (2020) 'Energy investigation framework: Understanding buildings

from an energy perspective view', *Journal of Building Engineering*, 28(November 2019), p. 101046. doi: 10.1016/j.jobe.2019.101046.

Granadeiro, V. *et al.* (2013) 'Envelope-related energy demand: A design indicator of energy performance for residential buildings in early design stages', *Energy and Buildings*, 61, pp. 215–223. doi: 10.1016/j.enbuild.2013.02.018.

Green, E., Hope, T. and Yates, A. (2015) *Sustainable Infrastructure: Sustainable Buildings*, *ICE Publishing*. Available at: https://www.icevirtuallibrary.com/isbn/9780727758064.

Gustavsen, A. *et al.* (2011) 'Key elements of and material performance targets for highly insulatingwindow frames', *Energy and Buildings*, 43(10), pp. 2583–2594. doi: 10.1016/j.enbuild.2011.05.010.

Halliday, D., Resnick, R. and Walker, J. (2014) *Fundamentals of Physics*. Tenth edit. John Wiley & Sons, Inc.

Harish, V. S. K. V. and Kumar, A. (2016) 'A review on modeling and simulation of building energy systems', *Renewable and Sustainable Energy Reviews*. Elsevier Ltd, pp. 1272–1292. doi: 10.1016/j.rser.2015.12.040.

He, D. *et al.* (2014) 'Building energy and control system modeling and simulation using Modelica', *The 26th Chinese Control and Decision Conference (2014 CCDC)*, pp. 2794–2797. doi: 10.1109/CCDC.2014.6852648.

He, D., Xiong, Q. and Shi, X. (2017) 'Modeling of the renewable energy system of an net zero energy community', *Proceedings of the 29th Chinese Control and Decision Conference, CCDC 2017*, pp. 3590–3595. doi: 10.1109/CCDC.2017.7979128.

Hirsch, J. J. (no date) *DOE-2*. Available at: http://www.ibpsa.org/proceedings/BS2019/BS2019_211268.pdf (Accessed: 22 June 2021).

HM Government (2010) 'Approved Document L2B: Conservation of fuel and power in existing buildings other than dwellings', *The Building Regullations 2010*. Available at: https://assets.publishing.service.gov.uk/government/uploads/system/uploads/attachment _data/file/540329/BR_PDF_AD_L2B_2013_with_2016_amendments.pdf.

HM Government (2013) 'Approved Document F: Means of ventilation', *UK Building Regulations*.

HM Government (2019) 'The Climate Change Act 2008 (2050 Target Amendment) Order 2019', *Legislation.Gov.Uk*, 2008(1056), p. 4. Available at: http://www.legislation.gov.uk/ukdsi/2019/9780111187654/pdfs/ukdsiem_97801111876 54_en.pdf.

HOMER - Hybrid Renewable and Distributed Generation System Design Software (no date). Available at: https://www.homerenergy.com/ (Accessed: 15 June 2021).

Hong, T., Chou, S. K. and Bong, T. Y. (2000) 'Building simulation: An overview of developments and information sources', *Building and Environment*, 35(4), pp. 347–361. doi: 10.1016/S0360-1323(99)00023-2.

Howarth, N. A. A. and Rosenow, J. (2014) 'Banning the bulb: Institutional evolution and the phased ban of incandescent lighting in Germany', *Energy Policy*, 67, pp. 737–746. doi: 10.1016/j.enpol.2013.11.060.

Illuminating Engineering Society of North America (1993) *Lighting Handbook: Reference & Application*. 8th Editio.

Introduction: EnergyPlus Essentials — EnergyPlus 9.6 (no date). Available at: https://bigladdersoftware.com/epx/docs/9-6/essentials/essentials.html#what-is-bem (Accessed: 24 December 2021).

Knier, G. (2008) *How do Photovoltaics Work? | Science Mission Directorate*, *Science Beta*. Available at: https://science.nasa.gov/science-news/science-at-nasa/2002/solarcells (Accessed: 5 July 2021).

Kothandaraman (2012) *Fundamentals of Heat and Mass Transfer*. New Age International Publisher.

Kottek, M. *et al.* (2006) 'World map of the Köppen-Geiger climate classification updated', *Meteorologische Zeitschrift*, 15(3), pp. 259–263. doi: 10.1127/0941-2948/2006/0130.

Kübler, S. and Norrefeldt, V. (2014) 'Enhancement of the building simulation software TRNSYS by coupling to the VEPZO model programmed in Modelica', *Proceedings of the 10th International Modelica Conference, March 10-12, 2014, Lund, Sweden*, 96, pp. 107–114. doi: 10.3384/ecp14096107.

Lawrence Berkeley National Laboratory (no date) *EnergyPlusToFMU*. Available at: https://simulationresearch.lbl.gov/projects/energyplustofmu (Accessed: 9 July 2021).

LETI (2020) 'Climate Emergency Design Guide', *How new buildings can meet UK climate change targets*, p. 158. Available at: https://www.leti.london/cedg.

Liang, X. *et al.* (2017) 'Analysis and Optimization on Energy Performance of a Rural House in Northern China Using Passive Retrofitting', *Energy Procedia*, 105, pp. 3023–3030. doi: 10.1016/j.egypro.2017.03.618.

Liu, L. *et al.* (2014) 'Comprehensive investigation on energy retrofits in eleven multi-family buildings in Sweden', *Energy and Buildings*, 84, pp. 704–715. doi: 10.1016/j.enbuild.2014.08.044.

Ma, Z. *et al.* (2012) 'Existing building retrofits: Methodology and state-of-the-art', *Energy and Buildings*, 55, pp. 889–902. doi: 10.1016/j.enbuild.2012.08.018.

Mauro, G. M. *et al.* (2015) 'A new methodology for investigating the cost-optimality of energy retrofitting a building category', *Energy and Buildings*, 107, pp. 456–478. doi: 10.1016/j.enbuild.2015.08.044.

Mazzeo, D. *et al.* (2020) 'EnergyPlus, IDA ICE and TRNSYS predictive simulation accuracy for building thermal behaviour evaluation by using an experimental campaign in solar test boxes with and without a PCM module', *Energy and Buildings*, 212. doi: 10.1016/j.enbuild.2020.109812.

Mcdowell, T. P. *et al.* (2017) 'TRNSYS 18 : The Continued Evolution of the Software', *Proceedings of the 15th IBPSA Conference*, pp. 1922–1930. Available at: http://www.ibpsa.org/proceedings/BS2017/BS2017_516.pdf.

McMullan, R. (2017) *Environmental science in building*. Eighth edi. Basingstoke, Hampshire : Palgrave Macmillan.

MHGLC (2018) 'English Housing Survey Headline Report, 2017-18'. Available at: https://www.gov.uk/government/statistics/english-housing-survey-2017-to-2018-headline-report.

Michelle, J., Ianakiev, A. and García-fuentes, M. Á. (2017) 'To examine appropriate deep-retrofit practice using simulation results in an EU-funded urban regeneration project', *Energy Procedia*, 105, pp. 2549–2556. doi: 10.1016/j.egypro.2017.03.733.

Modelica Association (2013) 'Modelica Libraries — Modelica Association', pp. 1–18. Available at: https://modelica.org/libraries.html (Accessed: 9 July 2021).

Murano, G. *et al.* (2017) 'The significant imbalance of nZEB energy need for heating and

cooling in Italian climatic zones', *Energy Procedia*, 126, pp. 258–265. doi: 10.1016/j.egypro.2017.08.150.

Nageler, P. *et al.* (2019) 'Co-simulation Workflow for the Dynamic Modelling and Simulation of Large-scale District Energy Systems Institute of Thermal Engineering , Graz University of Technology , Graz , Austria AEE – Institute for Sustainable Technologies , Graz , Austria Abstract', pp. 3698–3705.

Neroutsou, T. I. (2016) 'Lifecycle costing of low energy housing refurbishment: A case study of a 7 year retrofit in Chester Road, London', *Energy and Buildings*, 128, pp. 178–189. doi: 10.1016/j.enbuild.2016.06.040.

Nguyen, A. T., Reiter, S. and Rigo, P. (2014) 'A review on simulation-based optimization methods applied to building performance analysis', *Applied Energy*, 113, pp. 1043–1058. doi: 10.1016/j.apenergy.2013.08.061.

Nicolai, A. and Paepcke, A. (2017) 'Co-Simulation between detailed building energy performance simulation and Modelica HVAC component models', *Proceedings of the 12th International Modelica Conference, Prague, Czech Republic, May 15-17, 2017*, 132, pp. 63–72. doi: 10.3384/ecp1713263.

Niemelä, T., Kosonen, R. and Jokisalo, J. (2017) 'Energy performance and environmental impact analysis of cost-optimal renovation solutions of large panel apartment buildings in Finland', *Sustainable Cities and Society*, 32, pp. 9–30. doi: 10.1016/j.scs.2017.02.017.

Nouidui, T. S. and Wetter, M. (2014) 'Tool coupling for the design and operation of building energy and control systems based on the Functional Mock-up Interface standard', (December), pp. 311–320. doi: 10.3384/ecp14096311.

Pacheco, R., Ordóñez, J. and Martínez, G. (2012) 'Energy efficient design of building: A review', *Renewable and Sustainable Energy Reviews*, 16(6), pp. 3559–3573. doi: 10.1016/j.rser.2012.03.045.

Palmer, J. and Passivhaus Trust (2020) 'EPCs as Efficiency Targets', (April).

Parliament of the United Kingdom (2008) 'Climate Change Act 2008', *HM Government*, pp. 1–103. doi: 10.1136/bmj.39469.569815.47.

Peeters, L. *et al.* (2008) 'Control of heating systems in residential buildings : Current practice', *Energy and Buildings*, 40, pp. 1446–1455. doi: 10.1016/j.enbuild.2008.02.016.

Rahman, M. M., Rasul, M. G. and Khan, M. M. K. (2010) 'Energy conservation measures

in an institutional building in sub-tropical climate in Australia', *Applied Energy*, 87(10), pp. 2994–3004. doi: 10.1016/j.apenergy.2010.04.005.

Rees, S. J. (2016) *An introduction to ground-source heat pump technology*, *Advances in Ground-Source Heat Pump Systems*. Elsevier Ltd. doi: 10.1016/B978-0-08-100311-4.00001-7.

Roberts, S. (2008) 'Altering existing buildings in the UK', *Energy Policy*, 36(12), pp. 4482–4486. doi: 10.1016/j.enpol.2008.09.023.

Ruiz, G. R. and Bandera, C. F. (2017) 'Validation of calibrated energy models: Common errors', *Energies*, 10(10). doi: 10.3390/en10101587.

Sadineni, S. B., Madala, S. and Boehm, R. F. (2011) 'Passive building energy savings: A review of building envelope components', *Renewable and Sustainable Energy Reviews*, 15(8), pp. 3617–3631. doi: 10.1016/j.rser.2011.07.014.

Sajn, N. (2016) 'Energy efficiency of buildings: A nearly zero-energy future?', *European Parliamentary Research Service*, (May), p. 10. Available at: http://www.europarl.europa.eu/RegData/etudes/BRIE/2016/582022/EPRS_BRI(2016)5 82022_EN.pdf%5Cnhttp://www.csa.com/partners/viewrecord.php?requester=gs&c ollection=TRD&recid=20080322014046EA.

Serrano-Jiménez, A. *et al.* (2019) 'Decision-support method for profitable residential energy retrofitting based on energy-related occupant behaviour', *Journal of Cleaner Production*, 222, pp. 622–632. doi: 10.1016/j.jclepro.2019.03.089.

Soleimani-Mohseni, M., Nair, G. and Hasselrot, R. (2016) 'Energy simulation for a high-rise building using IDA ICE: Investigations in different climates', *Building Simulation*, 9(6), pp. 629–640. doi: 10.1007/s12273-016-0300-9.

Standard Assessment Procedure - GOV.UK (2013). Available at: https://www.gov.uk/guidance/standard-assessment-procedure (Accessed: 24 June 2021).

Tavares, P. *et al.* (2016) 'Control criteria of electrochromic glasses for energy savings in mediterranean buildings refurbishment', *Solar Energy*, 134, pp. 236–250. doi: 10.1016/j.solener.2016.04.022.

Terés-Zubiaga, J. *et al.* (2015) 'Energy and economic assessment of the envelope retrofitting in residential buildings in Northern Spain', *Energy and Buildings*, 86, pp. 194–202. doi: 10.1016/j.enbuild.2014.10.018.

The future of SAP calculations - Etude (no date). Available at: https://www.etude.co.uk/news/the-future-of-sap-calculations/ (Accessed: 24 June 2021).

The Regents of the University of California (through Lawrence Berkeley National Laboratory) (no date) *Open source library for building and district energy and control systems*. Available at: https://simulationresearch.lbl.gov/modelica/releases/v5.1.0/help/Buildings.html (Accessed: 6 June 2021).

Thorpe, D. (2010) *Sustainable Home Refurbishment: The Earthscan Expert Guide to Retrofitting Homes for Efficiency*. London: Routledge.

U.S. Department of Energy's (DOE) Building Technologies Office (BTO) (no date) *EnergyPlus | EnergyPlus*. Available at: https://energyplus.net/ (Accessed: 29 June 2021).

University of Strathclyde (2002) 'The ESP-r System for Building Energy Simulation'.

'University of Strathclyde' (2019) in *The Grants Register 2020*, pp. 1042–1044. doi: 10.1057/978-1-349-95943-3_939.

University of Wisconsin System (no date) *TRNSYS - Official Website*. Available at: http://sel.me.wisc.edu/trnsys/ (Accessed: 29 June 2021).

Valdiserri, P. *et al.* (2015) 'Retrofit strategies applied to a tertiary building assisted by Trnsys energy simulation tool', *Energy Procedia*, 78, pp. 765–770. doi: 10.1016/j.egypro.2015.11.091.

Virgin, L. N. (2019) *Mathematical Description*, *Introduction to Experimental Nonlinear Dynamics*. doi: 10.1017/9781139175227.006.

Wang, H. and Zhai, Z. (John) (2016) 'Advances in building simulation and computational techniques: A review between 1987 and 2014', *Energy and Buildings*, 128, pp. 319–335. doi: 10.1016/j.enbuild.2016.06.080.

Wang, Q., Ploskić, A. and Holmberg, S. (2015) 'Retrofitting with low-temperature heating to achieve energy-demand savings and thermal comfort', *Energy and Buildings*, 109, pp. 217–229. doi: 10.1016/j.enbuild.2015.09.047.

Wasilowski, H. A. and Reinhart, C. F. (2009) 'Modelling an existing building in designbuilder/energyplus: Custom versus default inputs', *IBPSA 2009 - International Building Performance Simulation Association 2009*, (January), pp. 1252–1259.

Wetter, M. and Haugstetter, C. (2006) 'Modelica versus TRNSYS–A comparison between an equation-based and a procedural modeling language for building energy simulation', *SimBuild IBPSA-USA*, 11(4), pp. 262–269. Available at: http://simulationresearch.lbl.gov/WETTER/download/WetterHaugstetter-2006.pdf%5Cnhttp://www.ibpsa.us/pub/simbuild2006/papers/SB06_262_269.pdf.

Wetter, M., Zuo, W. and Nouidui, T. S. (2011) 'Recent Developments of the Modelica"Buildings" Library for Building Energy and Control Systems'. Available at: https://www.osti.gov/biblio/1050666.

De Wit, S. (2004) *Advanced Building Simulation*. 1st edn, *Advanced Building Simulation*. 1st edn. Edited by A. M. Malkawi and G. Augenbroe. doi: 10.4324/9780203073674-11.

Wong, K. din and Fan, Q. (2013) 'Building information modelling (BIM) for sustainable building design', *Facilities*, 31(3), pp. 138–157. doi: 10.1108/02632771311299412.

Yang, L. *et al.* (2018) 'Integrated Platform for Whole Building HVAC System Automation and Simulation', (July).

Yu, S. *et al.* (2015) 'Impact of Civil Envelope on Energy Consumption based on EnergyPlus', *Procedia Engineering*, 121, pp. 1528–1534. doi: 10.1016/j.proeng.2015.09.130.

APPENDIX I

IDA ICE has been used in the initial part of this research work to provide an element of verification of the simulation results.

The simulation results from DesignBuilder and IDA ICE are compared in the following pages showing good matching. IDA ICE software has been used to model the pre-refurbishment building and the equivalent of the DesignBuilder model described in 6.3.1 (i.e., the "first model, main block 7 refurbished homes"). All the settings in terms of temperature, occupancy, ventilation and so on are the same in the two software, minor differences could be found in the material properties which have been selected from the libraries. Unlike the model in DesignBuilder the one in IDA ICE does not include the portion regarding PV system and EES, when the model was developed in fact the available software release did not allow a proper simulation of such systems (especially the EES was missing). The author wants to underline that following releases have not been investigated and as mentioned the research work has been carried on using DesignBuilder/EnergyPlus and Dymola, however this do not represent a judgment about IDA ICE potentialities or usefulness, and only applies to the specific moment and specific needs that were required at the time.

Appendix I 1 – Pre-refurbishment model, numerical results

Table Appendix I 1 SH energy consumption

	Space heating (kWh)									
	House									
	A	**B**	**C**	**D**	**E**	**F**	**G**	**H**	**I**	**TOT**
DB	11927	7412	7428	6961	7418	7425	7443	7561	11485	**75061**
IDA ICE	2089	1346	1366	1277	1366	1364	1365	1374	2043	**76053**
DIFF %	6.1	-6.9	-3.9	-10.5	-3.6	-3.5	-3.6	-3.9	7.9	**-1.4**

Table Appendix I 2 Heat demand in the main block with 9 homes heated

Heating demand per house – 9 homes model (kWh)									
	A	**B**	**C**	**D**	**E**	**F**	**G**	**H**	**I**	**TOT**
DB	10894	6770	6784	6358	6775	6782	6799	6906	10490	**68559**
IDA ICE	10236	7237	7053	7027	7022	7024	7043	7181	9664	**69487**
DIFF %	6.0	-6.9	-4.0	-10.5	-3.6	-3.6	-3.6	-4.0	7.9	**-1.4**

Table Appendix I 3 Heat demand in the main block with 7 homes heated

Heating demand per house – 7 homes model (kWh)									
	A	**B**	**C**	**D**	**E**	**F**	**G**	**H**	**I**	**TOT**
DB	10918	6784	6805	6450	8624	0	8827	10597	0	**59005**
IDA ICE	10134	7122	6944	7005	8941	0	9094	10961	0	**60201**
DIFF %	7.2	-5.0	-2.0	-8.6	-3.7	-	-3.0	-3.4	-	**-2.0**

Table Appendix I 1, Table Appendix I 2 and Table Appendix I 3 show the differences between the results from IDA and DesignBuilder in the simulation runs for the pre-refurbished building (the block of 9 terraced houses). The results in terms of total consumption are very close with DesignBuilder providing consumption and heat demand values slightly lower than IDA ICE, the difference is however in a range of 1.4 – 2%

Appendix I 2 – Post-refurbishment model numerical results

Table Appendix I 4 Case 1 heat demand

Heating demand per house – Case 1 (kWh)									
	A	**B**	**C**	**D**	**E**	**F**	**G**	**H**	**I**	**TOT**
DB	7911	5225	5090	5298	8225	0	8853	11036	0	**51639**
IDA ICE	7418	5351	5194	5340	8668	0	9350	11367	0	**52687**
DIFF %	6,2	-2,4	-2,0	-0,8	-5,4	--	-5,6	-3,0	-	**-2,0**

Table Appendix I 5 Case 2 heat demand

Heating demand per house – Case 2 (kWh)									
	A	**B**	**C**	**D**	**E**	**F**	**G**	**H**	**I**	**TOT**
DB	4989	3141	3039	3214	5185	0	5593	7043	0	**32204**
IDA ICE	4681	3373	3253	3314	5417	0	5983	7421	0	**33442**
DIFF %	6.2	-7.4	-7.1	-3.1	-4.5	-	-7.0	-5.4	-	**-3.8**

Table Appendix I 6 Case 3 heat demand

Heating demand per house – Case 3 (kWh)									
	A	**B**	**C**	**D**	**E**	**F**	**G**	**H**	**I**	**TOT**
DB	5089	3199	3057	3037	3146	3115	3104	3184	4963	**31894**
IDA ICE	4660	3336	3147	3093	3112	3283	3163	3281	4528	**31602**
DIFF %	8.4	-4.3	-2.9	-1.8	1.1	-5.4	-1.9	-3.0	8.8	**0.9**

Just like for the pre-refurbishment conditions also the post refurbishment models display results that are almost overlapping with a maximum difference in case 2 equal to 3.8%

Table Appendix I 7 Heat demand comparison by software

	Heating demand compared to pre-refurbishment scenario	
	DesignBuilder	**IDA ICE**
Case 1	-12.5%	-12.5%
Case 2	-45.4%	-44.4%
Case 3	-53.5%	-54.5%

Table Appendix I 7 highlights how the software indicate energy saving values which are very similar (maximum difference 1%) with case 1 having exactly the same results from both the software.

Assessment and optimisation of energy consumption in building communities using an innovative co-simulation tool

Giorgio Cucca *, Anton Ianakiev

Department of Civil Engineering, Nottingham Trent University, Nottingham, United Kingdom

ARTICLE INFO

ABSTRACT

Energy efficiency in building sector is attracting an increasing interest in the scientific community, due to its strong impact in terms of greenhouse gas emissions. In this context, the REMOURBAN H2020 project has carried out a pilot deep refurbishing work on a small cluster of 10 homes, implementing energy saving measures and a hybrid energy-supply system to satisfy the heating and domestic hot water demand. The system aims to achieve near-zero-energy homes level of performance at reasonable cost by offsetting the energy consumption with local energy microgeneration. It is designed as a local low temperature district heating system and includes ground source heat pumps, photovoltaic panels, electric and thermal energy storage devices. The management of the complex hybrid system requires a suitable control strategy to optimise the energy consumption and consequently running cost. With this purpose a co-simulation tool has been developed, coupling a model of the energy system built using Dymola-Modelica and the EnergyPlus model of the buildings. This allows to develop different control strategies aiming to reduce the energy consumption from the grid, maximize the self-consumption of photovoltaic energy and ultimately move away from fossil fuel to sustainable energy resources.

1. Introduction

Both the European Union and the United Kingdom are on the frontline addressing the root causes of the climate change. On November 28th, 2018 the European Commission presented a long-term strategic vision for a competitive carbon neutral economy by 2050 [1]. The United Kingdom, on the other hand, is tackling and responding to climate change through "The Climate Change Act 2008 (2050 Target Amendment) Order 2019", which states that "It is the duty of the Secretary of State to ensure that the net UK carbon account for the year 2050 is at least 100% lower than the 1990 baseline" [2].

In this scenario the research community is showing an increasing interest in buildings energy performance. This is due to the great impact that the building sector has on the energy demand, it accounts for roughly 40% of the energy demand in the European Union (EU)

[3] and 36% in the world with a forecasted growth of 28% by 2040 compared to the 2015 [4]. The growing population and the rising energy demand in developing countries could lead to a 50% increase in the energy demand from buildings by 2060. A fast growing economy like China had a 5.76% yearly increase in the carbon emissions from buildings in the last decade, with a total of 1.28 billion tons of CO_2 emitted in 2017 [5].

In the EU dwellings alone are responsible for 60% of building energy demand and 40–60% of this energy is used for heating [6]. In the specific case of the UK, the domestic sector accounts for around 40 $MtCO_2e$[1] on a total of 151.3 $MtCO_2e$ that represent the final consumption energy in the UK [7], the building sector is responsible for around 26% of all carbon emissions considering the direct and indirect ones[2] [8].

---

* Corresponding author

E-mail address: giorgio.cucca2017@my.ntu.ac.uk (G. Cucca).

[1] $MtCO_2e$ are Mega Tons of equivalent CO_2, see 4.4 for equivalent CO_2 definition.

[2] Direct emissions are from sources that are owned or controlled by the reporting entity. Indirect emissions are a consequence of the activities of the reporting entity but occur at sources owned or controlled by another. Indirect emissions are currently most commonly associated with electricity use.